Addis Ababa University
Addis Ababa Institute of Technology
School of Electrical and Computer Engineering

Designing Power Electronic Interfaces and Microsource Controllers for a MicroGrid

By: Mesfin Engdawork

THESIS SUBMITTED TO ADDIS ABABA INSTITUTE OF TECHNOLOGY IN PARTIAL FULFILLMENT OF THE REQUIREMENTS FOR THE DEGREE OF MASTERS OF SCIENCE IN ELECTRICAL ENGINEERING

Advisor: Dr. Mengesha Mamo

September 2017

Addis Ababa, Ethiopia

ADDIS ABABA UNIVERSITY

ADDIS ABABA INSTITUTE OF TECHNOLOGY

SCHOOL OF ELECTRICAL AND COMPUTER ENGINEERING

Designing Power Electronic Interfaces and Microsource Controllers for a MicroGrid

Mesfin Engdawork

Approved by Board Examiners

---	---
Chairman, Dept. Graduate Committee	Signature
Dr. Mengesha Mamo	---
Advisor	Signature
---	---
Internal Examiner	Signature
---	---
External Examiner	Signature

Declaration

I, the undersigned, declare that this thesis is my original work, has not been Presented for a degree in this or any other university, and all sources of materials used for the thesis have been fully acknowledged.

Mesfin Engdawork _____

Name Signature

Place: Addis Ababa

Date of submission: ----------

This thesis has been submitted for examination with my approval as a university advisor.

Dr. Mengesha Mamo _____

Advisor's name Signature

Abstract

Developing a Microgrid (MG) system supplied with feasible integrated microsources, such as renewable energy sources and fuel cell, is one of the major solutions to be envisaged in terms of the current trend of power demand, i.e. efficient, environmentally friendly and relatively cheap means of power generation. In a Microgrid the most indispensible devices are the Power Electronic Interfaces and Controllers which regulate electrical parameters of the microsources.

This research provides comprehensive overview, design and modelling of Power electronic interface (PEI) and Microsource Controllers (MCs) for a Microgrid supplied with Photovoltaic (PV) and Integrated Solid Oxide Fuel Cell/Gas Turbine (ISOFCGT). The PEIs to be designed includes Inverters and DC-DC boost converter for the three microsources, PV, SOFC and GT, and rectifier for the Gas Turbine (GT) unit. To avoid use of transformer in the MG, two-stage DC-DC boost converter is used. For the ease of controlling and reduction of THD, SPWM technique of inversion is applied.

In designing Microsource Controller a control technique known as Droop control, in which active and reactive powers are controlled during grid-connected mode of operation of the Microgrid, and voltage and frequency are controlled in island mode, is considered as a better option. By doing so the control of microsources is distributed and proportional power sharing among microsources is facilitated so that reliability of control is ensured as there is no central control unit which needs communication facilities.

In the Microgrid the PV is not dispatchable unless it is backed by battery storage system due to the intermittent nature of the solar power. But the cost of battery for PVs is very expensive and makes the system sophisticated due to power electronic interface for charging and other ancillary devices like charge controller. There is the possibility of not to use the battery and the ancillary devices by using the SOFC microsource instead of the battery storage system when the solar power is reduced or completely unavailable. So this thesis also considers the possible mechanism of sensing the intermittency of the solar

power in such a way that the SOFCGT can take over the PVs in partial or completely.

The designed PEIs could make the microsources to be integrated in to the proposed MG by converting their original DC and high frequency AC sources in to standard three phase AC wave forms of 380 V and 50 Hz. Also using the designed Microsource Controller it is possible to control V, f, P and Q by ensuring proportional power sharing among the microsources.

MATLAB/SIMULINK-Simpowersystem is used to simulate the designed PEIs and the MCs based on a model Microgrid so that the performance characteristics of the two systems can be demonstrated practically.

Key words: Microgrid, Microsource, Microsource Controller, Power Electronic Interface, Inverter, DC-DC converter, Rectifier, Droop Control, Photovoltaic, Integrated Solid Oxide Fuel cell/Gas Turbine.

Acknowledgement

I would like to thank my advisor Dr. Mengesha Mamo for his insightful comment on the ideas and contents to be included in this study. His comment could help me to shape the framework of this paper. The progressive ideas he has been telling me could help me to know more about the subject matter. He could also forward important comments as to add model Microgrid so that the real word application of the study can be revealed.

Mesfin Engdawork

Addis Ababa, September 2017

Table of Contents

Abstract iii

Acknowledgement v

List of figures ix

List of Tables xi

List of Acronyms xii

CHAPTER ONE 1

INTRODUCTION 1

1.1. Microgrid Concept 3

1.2. Power Electronic Interfaces 4

1.3. Microsource Controller 5

1.4. Research Objective and Methodology 8

1.4.1. Problem definition 8

1.4.2. Objectives 8

1.4.3. Methodology 9

1.5. Research Questions 9

1.6. Research Contribution 10

1.7. Outline of the Thesis 10

CHAPTER TWO 12

Literature Review 12

2.1. Introduction 12

2.2. Definition of Microgrid 12

2.3. Components of Typical Microgrid 13

2.3.1. Generation Units 13

2.3.2. Loads 14

2.3.3. Energy Storages 14

2.3.4. MicroGrid Controllers 17

2.4. Power Electronic Interfaces 25

2.4.1. PEIs for Photovoltaic 26

2.4.2. PEIs for SOFC 27

2.4.3. PEIs for Gas Turbine 28

2.5. Ancillary Devices 28

2.5.1. Static Transfer Switch 29

2.5.2. Phase Locked Loop 31
CHAPTER THREE 33
Microsources 33
3.1. Introduction 33
3.2. Photovoltaics 33
3.2.1. Basics of Photovoltaics 33
3.2.2. Types of Photovoltaic Cells 34
3.2.3. Electrical models of a photovoltaic cell 35
3.2.4. Dependent parameters of Photovoltaic panel 36
3.2.5. Maximum Power Point Tracking methods 37
3.3. Fuel Cell 38
3.3.1. Fuel Cell basics 38
3.3.2. Types of Fuel Cells 40
3.3.3. Solid Oxide Fuel Cell 41
3.3.4. Connecting individual SOFCs 43
3.3.5. Dynamic modelling of SOFC 44
3.3.6. Steady state characteristics of SOFC 45
3.3.7. Integrated SOFC/GT system 46
CHAPTER FOUR 48
Power Electronic Interface Design 48
4.1. Introduction 48
4.2. DC-DC converter 48
4.2.1. Principle of operation of DC-DC boost converter 49
4.2.2. Two stage boost converter 51
4.3. Rectifier 53
4.3.1. Three-phase bridge rectifier 54
4.4. Inverter 55
4.4.1. Components of inverter 56
4.4.2. Sinusoidal Pulse Width Modulation (SPWM) technique 57
4.4.3. Low pass filter 60
4.5. PEIs Design and Simulation Scenario 61
4.5.1. Load Estimation 61
4.5.2. PEIs for the SOFC 63
4.5.3. PEIs for the Photovoltaic 68

4.5.4. PEIs for Gas Turbine 72
CHAPTER FIVE 74
Microsource Controller Design 74
5.1. Introduction 74
5.2. Control functions of Microsource controller 75
5.3. Droop V-f control 77
5.3.1. Dqo transformation 77
5.3.2. Independent measurement of Active and Reactive Power 78
5.4. P-Q Droop control 81
5.4.1. PQ control scenario 83
5.5. Power sharing control 83
5.6. Design and Simulation of MS Droop controller 84
5.6.1. Power sharing simulation 94
CHAPTER SIX 100
Results and Discussion 100
6.1. Introduction 100
6.2. Power Electronic Interfaces 100
6.2.1. Inverter 100
6.2.2. DC-DC boost converter 103
6.2.3. Rectifier 105
6.3. Microsource Controller 107
6.3.1. V-f droop controller 107
6.3.2. PQ droop controller 108
6.3.2. Power sharing 108
6.4. Transition mode of MG operation 110
6.5. PV without Battery 112
CHAPTER SEVEN 113
Conclusion 113
7.1. Contributions 114
7.1.1. Power Electronic Interfaces 114
7.1.2. Microsource Controller 115
7.2. Future Duties 115
7.3. Recommendations 115
REFERENCES 117

List of figures

Figure 1-1: Structure of typical Microgrid 2
Figure 2-1: Microgrid Architecture 13
Figure 2-2: Flywheel storage system 16
Figure 2-3: The theory of PQ control: (a) frequency droop characteristic and (b) voltage droop characteristic 18
Figure 2-4: PQ control schematic 20
Figure 2-5: The theory of V/f control: (a) frequency droop characteristic and (b) voltage droop characteristic 21
Figure 2-6: General V/f control Scheme in a Distribution Network 22
Figure 2-7: Dual mode operation inverter structure of PQ-V/f control 24
FFigure 2-8: Schematic of PEIs for PV 27
Figure 2-9: SOFC system configuration with DC-DC and DC-AC converters 28
Figure 2-10: Gas Turbine with cascaded AC-DC and DC-AC converters 28
Figure 2-11: STS basic structure 29
Figure 2-12: Component parts of PLL 31
Figure 2-13: Block diagram of PLL in three phase system 31
Figure 3-1: Air mass depending on the sunlight path 34
Figure 3-2: Electrical models of a photovoltaic cell 35
Figure 3-3: The effect of environmental conditions on PV characteristic curves 37
Figure 3-4: I-V and P-V Solar Cell Characteristics with MPP 37
Figure 3-5: The basic workings of a fuel cell with proton flow through the electrolyte. 39
Figure 3-6: Schematic diagram of Solid Oxide Fuel Cell 42
Figure 3-7: Planar SOFC (two cell array) 43
Figure 3-8: V-I characteristics of the SOFC model at different temperatures 45
Figure 3-9: P-I characteristics of the SOFC stack model at different temperatures. 46
Figure 3-10: Main components of Integrated SOFC/GT (ISOFC/GT) system 47
Figure 4-1: Schematic diagram of the boost DC-DC converter 49
Figure 4-2: Principle of operation of the boost dc-dc converter 50
Figure 4-3: Two stage DC-DC boost converter 52
Figure 4-4: Three - phase full bridge rectifier 54
Figure 4-5: Different power semiconductor switches 56
Figure 4-6: Three-phase voltage source inverter 57
Figure 4-7: Conventional SPWM generation technique for three phase voltage source inverter 59
Figure 4-8: 3rd order LCL filter for three phase system 60
Figure 4-9: Bridge Inverter with Switching gate signal 64
Figure 4-10: SIMULINK model of LCL filter 65
Figure 4-11: The overall SIMULINK model of the inverter with measuring units 65
Figure 4-12: A Phase to phase AC output voltage and current 66
Figure 4-13: Three phase output voltage and current wave form for SOFC 66
Figure 4-14: SIMULINK model of the two stage DC-DC boost converter 68
Figure 4-15: The output voltage wave form of the DC-DC boost converter 68
Figure 4-16: SIMULINK model of the inverter with measuring units for the PV 69
Figure 4-17: Inverter phase to phase output voltage and current for PV 70

Figure 4-18: The three phase output voltage and current for PV 70
Figure 4-19: SIMULINK model of two stage boost converter for PV 71
Figure 4-20: Output voltage waveform of the two stage DC-DC boost converter 72
Figure 4-21: SIMULINK model of rectifier for the Gas Turbine. 73
Figure 4-22: Waveform of the rectifier output DC voltage for the GT 73
Figure 5-1: Clark and Park Transformations 77
Figure 5-2: Basic VSI converter system 79
Figure 5-3: Droop characteristic curve of a microsource 80
Figure 5-4: V-f droop control system schematic 81
Figure 5-5: Current mode control for intermittent renewables 82
Figure 5-6: Current mode power flow control for dispatchable sources 83
Figure 5-7: SIMULINK model of abc-dqo converter 85
Figure 5-8: Active and reactive power calculation unit in SIMULINK 86
Figure 5-9: Frequency and voltage droop control unit in SIMULINK 86
Figure 5-10: Modulating signal generation unit 87
Figure 5-11: Complete features of MS controller during islanding in SIMULINK 89
Figure 5-12: The output voltage wave form of MS controller during islanding 90
Figure 5-13: Standard wave form generated from sine wave generator 91
Figure 5-14: SIMULINK model of PQ droop controller 91
Figure 5-15: Non-droop PQ controller in grid connected mode for PV 93
Figure 5-16: Output voltage wave form of the PQ controller 94
Figure 5:17: SOFC Subsystem 95
Figure 5-18: MS droop controller subsystem 95
Figure 5-19: Flow diagram of modes of operation of the MG 96
Figure 5-20: Power sharing simulation model of the Microgrid 97
Figure 5-21: Active power output of the SOFC in switched modes 98
Figure 5-22: Active power output of the PV in switched modes 98
Figure 5-23: Active power output of the GT in switched modes 99
Figure 6-1: dqo output wave form of the AC voltage from inverters 101
Figure 6-2: Simulation results of LC and LCL filtering techniques 102
Figure 6-3: Output voltage response change Vs change in sample time 105
Figure 6-4: Change in ripple content and response of output voltag 107
Figure 6-5: The simulation result of PQ droop controller 108
Figure 6-6: Total current response to change in load 109
Figure 6-7: STS mechanism of operation in SIMULINK 110
Figure 6-8: The switching of STS from grid connected mode to islanding 111
Figure 6-9: Logic Flowchart for Synchronization Determination. 111

List of Tables

Table 4-1: Estimated loads 62
Table 4-2: Microsource's power supply 63
Table 4-3: Components and design and specification of inverter for SOFC 63
Table 4-4: Specification of switching MOSFET for inverters…. 64
Table 4-5: Design Specification for two stage DC-DC boost converter for SOFC 67
Figure 4-6: Specification of diodes used in the DC-DC boost converter 67
Table 4-7: Design specification of two stage DC-DC converter for PV 71
Table 4-8: Design specifications of rectifier for GT 73
Table 5-1: Summary of microsource data 85

List of Acronyms

AFC Alkaline Fuel Cell

CHP Combined Heat and Power

DAFC Direct Alcohol Fuel Cell

DER Distributed Energy Resource

DMFC Direct Methanol Fuel Cell

FAFC Phosphoric Acid Fuel Cell

FC Fuel Cell

FESS Flywheel Energy Storage System

GT Gas Turbine

HFAC High Frequency Alternating Current

ISOFC/GT Integrated Solid Oxide Fuel Cell Gas Turbine

LFAC Low Frequency Alternating Current

LV Low Voltage

MC Microsource Controller

MG Microgrid

MGCC Microgrid Central Controller

MPPT Maximum Power Point Tracking

MS Microsource

PCC Point of Common Coupling

PEI Power Electronic Interface

PEMFC Polymer Electrolyte Membrane Fuel Cell

PLL Phase Locked Loop

PQ Active-Reactive Power

PV Photovoltaic

SOFC Solid Oxide Fuel Cell

STC Standard Test Condition

STS Static Transfer Switch

THD Total Harmonic Distortion

V/f Voltage/frequency

VCO Voltage Controlled Oscillator

CHAPTER ONE

INTRODUCTION

These days the world is witnessing two competing scenarios as far as power generation is concerned. On one hand, there is a rapid rise in demand of electric power. On the other hand, the issue of generating power using generators which are environmentally friendly is becoming a leading agenda so as to avert the crisis of global warming and environmental pollution that the world is facing. This is despite the fact that the traditional means of power generation is mostly powered by fossil fuel. Again there is a reasonable interest on efficiency and cost of power generation and transmission.

Amidst of all these very important needs, investigating alternative energy resources which are environmentally friendly, efficient and relatively cheap is becoming top priority of leading engineers of the world. Renewable energy resources such as Photovoltaic (PV) and wind turbine, and other non-conventional energy resources such as Fuel cell (FC) are being considered as the leading alternative resources. But it does not mean that they are being utilized as a central generator which produces huge amount of power. They are rather used as energy resources which give support to the main Grid. Organizing these non-conventional resources into a power system so that they can be integrated with the utility or supplying power in a stand-alone mode is one of the most challenging engineering fields of study in which enormous researches have been undergoing.

Additionally, demand-supply matching, controlling and other technical issues are among the challenges being faced in integrating non-conventional energy resources in to a utility network. These sources typically would be connected to a weak distribution network which in turn introduces power quality issues within the network. Also the direction of power flow may be in the opposite direction to conventional power flow, thus new protection schemes may be required.

The Microgrid concept is a solution which has been suggested to use alternative energy sources effectively while enabling increased amounts of

renewables to connect to the utility network. A typical Microgrid contains several generation units which are known as microsources. Further a Microgrid could be connected to the utility network to export or to import power. It makes use of two concepts. Firstly net power flow to or from the main utility network is controlled, improving the apparent behaviour of local microsources. Secondly the Microgrid may island from the main network, continuing to supply power to loads during network disturbances. Figure 1-1 presents the structure of typical Microgrid.

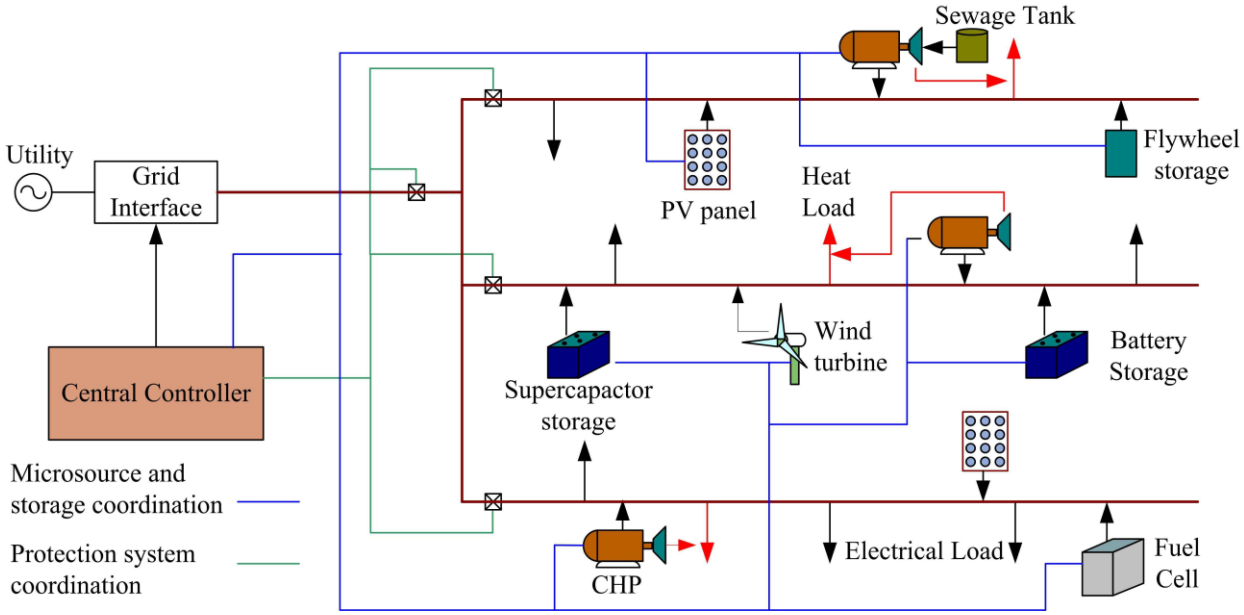

Figure 1-1: Structure of typical Microgrid [6]

In most cases microgrids are supplied with integrated distributed energy resources, especially with that of renewable ones called microsource. They use different resources to supply both electric power and heat to a community or an industry. The integration of wind, solar thermal, solar photovoltaic, Fuel Cell and steam turbine is among Combined Heat and Power (CHP) system to be cited as an example of a Microgrid.

Apart from such combinations it is possible to establish a Microgrid which is supplied with a hybrid of a renewable energy resource and a Fuel Cell (FC). Among such possibilities a hybrid of PV and Integrated Solid Oxide Fuel Cell/Gas Turbine (ISOFCGT) is considered as a reasonable coupling in terms of efficiency, minimum emission, cheaper cost and simpler design. In the ISOFCGT

system the Solid Oxide Fuel Cell (SOFC) generates both heat and electricity in parallel so that the efficiency of the Microgrid is enhanced. This is due to the fact that the operating temperature of the SOFC is very high (600-1000) ^{0}C. So the exhaust gas from its anode can be used to generate further electric power using cascaded Gas Turbine (GT) other than that of the SOFC.

So the advantages provided by the proposed Microgrid (MG) include use of renewable energy sources, use of waste heat during generation, efficiency, cheap cost of operation and infrastructure and improved reliability of power. However, the implementation of Microgrid introduces many challenges such as lack of proven technology, efficient power electronic interfaces, well designed MG controllers, Protection units, etc. which make the system sophisticated and challenging to implement [6].

1.1. Microgrid Concept

Microgrids are small-scale, LV CHP supply networks designed to supply electrical and heat loads for a small community, such as a housing estate or a suburban locality, or an academic or public community such as a university or school, a commercial area, an industrial site, a trading estate or a municipal region [1]. Microgrid is essentially an active distribution network because it is the conglomerate of DG systems and different loads at distribution voltage level. The generators or microsources employed in a Microgrids (MGs) are usually renewable/non-conventional DERs integrated together to generate power at distribution voltage.

From operational point of view, the microsources must be equipped with power electronic interfaces (PEIs) and controllers to provide the required flexibility as to ensure operation of a MG as a single aggregated system and to maintain the specified power quality and energy output. This control flexibility would allow the Microgrid to present itself to the main utility power system as a single controlled unit that meets local energy needs for reliability and security.

The key differences between a Microgrid and a conventional power plant are as follows [5]:

a) Microsources are of much smaller capacity with respect to the large generators in conventional power plants.
b) Power generated at distribution voltage can be directly fed to the utility distribution network.
c) Microsources are normally installed close to the customers' premises so that the electrical/heat loads can be efficiently supplied with satisfactory voltage and frequency profile and negligible line losses.

The technical features of a Microgrid make it also suitable for supplying power to remote areas of a country where supply from the national grid system is either difficult to avail due to the topology or frequently disrupted due to severe climatic conditions or man-made disturbances.

From grid point of view, the main advantage of a Microgrid is that it is treated as a controlled entity within the power system. It can be operated as a single aggregated load. This ascertains its easy controllability and compliance with grid rules and regulations without hampering the reliability and security of the power utility [1]. From customers' point of view, Microgrids are beneficial for locally meeting their electrical/heat requirements. They can supply uninterruptible power, improved local reliability, reduce feeder losses and enhance power quality [3]. From environmental point of view, Microgrids reduce environmental pollution and global warming through utilisation of low-carbon technology.

1.2. Power Electronic Interfaces

Microsources (MSs) of a Microgrid such as PV and Fuel cell produce dc voltage, and generators like wind turbine and gas turbine produce variable voltage at a certain frequency. Thus power electronic converters must be used to interconnect the microsources to a Microgrid. Those which produce dc voltage should be converted in to appropriate dc voltage level so as to be converted in to standard AC form. And the DC source voltage of microsources like fuel cell and photo voltaic varies with the current to be supplied, also the DC source voltage is needed to be stepped up so as to reduce the cost of DGs and avoid the use of transformer [5]. So dc-dc converter should be used for the stated purposes. But those which operate at alternating voltage should be connected to a rectifier prior to being connected to DC-DC converter and then to an

inverter. Finally both types of microsources are connected to the respective inverter in order to be integrated in to a Microgrid.

Moreover, microsources are relatively slow to respond to load changes in a Microgrid [3]. It may take more than a minute in case of fuel cell. A Storage unit such as battery, flywheel or super capacitor should be connected to the MG so as to facilitate instant response to the load changes till the microsources in the Microgrid takeover the required supply. The storage units cannot be connected directly to the MG. They are connected to a MG through Power Electronic Interfaces (PEI) too. However, more emphasis is given to developing PEIs (rectifier, DC-DC boost converter and inverter) for the microsources of the proposed MG as far as this study is concerned as in most cases storage units, especially fly wheel, have their own in built PEIs. Plus similar techniques of PEIs design as that of MSs can be followed.

1.3. Microsource Controller

Microgrids can be developed as either grid-connected or stand-alone mode. When the Microgrid (MG) is connected to the utility, it has the advantage of power supply and power quality support. And it operates in island and grid-connected mode in accordance with the availability of utility supply in terms of power quality and reliability. When the MG is connected to the utility, loads are supported from both the utility and the Microgrid in terms of power supply and voltage and frequency regulation. When power is interrupted from the utility due to faults, loads in a MG are shared among microsources and regulation of voltage and frequency are switched to individual control system known as Microsource Controller (MC).

As far as MS controller in a MG is concerned, there are two types of controller; central controller and distributed controller. This paper opts for studying the distributed one where each microsource of a MG has its own controller. When a MG is grid-connected, power flow is controlled (regulated) so that a specified amount of active and reactive power are supplied either from the utility to MG or vice versa. This kind of operation is called PQ control. During islanding mode of operation, the MG averts in to controlling the voltage and frequency of the MG as the respective reference quantities from the utility are interrupted. This mode of controlling is known as V-f control. There are two options of carrying

out the two modes of controlling. The first is to switch between the PQ and V/f control mode as required. The second option using a technique called droop control where P and Q are controlled by measuring frequency and voltage, and controlling V and f by measuring P and Q. This study designs the microsource controller based on the droop technique.

Another important feature of the droop controller is that it ensures proportional load sharing among microsources during islanding through droop characteristic equations. According to [5] load sharing in islanding mode can be undertaken in such a way that either the MG can accommodate all loads or it continues to supply sensitive-loads while disconnecting the non-sensitive ones as per the available capacity of the microsources. It is for the grid-connected type of Microgrid which share power supply with the utility in interconnected mode and shades non-sensitive loads in islanding that this study is going to develop a Microsource Controller.

Microgrids operating in coordination with the utility grid have the advantage of active and reactive power support, voltage and frequency operating point setting, continuous supply of loads without interruption fully or in partial as per the type of connections we choose to develop among the available options [8]. The following are the type of possible connections between the Microgrid and the utility:

i. The Microgrid and the utility are connected through static switch in such a way that sensitive and non-sensitive loads are connected in to separate feeders so that either all loads are supplied with power when the MG and the utility are connected, or only sensitive loads are supplied when power is interrupted from the utility. This is the type of connection this study deals with.
ii. Both the sensitive and non-sensitive loads are supplied with power either in grid-connected or islanded mode. What the utility does in this option is that it supports by supplying power in partial and setting the operating voltage and frequency. In the island mode all the power supply are accommodated from the microsources of a Microgrid.
iii. In the above two options power is allowed to flow only from the utility to the Microgrid bur not in the reverse direction. But it is possible to allow power flow in both directions when the Microgrid DGs can

generate extra power so that it can supply the utility. Either of the above configurations is possible as far as the extent of power supply is concerned from the two sources.

Load sharing among the DGs of a Microgrid and maintaining the system frequency and voltage are among the major processes in a Microgrid. According to [6], during islanding DGs of a MG are responsible for maintaining the system voltage and frequency while sharing the real and reactive power. Load sharing without extensive communication facilities is the best option as the network can be complex and can span over a large area. The most common method for this purpose is the use of droop characteristics where power sharing among the parallel sources is achieved while controlling two independent quantities – the system frequency and the fundamental voltage magnitude [5].

Static transfer switch (STS) interconnects the MG with the utility. The STS disconnects the MG from the utility when the voltage and frequency do not meet the standard specification in which case the MG islands and the MS controller switches to V-f control. The STS remains switched off till the voltage and frequency levels of the utility return back to their standard value. The topology of the MG should allow the proper position of the STS so that sensitive loads continue to operate while non-sensitive ones ride through during faults, i.e. the power supply for sensitive loads is interrupted while supply for sensitive loads continues during islanding mode.

A smooth transfer between grid-connected and islanded modes is essential for the reliability of a Microgrid. When grid faults occur, in order to protect the power electronic devices and some sensitive loads, the STS disconnect the Microgrid from the main grid and the V-f control unit of the MS controller undertakes voltage and frequency regulation. At the same time, DGs must immediately increase their power output in a predetermined manner so as to continue supplying power to critical loads. When the clearance of faults takes place, the voltage at the common bus should track that of the grid with the help of STS, in terms of frequency, magnitude and phase, in order to achieve smooth and fast resynchronization. The overall process which takes place in a grid-connected Microgrid be described as grid-connected mode of operation,

islanding mode of operation and resynchronization. All the three states of operation needs dedicated controllers.

1.4. Research Objective and Methodology

1.4.1. Problem definition

A Microgrid mainly includes microsources, Power Electronic Interfaces, MS controllers and storage units. For the microsources to be integrated with the MG, they have to be connected through PIEs in one or more stages depending on the type of power they generate. Accordingly the conversion may take AC-DC, DC-DC, DC-AC, etc. The conversion process depends on the type of micro-generator, the level of the power to be generated, the form of generation, AC or DC, etc. So microsources (MSs) need specific type of PIEs to be designed as to realize the proper integration with the utility. When MSs are allowed to be connected with the MG, they have to be controlled as the MG switches between grid-connected and island mode of operation. During grid-connected mode, the active and reactive power have to be controlled as the MG is expected to contribute a specified amount while the voltage and frequency are maintained constant as the utility values used as reference. During islanding mode the voltage and frequency have to be maintained to their nominal values so that sensitive equipment continues to operate properly and seamless transition between the two modes of operation can be realized. Still all these list of control requirements need specifically designed MS controller. Therefore we can't separate the design of PIEs from that of the MS controller for the proper operation of a MG to meet its purpose.

1.4.2. Objectives

Main Objective

The main objective of this paper is to design a power electronic interface system and Microsource Controller for a Microgrid consisting of Photovoltaic and Integrated Solid Oxide Fuel Oxide/Gas Turbine microsources based on the specific requirements of the microsources in particular and the proposed MG in general.

Specific Objectives

- To investigate the weaknesses and strength of the existing technologies of Power Electronic Interfaces and Microsource Controllers of various Microgrids so as to achieve a reliable design.
- To develop simulations for PEIs and MCs of a Microgrid in the MATLAB/SIMULINK software to test their performance characteristic.
- To introduce new type of system design to come up with better architecture of the proposed Microgrid in terms of cost, efficiency and reliability.

1.4.3. Methodology

- **Literature survey**: Various literatures related to MicroGrids, types of fuel cells, Solid Oxide Fuel Cell, Gas Turbine, Photovoltaic, Microsource Controllers, and Power Electronic Interfaces i.e. DC-DC converters, rectifiers, inverters, and island detection units, etc. were studied.
- **Reviewing the existing technologies:** the existing available technologies of Power Electronic Interfaces and Microsource Controllers of various Microgrids were investigated to find out a better alternative design which suits for the proposed MG.
- **Collecting data on the type of loads:** an institution, Black Lion Hospital, which has sensitive and non-sensitive loads was selected and load estimation has been carried out for the PEIs and MS controller design to compatible with the level and type of loads.
- **Simulation:** The newly developed PEIs and MCs are simulated on MATLAB/SIMULINK-Simpowersystem environment based on the real world implementation.

1.5. Research Questions

In the context of this research, my goal is to address the following three research questions:

1. How micro-generators, renewable and non-renewable, can be integrated into a MG generating the nominal or standard electrical quantities with relatively low cost?
2. What kinds of Power Electronic Interfaces are needed in terms of the nature of the microsources and special needs in the MG?
3. What kind of Microsource Controller is required to operate the Microgrid in both grid-connected and island modes of operation reliably with ease of flexibility?

1.6. Research Contribution

This research provides the following contributions:

1. Specifies the type of power electronic converters required for specific purposes in a MG in terms of their topology, rating and complimentary devices.
2. Defines control strategy for grid-connected and island modes of operation of a Microgrid.
3. Shows alternative design approaches of both PEIs and MS controllers.

1.7. Outline of the Thesis

The works in this thesis are structured as follows:

- Chapter one provides a comprehensive overview of what to be covered in this study briefing the concept of Microgrid and what it includes. It also formulated the research objectives, and described the technological contributions of this study.
- Chapter two introduces the study by reviewing the literatures according to the themes of the study to be covered.
- Chapter three introduces the scientific and engineering aspects of the micro-generators of the proposed Microgrid.
- Chapter four provides the processes of designing of Power Electronic Interfaces (PEIs) of the MG by demonstrating the theoretical background of the PEIs first, and finally simulation with SIMULINK is followed.

- Chapter five provides the processes of design of Microsource Controller (MC) of the MG by demonstrating the theoretical background of the MC first, and finally simulation with SIMULINK is followed.
- Chapter six discusses on the result obtained from the design of PEIs and MC, and key issues which need further explanations.
- Chapter seven summarizes the main conclusions of the thesis and identifies further proceedings that may be undertaken in the future.

CHAPTER TWO

Literature Review

2.1. Introduction

In this chapter the definition of a Microgrid and the structure of a typical Microgrid are explained. Further a brief introduction to the components of a Microgrid is given. The benefits, features and issues are also discussed. Further some of the proposed power electronic interfaces and microsource control techniques are presented.

2.2. Definition of Microgrid

The definition and typical composition of a Microgrid are both not standardised and still evolving [6]. According to [4], “Microgrid concept assumes a cluster of loads and microsources operating as a single controllable system that provides both power and heat to its local area”. Alternatively a “Microgrid is a small grid in which distributed generators and electric loads are placed together and controlled efficiently in an integrated manner” according to [4]. Alternatively “A Microgrid can be defined as an LV network (e.g., a small urban area, a shopping centre, or and industrial park) plus its loads and several small modular generation systems connected to it, providing both power and heat to local loads [combined heat and power (CHP)]” according to [6].

A Microgrid is thus a power network which is comparatively lower in total generation capacity compared with a conventional power system. It typically consists of loads, several small generation units, power electronic interfaces and possibly storage and some degree of intelligent control [6]. Critically, a Microgrid is designed to be capable of operating either in grid-connected mode or islanded mode. In addition to electrical loads, heat loads are also often connected to this small power system. A Microgrid typically only consists of part of a distribution network, and the distance between loads and generation units are close.

2.3. Components of Typical Microgrid

The schematic architecture of a typical MicroGrid is presented in Figure 2-1. The main components of a MicroGrid are generation units, loads, energy storage, the actual distribution network, the protection system, the control system and the grid interface unit.

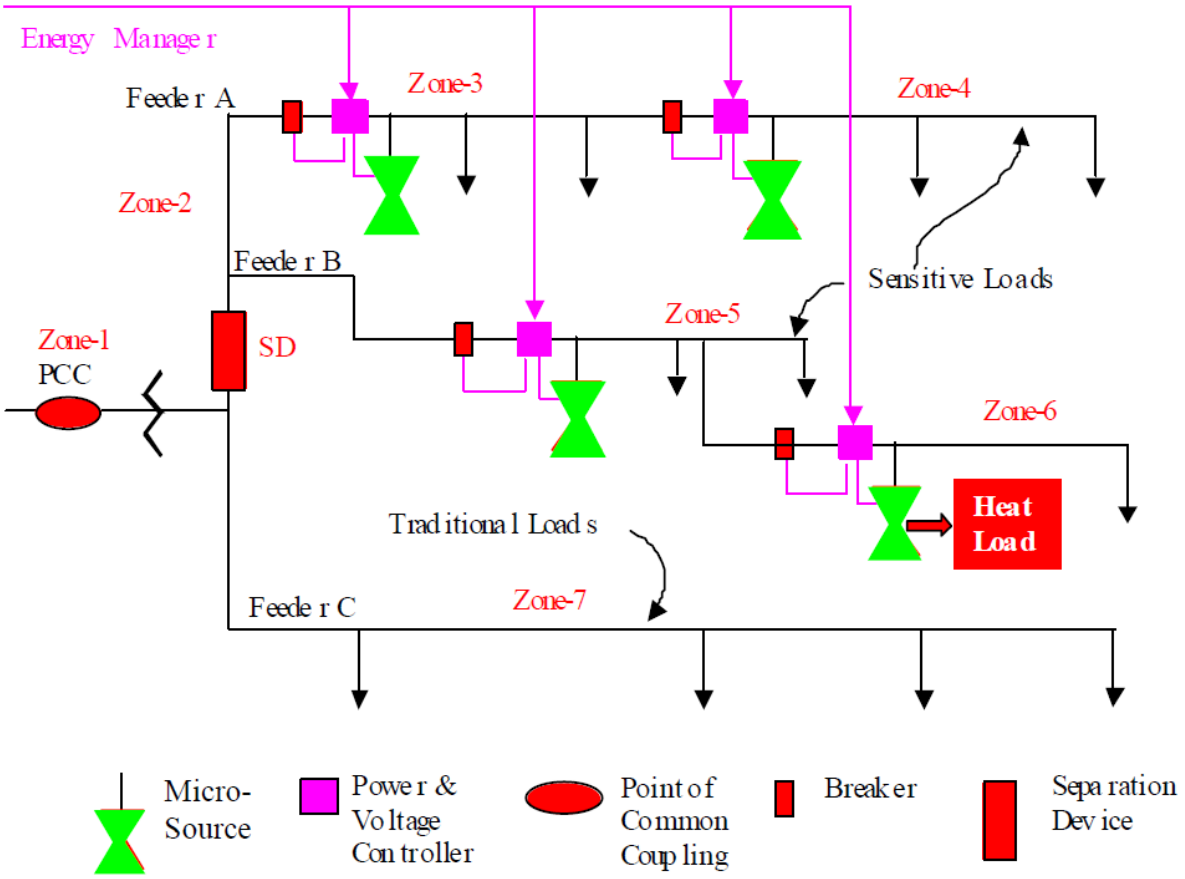

Figure 2-1: Microgrid Architecture [8]

2.3.1. Generation Units

The capacity of generation units connected to a Microgrid is relatively small in capacity compared with conventional power stations, and thus they are known as microsources [2]. In most cases, the upper limit of the capacity of a microsource is below 500kW [1]. Renewable energy sources such as photovoltaics (PV), wind turbines and hydro power plants are proposed and used in various pilot Microgrids. The output power of renewable sources is subjected to environmental conditions, and this introduces availability

constraints which creates problems in matching demand to supply when the Microgrid is not connected to the remaining utility network. Dispatchable microsources which have been proposed for use in a Microgrid are fuel cells, microturbines and diesel generators [10]. These are 'dispatchable' because in theory the fuel source is readily available without significant supply constraints. There is also a possibility of combining the dispatchable unit with that of non-dispatchable so as to gain economic advantage [2]. Such kind of combination incudes Fuel cell-Photovoltaics hybrid generation system in which the FC substitutes the storage battery of the PV cells during severe climatic conditions and night time. However if heat generated from the microsources such as microturbines and fossil fuel generators are used for heating purposes (i.e. in Combined Heat and Power plants) then a constraint is imposed requiring reasonable economic use of such heat.

2.3.2. Loads

Microgrids (MGs) can be classified in to two according to the arrangement of their loads whether a Microgrid can supply power to them fully or in partial during islanding. When the MG is designed to supply only some specific loads when it islands, the loads are classified as critical and non-critical loads. In this type of load arrangement, continuous power to the critical loads is ensured. Generation-demand mismatch during islanded operation mode may results in disconnection of non-critical loads. Authors in [2, 3] have proposed to use separate feeders for critical and non-critical loads which makes the disconnection process easier. Loads connected to a typical MicroGrid are not only electrical loads but also heating loads. Heating loads are linked to the Microgrid both by direct heat loads and by CHP plants. The potential interactions between loads and generation source are thus relatively complex.

2.3.3. Energy Storages

The response to load changes in a Microgrid is different among microsources. It may take up to few minutes for microsources such as fuel cell [3]. However the response should be as instantaneous as possible. So, relatively slow response of microsources can be compensated by connecting a storage unit in parallel with the microsources through power electronic converter. The other problem which causes difficulty in a MG with regard to the inadequacy of

microsources is the occurrence of power fluctuation transients. In order to withstand such transients the same storage unit compensates the shortage of power. Most of the real-world Microgrids have used batteries as the storage units while some have used flywheels and ultracapacitors along with the batteries [11]. Authors in [13] have studied the possibility of operation of a MicroGrid with a flywheel as the only storage method. This paper also gives preference to fly wheel as a storage unit in the proposed MG for its advantages of simple maintenance, clean storage unlike batteries, high reliability, rapid response, ease of control, long service life and low per cycle cost.

Energy storage could be either centralised where the total storage capacity is in a single unit or distributed where the total capacity is distributed across the Microgrid in several units. With distributed energy storage, incremental expansion of storage is less costly. Also storage units can be classified in two in terms of the duration they can sustain supplying the required power support to their capacity [13];

I. Long term storage: Where the period of storage is above 10 minutes and the well-known types of long term storage units are batteries, storage under potential form of water.
II. Short term storage: Where the period of storage is less than 10 minutes and well-known types of short term storage units are Flywheel, super capacitor.

Flywheel storage unit

Flywheels are very popular as energy storage due to the simplicity of storing kinetic energy in a spinning mass [13]. For more than 20 years, it has been a primary technology used to limit power interruptions in motor/generator sets where steel wheels increase the rotating inertia, providing short power interruptions protection and smoothing of delivered power [13]. Conversion from kinetic to electric energy is accomplished by electromechanical machines. Many different types of generator machines are used in flywheel systems, such as permanent magnet machines, induction machines, and switched reluctance machines.

The key design element is to match the decreasing speed of the flywheel during discharge and the increasing speed during charging with a fixed frequency electrical system. Along with electromechanical machines, two methods are used to match system frequencies, mechanical clutches, and power electronics. The basic operation of a flywheel can be summarized as follows: When there is excess in the generated power with respect to load demand, the difference is stored in the flywheel that is driven by the electrical machine operating as a motor. On the other hand, when a fluctuation in delivered power is detected in the loads, the electrical machine is driven by the flywheel and operates as a generator supplying the extra energy needed. Such systems tend to be designed according to power needs and thus operate over shorter periods (on the order of one minute). Figure 2-2 below shows the main component parts of the storage system based on flywheel.

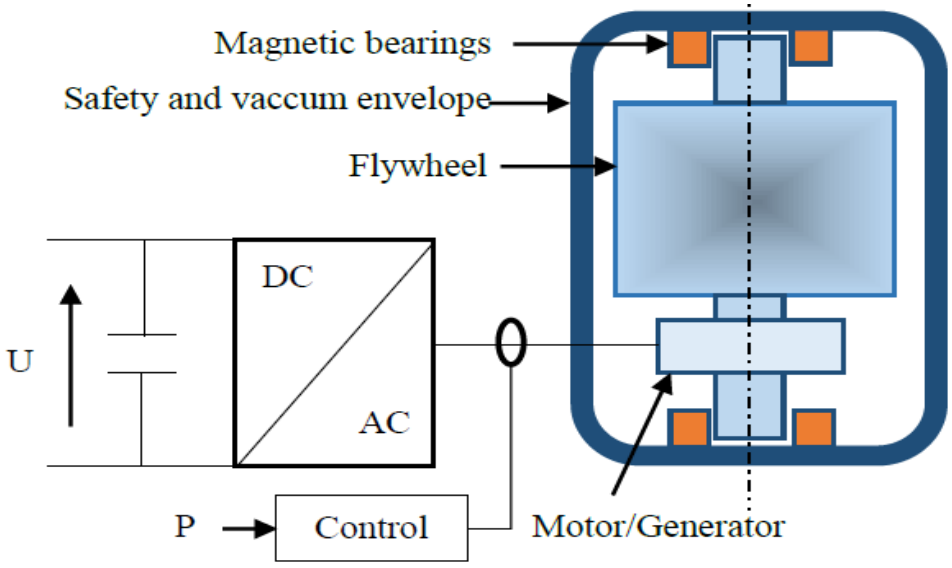

Figure 2-2: Flywheel storage system [13]

The main parts of FES include:

- the electromagnetic motor/generator,
- the flywheel,
- the bearings,
- the vacuum and safety envelope,
- the static converter (rectifier).

2.3.4. MicroGrid Controllers

From the view of the bulk grid system, Microgrid is an aggregation unit as a generation or load. On the other hand, Microgrid is a power system that operates autonomously, supplying reliable and high quality electric power from the view of customer side. Therefore, a good performance Microgrid control and management system is needed.

According to the integral control strategy, Microgrid control can be divided into master-slave control and peer-to-peer control [13]. There is a main control unit in master-slave control to maintain the constant voltage and frequency. The main control unit adopts Voltage/frequency (V/f) control while other distributed generations adopt PQ control to output certain active and reactive power. Master-slave control is composed of upper master control and sub-layer slave control. The upper master controller sends control command towards sub-layer slave control. Peer-to-peer (distributed) control, based on the idea of "plug-and-play", contain a number of equal-status microsources, one of which changes won't affect the others. The control strategy of DG can be divided into three categories: PQ control, V/f and Droop control, according to the control method of individual DG. Droop control is a common control strategy in peer-to-peer control. Also this study opts for the droop technique of V-f and PQ methods of control as they favour plug-and-play strategy and every microsource is controlled independently so that there is no need of communication among the micro-generators which enhances reliability.

Generally the following are purposes of Microgrid control in the context of distributed (peer-to-peer) method of control:

- New microsources can be added to the system without modification of existing equipment.
- The Microgrid can choose operation point autonomously.
- The Microgrid can connect to or isolate itself from the grid in a rapid and seamless fashion.
- Reactive and active power can be independently controlled.
- Voltage sag and system imbalances can be corrected.
- The Microgrid can meet the grid’s load dynamics requirements.

As already mentioned above, there are three Microgrid inverter control strategies: they are PQ control, V/f control and droop control. Detail explanation follows:

PQ control

The main purpose of using PQ control is to make distributed energy sources generate specified active and reactive power according to reference, namely when the frequency and voltage of AC bus with which inverter connects change within a certain range, the active and reactive power of distributed energy sources remain the same [15]. Active and reactive powers flowing out of an inverter are controlled by voltage mode control, where the active and reactive power are controlled using the phase angle and voltage magnitude of the inverter AC side with respect to the same quantities on the PCC side. Figure 2-3 illustrates the frequency and voltage droop characteristic PQ control theory.

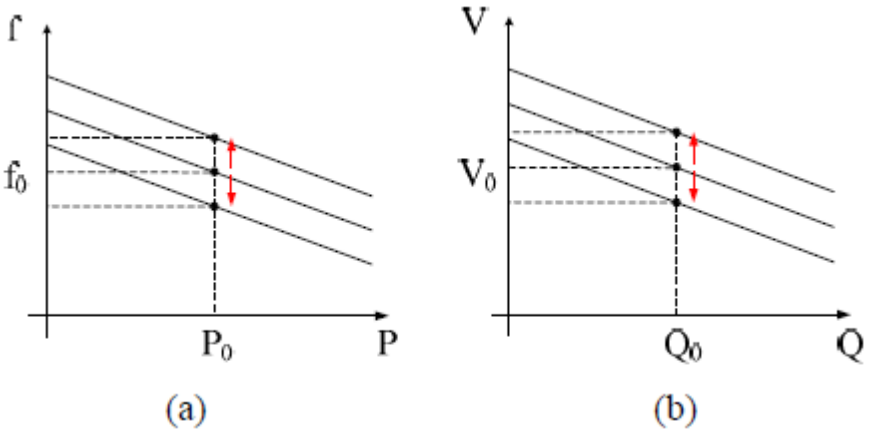

2-3: The theory of PQ control: (a) frequency droop characteristic and (b) voltage droop characteristic [3]

When Microgrid bus bar frequency changes within an allowed range ($f_{min} \leq f \leq f_{max}$), the active power of inverter will keep at the given reference value P_0; When Microgrid bus bar voltage changes within an allowed range ($V_{min} \leq V \leq V_{max}$), the reactive power of inverter will keep at the given reference value Q_0. In this approach the active and reactive power are controlled by controlling the

frequency and magnitude of the inverter AC side voltage with respect to the PCC current quantities [14]. PQ mode of control is applied when a MG is under grid-connected mode of operation.

The main function of an inverter in a Microgrid which is in grid-connected mode of operation is to control the active and reactive power flow between the microsource and AC system. In this section the variables which influence the flow of active and reactive power through the inverter will be discussed. The power flow between two AC sources – microsource inverter and the utility is represented by:

$$P = \frac{VE}{X} \sin\left(\theta_V - \theta_E\right) \quad (2.1)$$

$$Q = \frac{V^2}{X} - \frac{VE}{X} \cos\left(\theta_V - \theta_E\right) \quad (2.2)$$

Where P and Q are the active and reactive power flowing between the inverter and the Microgrid. V is the voltage at the AC side of the inverter and E is the voltage at the Microgrid. Θ_V and Θ_E are the power phase angles at the AC side of Inverter and the Microgrid side respectively. X is the impedance connected in between the inverter and the Microgrid. From the equations it is observed that the active power is predominantly dependent on inverter AC side and the Microgrid power phase angle difference (power angle). Assuming that the angle difference is very small, $\sin(\Theta_V - \Theta_E) = (\Theta_V - \Theta_E)$ and $\cos(\Theta_V - \Theta_E) = 1$, then equations (2.1) and (2.2) will give:

$$V = \frac{QX}{V-E} \quad (2.3)$$

$$\Theta_V - \Theta_E = \frac{PX}{VE} \quad (2.4)$$

Thus from the above equations it can be seen that for a reference active and reactive power the Voltage and power phase angle at the inverter AC side can be controlled with respect to the Voltage and power phase angle at the Microgrid side. PQ control is shown schematically in Figure 2-4 below.

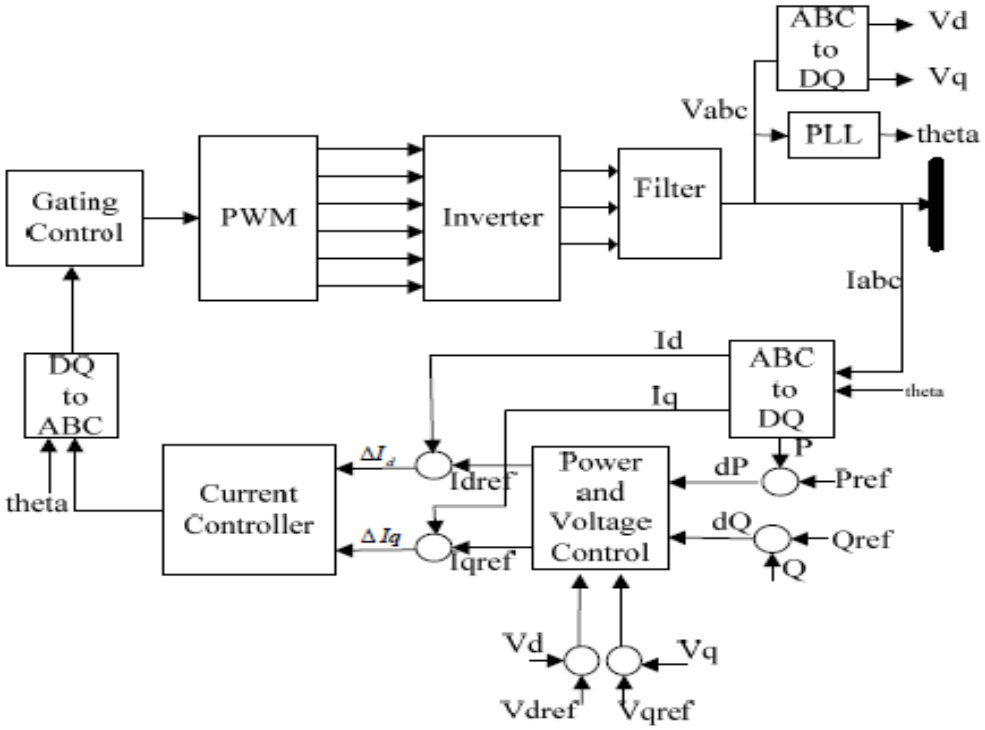

Figure 2-4: PQ control schematic [46]

To control the active and reactive output powers, the developed control system is implemented in the dq0 reference frame, i.e. Park's transformation is used to convert the three-phase voltages and currents at the grid side into the rotating reference frame components. The inverter output current components, I_d and I_q, are controlled by means of some current reference values, I_{dref} and I_{qref}, obtained from the outputs of the power control block shown in Figure 2-4. Power measurement is made at the inverter output and the powers are compared with the power reference values, P_{ref} and Q_{ref}. The difference between the output and the reference powers, dP and dQ, provides inputs to a PI controller which allows generation of the reference signals, Id_{ref} and Iq_{ref}. Thus, as comparison is made to provide the error signals which are subsequently passed through the PI controller to obtain the inverter modulating signals of the PWM. Then, by using the dq0-to-abc transformation block, the pulse signals for the inverter are obtained [46].

V/f Control

In islanded mode the distributed sources operating with PQ control strategy lose their voltage and frequency references, which were previously dictated by the main grid. The storage device which was previously being operated with a PQ control changes to V/f control. The storage device provides the power imbalance that was being supplied from the main grid to the microgrid before the islanding instant. Rest of microsources could either be operated at the same set points or may change their set points based on the supply and demand. It is assumed that the storage device has an adequate reserve to be able to provide the same power imbalance as the main grid [18]. The purpose of using V/f control is that no matter the storage unit inverter power change, the amplitude and frequency of output voltage remain the same, the inverter V/f control can provide voltage and frequency support for microgrid during islanded operation, and has certain character of following load power. Figure 2-5 illustrates the frequency and voltage droop characteristic of V/f control theory.

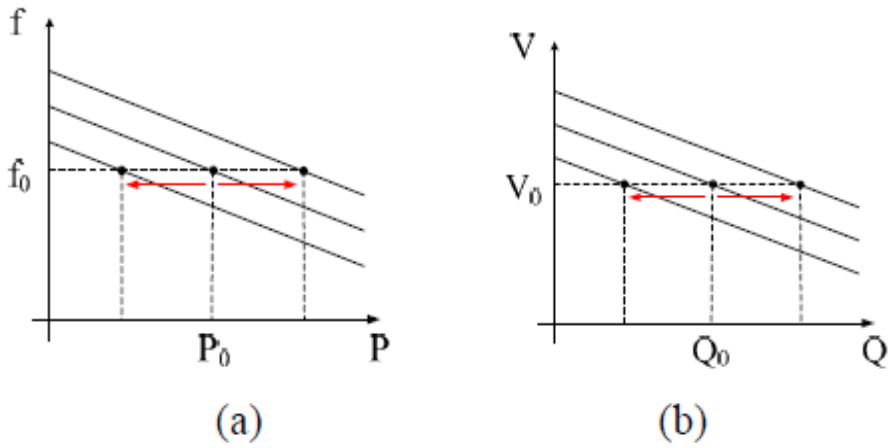

2-5: The theory of V/f control: (a) frequency droop characteristic and (b) voltage droop characteristic [3]

The schematic of V/f controller is shown in figure 2-6 below. The same inverter that connects the Storage device experiences a change in gating pulses which is now dictated by a V/f control scheme instead of the PQ control. The V/f control strategy is a tight closed loop control with the reference values of

voltage, V_0 and frequency, f_0 being the nominal values of the LV test-bed. In most cases the reference voltage and frequency levels are generated by storage units connected through dedicated PEIs.

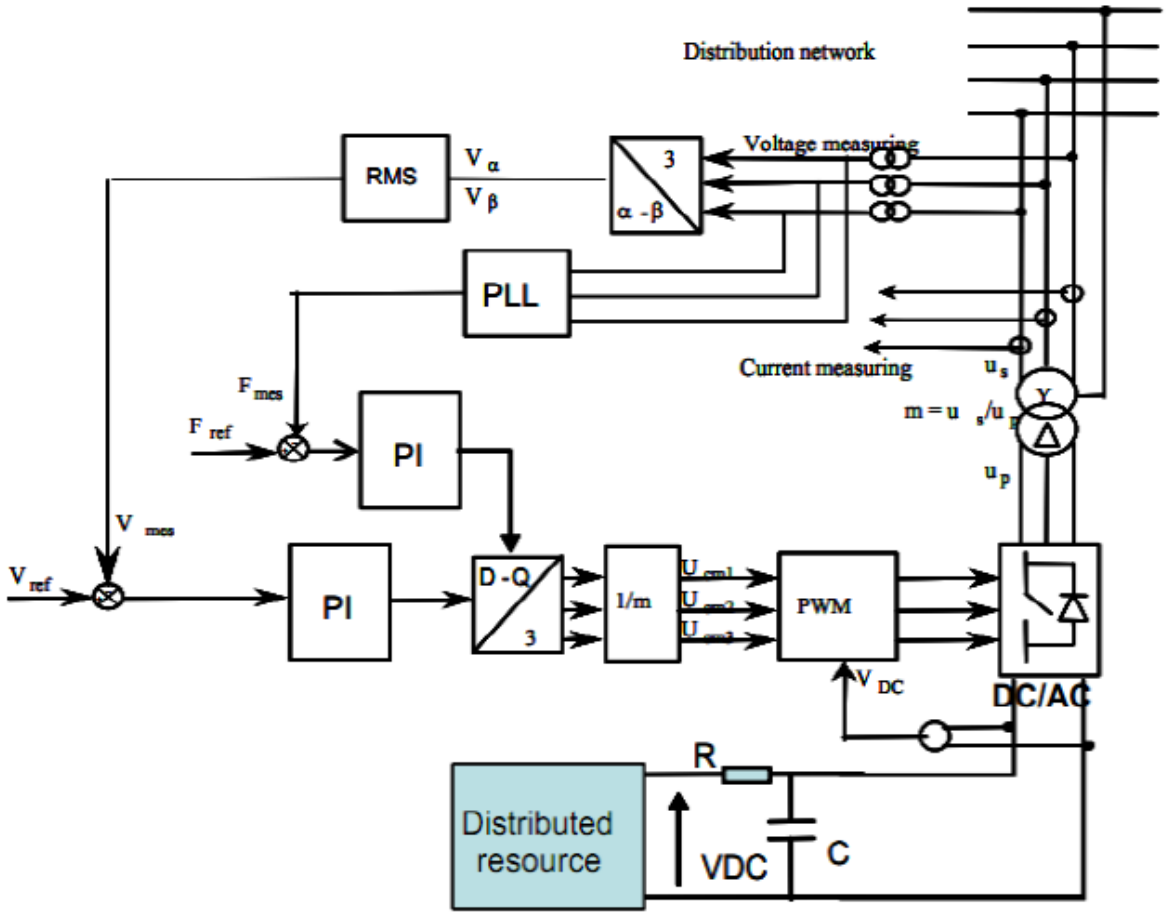

Figure 2-6: General V/f control Scheme in a Distribution Network [47]

The frequency is measured using a three-phase PLL. In the V/f control scheme two separate PI compensators are used to process the error caused by the difference of the measured value and the reference set-points and attempts to minimize the error by adjusting the process control units. The power imbalance is automatically detected by the storage system and it supplies the remaining power. Even in case of excess power generation within the islanded microgrid the storage device readily absorbs the power to charge itself. In case the power flow from the storage device exceeds its limits the battery storage would have to shut down. In case there is extra power available from controllable power sources like a reserve storage device which for example could be HEV's batteries, their power settings can be modified in order to limit

the Main storage power flow within its rated value. If all the power limits of the DG's are exceeded then load shedding of non-critical loads become inevitable. When the signal for resynchronization is given, the storage systems returns to its normal PQ control [47].

Droop control

In a complex power system, when multiple DGs are attached to the microgrid, the power sharing among them is made properly with the help of a control strategy called droop control. The role of droop control in power sharing is that it controls the real power on the basis of frequency droop control and it controls the reactive power on the basis of voltage control. The voltage and frequency can be manipulated by regulating the real and reactive power of the system. This forms a conventional droop control equation based on the equations (2.3) and (2.4) which show that the power can be controlled by regulating the real power P of a microsource, and the inverter voltage V can be controlled by regulating the its reactive power Q. Dynamically, the frequency control leads to regulate the power angle and this in turn controls the real power flow. Therefore, the frequency and voltage amplitude of the microgrid are manipulated by adjusting the real and reactive power autonomously. As a result, the frequency and voltage droop regulation can be determined as:

$$\omega = \omega_0 - m\,(P - P_0) \tag{2.5}$$

$$V = V_0 - n\,(Q - Q_0) \tag{2.6}$$

Where f, V = the frequency and voltage at a new operating point; P, Q = Active and reactive power at a new operating point; ω_0, V_0 = base frequency and voltage; P_0, Q_0= Temporary set points for the real and reactive power; m, n = P-f and Q-V droop coefficients respectively.

2.3.5. Seamless switching of Microgrid

Because there are grid connected and islanded modes of operation in a Microgrid, its inverters as a basic component unit of Microgrid must have the ability to operate steadily during two operation modes and there has to be a smooth switching between the two operation modes.

During grid-connected operation, the output voltage is forced to grid voltage. Inverter voltage and grid voltage can be synchronized by Phase Locked Loop (PLL) technology, but when Microgrid switches to islanded operation, due to lack of support of grid voltage and frequency, the inverter of PQ current mode control cannot operate alone; there must be other units with stable voltage and frequency to provide frequency and voltage support for the Microgrid. A storage system connected through power electronic converter is recommended in many literatures as a controlled voltage source which can maintain the voltage and frequency of a Microgrid in the islanding mode.

So a Microgrid should be supported by dual modes of operation so as to perform steadily in both grid-connected and islanded modes [12]. During grid connected operation it uses PQ mode of control in which voltage and frequency are maintained constant using the corresponding grid parameters as references. Microgrid and the utility are synchronized by three-phase PLL technology. During islanded operation, because Microgrid loses the support of grid, inverter must afford the regulation task of voltage and frequency. Inverters use V/f mode of control so that a Microgrid ensures continuous power supply of local load at steady voltage and frequency of the storage unit. Therefore the storage unit operating in generating constant voltage and frequency with fast response during islanding, and the V/f control strategy of microsources ensure seamless transition of a MG between the two modes of operation.

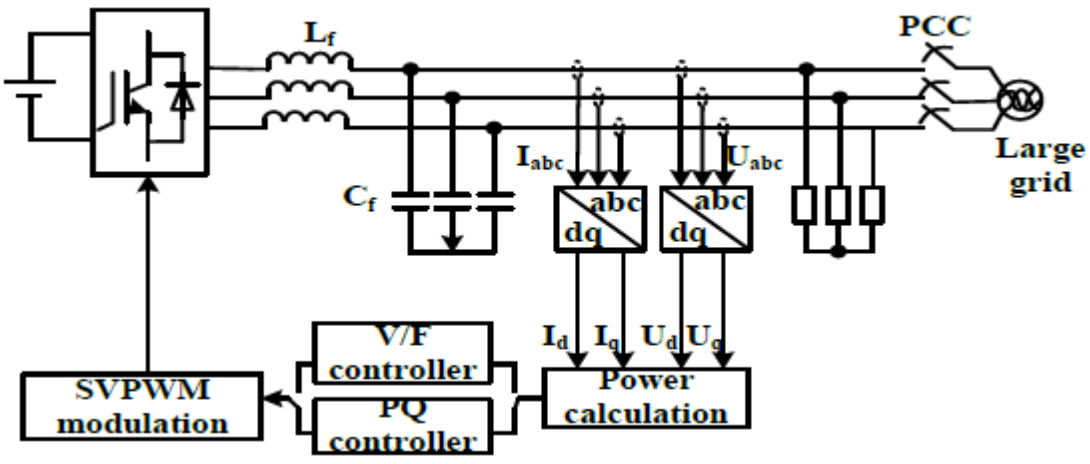

Figure 2-7: Dual mode operation inverter structure of PQ-V/f control [3].

Generally, a Microgrid needs to have PQ and V/f controllers in order to operate steadily in grid-connected and islanded states. To realize this phenomenon, the Microgrid needs to switch between the two modes of control in such a way that island detection and resynchronization mechanisms play major roles for the switching to occur between the two states. But there might be a switching failure which can make the Microgrid out of control; i.e. whenever unplanned islanding happens and if the islanding cannot be detected in time. So the remedy for these kinds of incidents not to happen is that to develop a droop controller which can operate in the two modes of control. [16] Proposes a droop control strategy in which there is voltage magnitude and frequency restoration mechanism to maintain the two parameters at their nominal values after an island is occurred so that the MG is kept stable in grid-connected and islanding modes of operation.

2.4. Power Electronic Interfaces

All of the Distributed Energy Resource (DER) technologies in a MG require specific Power Electronics Interfaces (PEI) to convert the power generated into useful power that can be directly interconnected with the utility grid. Since micro-generators can produce either DC or AC voltages, the general structure of electronically-coupled DER units consequently falls into two categories. For wind turbine, Internal Combustion Engine and microturbine generation systems, the outputs are either High Frequency AC (HFAC) or Low Frequency AC (LFAC) voltages, whereas the Photovoltaic (PV), Fuel Cell (FC) power systems and battery systems produce DC voltages. The output voltages from those energy resources are then converted by means of a power electronics converter to the voltages that are compatible to the Microgrid. Hence the type of output voltage from microsources determines the topologies of power electronics interfaces.

The power electronics interface accepts power from the distributed energy source and converts it to power at the required voltage and frequency. The design of the input converter module depends on the specific energy source or storage application. The DER systems that generate AC output, often with variable frequencies, such as wind, microturbine, IC engine, or flywheel storage

needs an AC-DC converter. For DC output systems like PV, fuel cells, or batteries, a DC-DC converter is typically needed to change the DC voltage level. The DC-AC inverter module is the most generic of the modules and converts a DC source to grid-compatible AC power. The output interface module filters the AC output from the inverter and the monitoring and control module operates the interface, containing protection for the DER and utility point-of-common-coupling (PCC). The microsources included in the proposed Microgrid with their appropriate PEIs are described in the following sub-sections.

2.4.1. PEIs for Photovoltaic

For a PV system, the voltage output is a constant DC whose magnitude depends on the configuration in which the solar cells/modules are connected. On the other hand, the current output from the PV system primarily depends on the available solar irradiance. The main requirement of power electronic interfaces for the PV systems is to convert the generated DC voltage into a suitable AC for consumer use and utility connection.

Generally, the DC voltage magnitude of the PV array is required to be boosted to a higher value by using DC-DC boost converters before converting them to the utility compatible AC. The DC-AC inverters are then utilized to convert the voltage to 50 Hz AC. The process of controlling the voltage and current output of the array must be optimized based on the weather conditions. Specialized control algorithms have been developed called maximum power point tracking (MPPT) to constantly extract the maximum amount of power from the array under varying conditions. The MPPT control process and the voltage boosting are usually implemented in the DC-DC converter, whereas the DC-AC inverter is used for grid-current control. The schematic of PEIs integrating the PV into the MG is shown below.

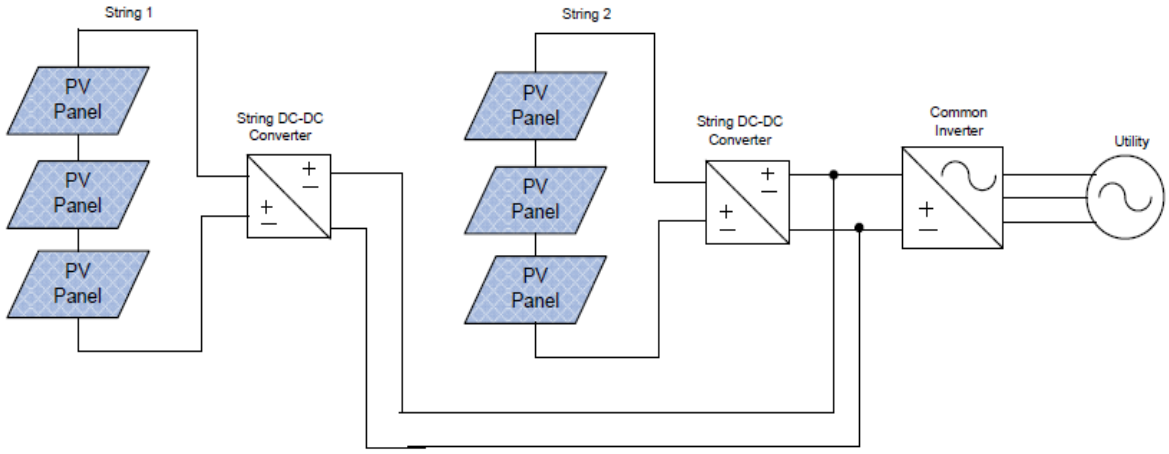

Figure 2-8: Schematic of PEIs for PV [32]

2.4.2. PEIs for SOFC

Fuel cells are similar to PV systems in that they produce DC power. Power conditioning systems, including inverters and DC-DC converters, are often required in order to supply normal customer load demand or send electricity into the grid. The simplest form of fuel system configuration consists of a fuel system stack followed by the DC-AC inverter. If the isolation or a high ratio of the voltage conversion is required, a transformer is usually integrated into the system. The main drawback for this configuration is that the low-frequency transformer placed at the output of the inverter makes the system very bulky and expensive [32].

A DC-DC converter is usually put between the fuel cell and the inverter, as shown in Figure 2-9. The DC-DC converter performs two functions: 1) it acts as the DC isolation for the inverter; and 2) it produces sufficient voltage for the inverter input so that the required magnitude of the AC voltage can be produced. The inverter can be single-phase or three-phase depending on the utility connection.

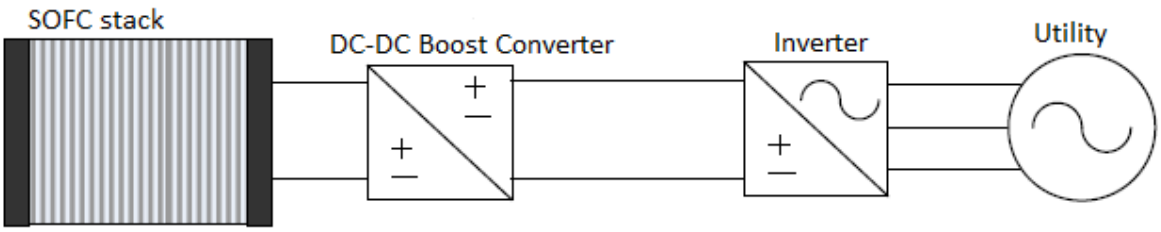

Figure 2-9: SOFC system configuration with DC-DC and DC-AC converters [32]

2.4.3. PEIs for Gas Turbine

In conventional low-speed gas turbine applications, synchronous generators have an advantage as they can be connected directly to the grid if speed is properly regulated [32]. This is generally not the case in high-speed microturbine applications. For all generator types, the generated three-phase high-frequency voltage, typically in the range of 1000 Hz to 3000 Hz, must be converted to line frequency before the generated power becomes usable for the consumers and/or for the utility.

The most common power converter topology that is used for connecting Gas Turbine to the grid is the DC-link converter. The high-frequency power from the generator must be converted to DC first either by using a diode-bridge passive rectifier or a self-commuted active rectifier. The DC-link is then used to construct three phase voltages at 50 Hz using a DC-AC inverter. Figure 2-10 shows a Gas Turbine generator feeding power to the utility by DC-link converter.

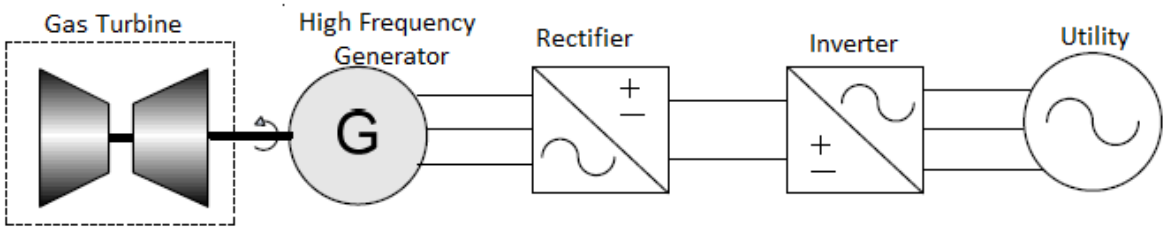

Figure 2-10: Gas Turbine with cascaded AC-DC and DC-AC converters [32]

2.5. Ancillary Devices

In the context of this study, ancillary devices are devices which provide complementary services to a MG other than PEIs, MS controller, microsources

and storage units. These devices include mainly Static Transfer switch (STS) and Phase Locked Loop (PLL). The STS is responsible for the connection and disconnection of the Microgrid from the utility network. The PLL is used to measure the frequency of the microsources when the MG is in grid-connected so that synchronization with the utility can be realized.

2.5.1. Static Transfer Switch

In standard MG like that of Consortium for Electric Reliability Technology Solutions (CERTS) the Static Transfer Switch has the task of disconnecting all the sensitive loads from the grid once the quality of power delivered starts deteriorating. The static switch does not disconnect the local system from the grid, but it disconnects only the sensitive loads. The basic feature of the STS is the possibility of rapidly switching the power supply to the load between two alternative energy sources (utility and MG), to avoid even temporary interruptions in the power supplied to the load. The two sources, at the STS inputs, are different and completely independent of one another. As illustrated in Figure 2-11, the STS block diagram is very simple: the switching units at both inputs consist of pairs of anti-parallel SCRs (static switches). However, this simple power structure is managed by a complex control which must cope with and manage many different operating conditions.

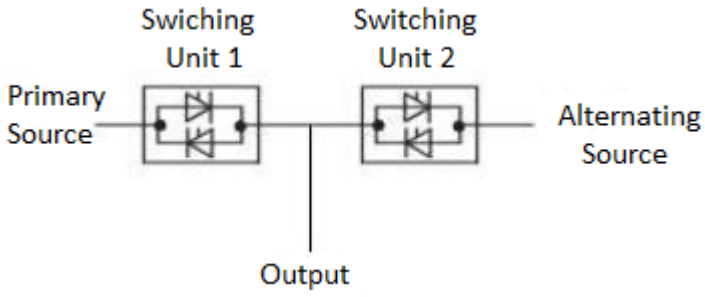

Figure 2-11: STS basic structure [45]

There are two main reasons to adopt a static switch to implement the connection and disconnection from the grid: first a static switch does not have mechanical moving parts, therefore its operating life will be extensively elongated compared to a traditional contactor with moving parts [4]. The second reason to use a dedicated switch is because during reconnection with

the grid a complex series of synchronization checks need to be performed. A normal interrupting breaker would be able to perform the function of disconnecting to the grid, but a sophisticated static switch is required to properly reconnect to the utility system without creating hazardous electrical transients across the Microgrid.

The static switch plays a key role in the interface between the Microgrid and the utility system. This device needs to be controlled by a logic that verifies some constraints at the terminals of the switch before allowing for synchronization. The same logic applies to the circuitry that controls the action of the contactor, the device used to physically connect a microsource to the feeder. Disconnection at the static switch is regulated differently than at the contactor. According to [4] disconnection at the static switch takes place because of deterioration of quality of electric power delivery from the utility system. More in particular, there are at least five conditions that will enable the disconnection logic and command the transfer to intentional island:

I. Poor voltage quality from the utility, like unbalances due to nearby asymmetrical loads,
II. Frequency of the utility falls below a threshold, indicating lack of generation on the utility side,
III. Voltage dips that last longer than the local sensitive loads can tolerate,
IV. Faults in the system that keep a sustained high current injection from the grid,
V. Any current that is detected flowing from the microgrid to the utility system for a certain period of time.

Synchronization conditions are detected by verifying two constraints: the first is that the voltage across the switch has to be very small (ideally zero), and the second is that the resulting current after the switch is closed must be inbound from the utility system towards the microgrid. The second condition needs to be re-spelled for the case of a contactor connecting two microsources in island mode: in this scenario the resulting current must always be from the highest frequency source to the lower one (which is by the way the same constraint that is enforced when connecting to the grid).

2.5.2. Phase Locked Loop

Phase Locked Loop (PLL) is a vital part of a grid-connected MG as it is used to synchronize the phase angle and frequency of the connected MG with the grid in reference with the values at the PCC [48]. PLL is a negative feedback system mainly consisting of a phase detector, a loop filter and a voltage controlled oscillator (VCO) as shown in figure 2-12 below.

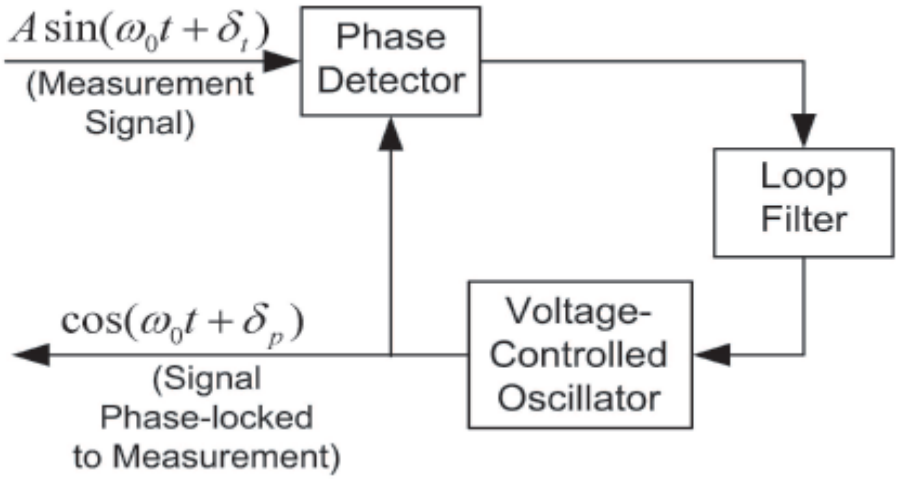

Figure 2-12: Component parts of PLL [48]

A phase detector is utilized to compare the input and VCO in order to change its frequency in reference to the phase error. Through negative feedback process, the phase difference of utility voltage vector and a voltage reference frame input can be reduced. A block diagram of PLL used in a three phase system is shown in figure 2-13 below.

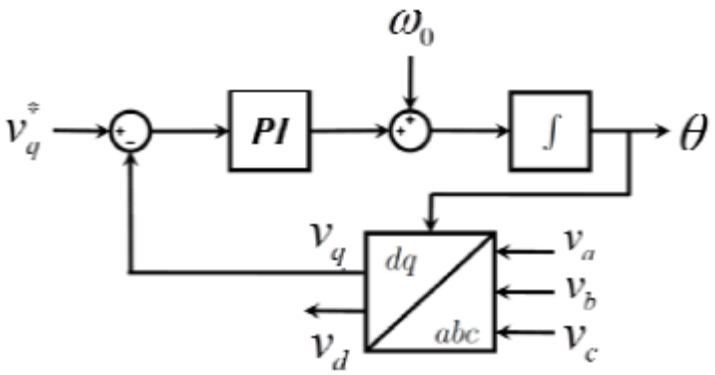

Figure 2-13: Block diagram of PLL in three phase system [39]

From figure 2-13, the phase detector compares the voltage reference frame v_q^* and the vector of three phase voltage, v_a, v_b, v_c, are transformed in dq frame. Difference between v_q and v_q^* is sent to Proportional Integral (PI) controller to produce angular speed values that will be compared with the actual angular speed, ω_0. The difference in angular speed will be integrated into phase angle, Θ, which is assigned to the VCO in order to change its frequency in a way that reduces the phase error. This process will eventually synchronize the three phase voltage with the reference frame [39].

CHAPTER THREE

Microsources

3.1. Introduction

The microsources of the MicroGrid which is the subject of this study are intended to be that of Photovoltaics (PV) and Integrated Solid Oxide Fuel Cell Gas Turbine (ISOFC/GT). A brief overview of these microsources is presented in this chapter. In ISOFC/GT, the microsource is mainly considered to be the SOFC as the gas turbine operates with the high temperature exhaust gas from the SOFC. As the gas turbine is cascaded with the SOFC to enhance its electrical efficiency, it is possible to consider the two units as one microsource. So, relatively wide coverage is given to the SOFC together with the Photovoltaic.

3.2. Photovoltaics

3.2.1. Basics of Photovoltaics

A photovoltaic cell converts sunlight into electricity and each cell generates a few watts of electricity. A photovoltaic panel or module is a collection of cells and typically cells are connected in series to increases the output voltage and the output power [6]. The output power of a panel varies from 40 W to 300 W [6]. In most applications, a number of panels are connected in series or parallel to increase the output power. Such a system is known as photovoltaic array. The performance of photovoltaic panel is presented under special conditions known as Standard Test Conditions (STC). A panel is said to be tested under standard test conditions, if a) the panel is tested at 25°C, b) the incident irradiance is 1000W/m^2 and c) the air mass (AM) is 1.5 [6]. Air Mass represents the angle between the sun light and zenith as shown in Figure 3-1 [6]. On the earth's surface the air mass varies but it is typically around 1.5 thus this value is selected for the standard test conditions [6].

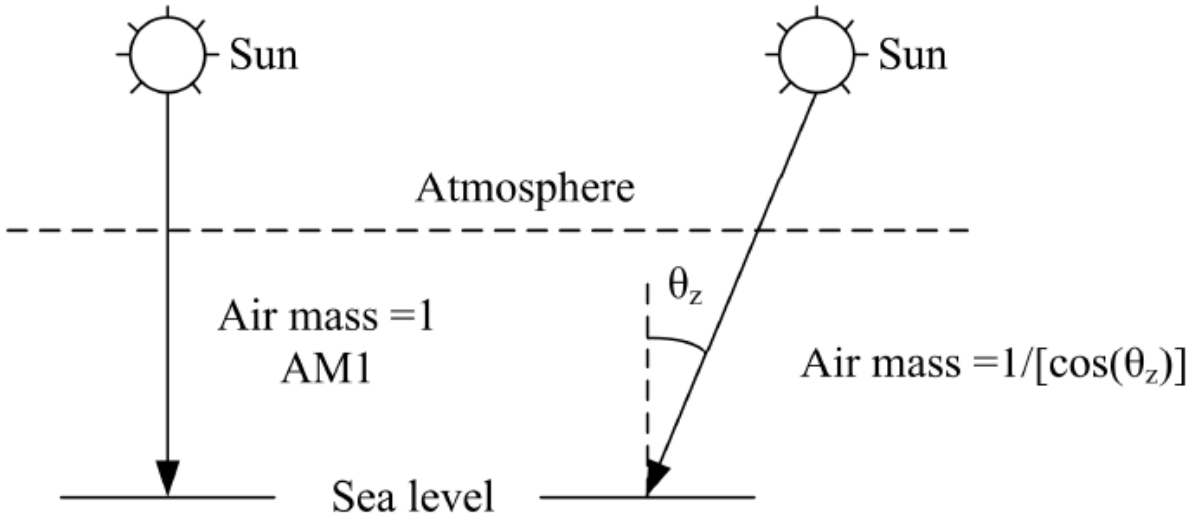

Figure 3-1: Air mass depending on the sunlight path [6]

3.2.2. Types of Photovoltaic Cells

The major cell types are crystalline silicon and thin film cells. At present the highest market share belongs to crystalline silicon cells which are manufactured from very small slices of silicon wafers [6]. These are further divided into two categories: mono and multi crystalline cells. The efficiency of a crystalline cell is around 14-17% while the efficiency of a module is around 12-15% [6]. The commercial thin film cells are based on amorphous silicon (a-Si), copper indium diselenide (CIS) and cadmium telluride (CdTe) [6]. These photosensitive materials are coated on a low cost material such as glass or plastic. Efficiency of thin film based cells varies between 6 and 11%. Thin film panels are cheaper than crystalline silicon panels. However to generate the same output power, more thin film panels are required when compared with crystalline silicon panels.

The efficiency of concentrator cells is about 30% [6]. This cell type generates more electrical power from fewer cells. A disadvantage of this method is that electricity is only produced from direct sunlight. Heat generation and expensive concentrating optics are challenges for concentrator cells. Bifacial photovoltaic cells generate electricity from the back side as well as the front side of the cell. Typically the front side is oriented directly to the light and the back side generates power from the light reflected from surroundings.

Efficiency of a bifacial cell is increased by 5 to 20% comparing with conventional cell, without increasing the cost significantly.

3.2.3. Electrical models of a photovoltaic cell

Figure 3-2 presents some of the electrical models of a photovoltaic cell which could be found in literature [6]. The simplest model contains a current source and a diode which is connected anti-parallel to the current source. The model presented in Figure 3-2(b) contains a resistor in series at the output which represents the electrical losses of the cell. A more complex model contains a resistor in parallel to the current source and a resistor in series with the output as shown in Figure 3-2(c). The model shown in Figure 3-2(d) consists of two anti-parallel diodes [6]. Characteristics of each diode are slightly different, thus better curve fitting could be achieved with this model.

Equation 3-1 gives the characteristic equation of a photovoltaic cell for the model shown in Figure 3-2 (b) where $I_{pv,}$ I_{ph}, I_{sat}, V_{pv}, R_s and V_t represent the PV panel current, the photocurrent, the diode saturation current, the PV panel voltage, the series resistance and the thermal voltage respectively.

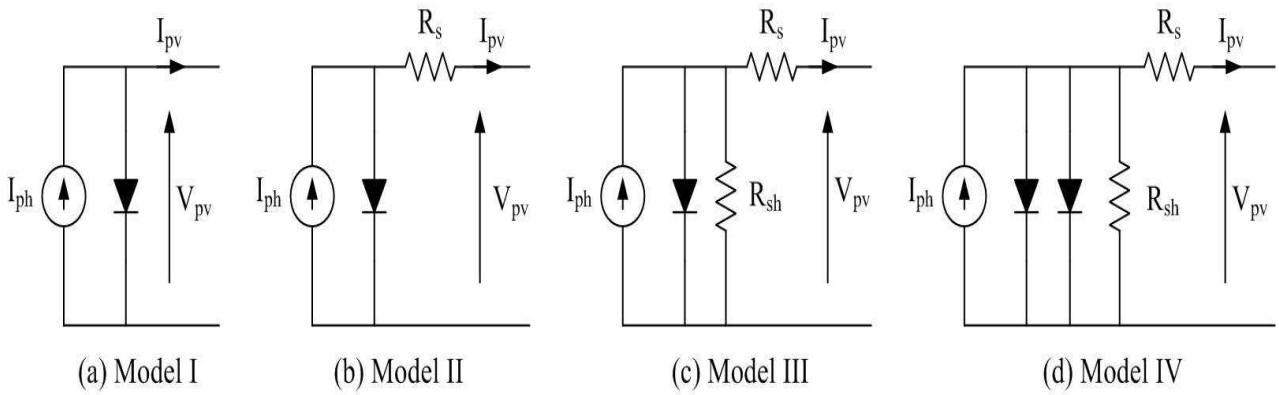

Figure 3-2: Electrical models of a photovoltaic cell [6]

$$I_{PV} = I_{ph} - I_{sa}[exp[\frac{V_{PV}+I_{PV}R_s}{V_t}]-1] \quad (3.1)$$

$$V_t = \frac{AkT}{q} \quad (3.2)$$

The thermal voltage is related to the ideality factor (A), the Boltzmann constant (k), the temperature (T) and the charge of an electron (q) as given in Equation 3-2 [6]. The ideality factor is a constant which depends on the material of the cell and typically it varies between one and two [6].

3.2.4. Dependent parameters of Photovoltaic panel

The output power of a photovoltaic panel depends on the environmental temperature and the irradiance incident on the panel [6]. Figure 3-3 highlights the effect of temperature and irradiance on the characteristic curves of SM110-24P photovoltaic panel [6]. Irradiance affects the short circuit current as well as the open circuit voltage. However, the effect on the short circuit current is more significant than that on the open circuit voltage. The output power at the maximum power point increases as the irradiance increases. Temperature affects the open circuit voltage of the panel and the open circuit voltage decreases due to an increase in temperature.

Equation 3-3 and Equation 3-4 present the relationship of temperature and irradiance with the short circuit current and the open circuit voltage G_a, I_{sc}, T, V_{oc}, ΔI_{sc} and ΔV_{oc} represent the irradiance, the short circuit current, the temperature, the open circuit voltage, the temperature coefficient of the short circuit current and the temperature coefficient of the open circuit voltage respectively. Constants with an additional letter‘s’ correspond to the values at standard test conditions.

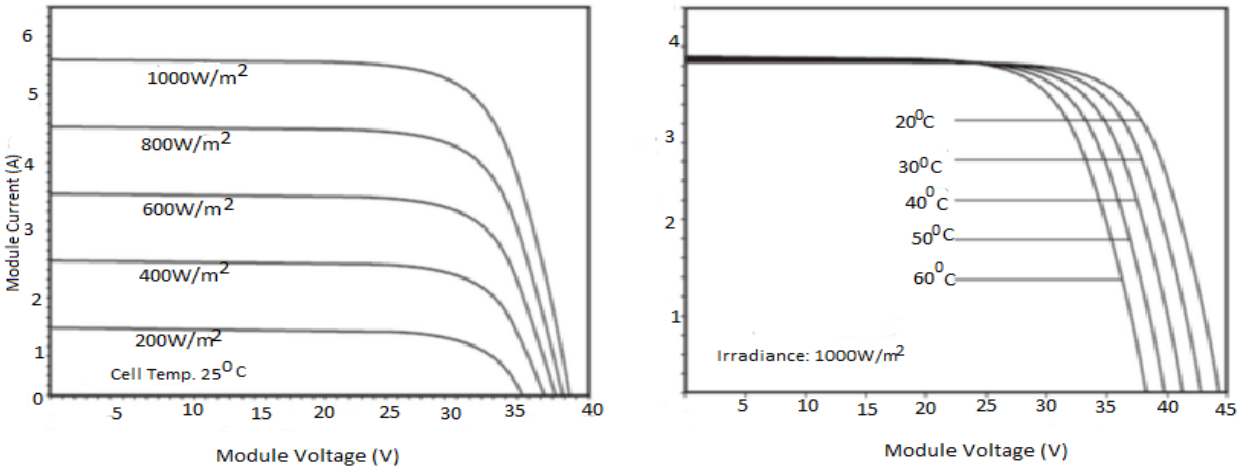

a) Irradiance b) Temperature

Figure 3-3: The effect of environmental conditions on PV characteristic curves [6]

$$I_{sc} = \frac{G_a}{G_{as}} [I_{scs} + \Delta I_{sc}(T - T_s)] \quad (3.3)$$

$$V_{oc} = V_{ocs} + \Delta V_{oc}(T - T_s) + \ln\left(\frac{I_{sc}}{I_{scs}}\right) \quad (3.4)$$

3.2.5. Maximum Power Point Tracking methods

The characteristic curve of a photovoltaic panel, as indicated in figure 3.4, shows that the panel should operate at the Maximum power point (MPP) to extract the maximum available power. Maximum Power Point Tracker (MPPT) is the device used to track the maximum power point.

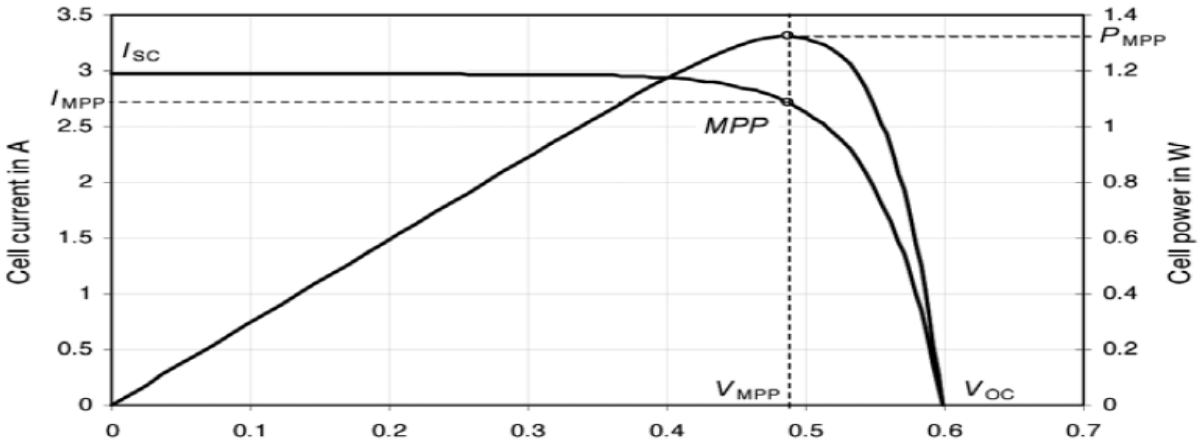

Figure 3-4: I-V and P-V Solar Cell Characteristics with MPP [54]

Almost all the PV panels are connected through power electronic converters. A converter is associated with a controller and the controller makes sure that the converter is operating at a given reference voltage. In a photovoltaic system, MPPT generates the reference voltage applied to the controller of the converter.

The simplest MPPT generates a predefined voltage reference which is the voltage at maximum power point corresponding to a particular environmental condition [54]. This would be the cheapest MPPT as it neither requires any sensor nor needs to perform complex calculations. The voltage reference does not change dynamically. Thus the panel would not operate at the MPP all the time, which is the main drawback of this method.

The voltage at the maximum power point is approximately equal to 70-80% of the open circuit voltage while the current at the maximum power point is approximately equal to 90% of the short circuit current [54]. There are MPPTs built based on these two factors and such a MPPT requires either a current sensor or a voltage sensor. A voltage sensor is typically cheaper than a current sensor therefore a MPPT based on the open circuit voltage would be cheaper than a MPPT based on the short circuit current. The open circuit voltage and the short circuit current are measured periodically in respective MPPT methods. This process disrupts the continuous power flow. Authors in [54] have indicated that some systems proposed a pilot cell to measure the open circuit voltage for MPPTs based on open circuit voltage. Both of these MPPTs are better than the previous method as dynamic tracking is available.

3.3. Fuel Cell

3.3.1. Fuel Cell basics

Fuel cells (FCs) are devices that utilize an electrochemical process to convert chemical energy of a fuel into electrical energy. This electrical energy can be used to power vehicles, electronic devices, houses, or be delivered to an electrical grid. Over the last few decades increased attention has been given to fuel cell technology due to its high efficiency and clean processes. Unlike a battery that stores energy, a fuel cell converts chemical energy of its input fuel

into electrical energy without the use of stored materials within its structure. Fuel cells also differ from conventional heat engines in that they produce electricity directly from chemical energy without an intermediate conversion into mechanical power [56]. When hydrogen is used as fuel, the only by-products of the fuel cell operation are water and heat.

Fuel cells are static energy conversion devices that convert the chemical energy of fuel directly into DC electrical energy. The physical structure of a fuel cell consists of two porous electrodes (anode and cathode) and an electrolyte layer in the middle. Figure 3.5 shows the basic workings of a fuel cell with positive ion flow through the electrolyte. Hydrogen and oxygen molecules combine to form water. The process is caused by the fact that charged particles migrate toward regions of lower electrochemical energy. The charged hydrogen and oxygen particles move toward each other and bond to one another because the final product of this reaction has a lower overall electrochemical energy.

Electrical energy is generated as a result of the movement of the charged hydrogen and oxygen particles, which is essentially the controlled movement of electrons.

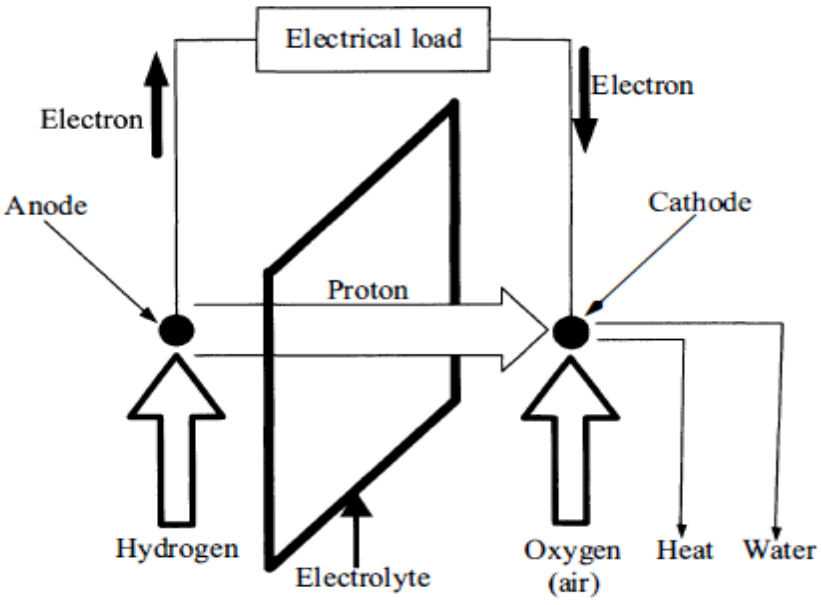

Figure 3-5: The basic workings of a fuel cell with proton flow through the electrolyte. [55]

The actual chemical reaction inside a hydrogen fuel cell can be broken down into two half reactions, the oxidation half reaction and the reduction half reaction. The oxidation half reaction, represented by (3.5), shows the dissociation of hydrogen molecules to protons and electrons at the anode. After the dissociation, the protons are free and pass through the electrolyte, and recombine with the electrons (which move through the external circuit) at the cathode. In this process, which is often called the reduction half reaction, the electrons and hydrogen protons combine with the oxygen molecules from the surrounding air, according to (3.6), to form water.

$$2H_2 \rightarrow 4H^+ 4e^- \quad (3.5)$$

$$O_2 + 4H^+ + 4e^- \rightarrow 2H_2O \quad (3.6)$$

The type and chemical properties of the electrolyte used in fuel cells determine their operating characteristics and internal operating temperature. The polarity of an ion and its transport direction can differ for different fuel cells, determining the site of water production and removal. If the working ion is positive, like shown in Figure 3-5, then water is produced at the cathode. On the contrary, if the working ion is negative, like in solid oxide fuel cell, water is formed at the anode. In both cases electrons pass through an external circuit and produce electric current.

3.3.2. Types of Fuel Cells

Fuel cells are generally classified by the type of electrolyte they use, and the choice of electrolyte dictates the range of their operating temperature and the degree of fuel processing required [56]. Low-temperature fuel cells are generally limited to temperatures below or around 200°C because high-temperature vapour causes rapid degradation of their electrolyte material. The most common type of low-temperature fuel cells are Alkaline Fuel Cell (AFC), Phosphoric Acid Fuel Cell (PAFC), and Polymer Electrolyte Membrane Fuel Cell (PEMFC). In these fuel cells all the fuel must be converted to hydrogen prior to entering the fuel cell. In addition, the catalyst used in these fuel cells (mainly platinum) is strongly poisoned by carbon monoxide (CO). Therefore, the hydrogen entering these fuel cells needs to be pure. This is a downside of the low-temperature fuel cells.

In high-temperature fuel cells, CO and even hydrocarbons (e.g., CH_4) can be internally converted to hydrogen or even directly oxidized [27]. The most common types of high-temperature fuel cells are Molten Carbonate Fuel Cell (MCFC) with operating temperature range of 600-700°C, and solid oxide fuel cell (SOFC) operating in the temperature range of 600-1000° C.

In addition to the above types of fuel cells, there is another category of fuel cells, which can utilize non-hydrogen fuels directly without internal or external reforming process. Two common types in this category are Direct Methanol Fuel Fell (DMFC) and Direct Carbon Fuel Cell (DCFC). DMFC, also called Direct Alcohol Fuel Cell (DAFC), is a low-temperature polymer electrolyte fuel cell, which uses alcohol as fuel without reforming. Its application is mainly in low power portable electronics. DCFC uses carbon (as fuel) directly in the anode, without an intermediate gasification step. The carbon can be derived from coal, biomass or pet-coke. Among the different types of fuel cells, PEMFC, MCFC, and SOFC are most likely to be used for distributed generation (DG) applications.

3.3.3. Solid Oxide Fuel Cell

SOFCs are high temperature fuel cells operating at 600-1000°C [56]. They use a solid (ceramic-type metal oxide) electrolyte, usually dense yttria-stabilized zirconia (Y_2O_3 stabilized with ZrO_2). This material is an excellent conductor of negatively charged ions (O^{2-} in the case of SOFC) at high temperatures. The anode (fuel electrode) is typically made of a cement type material, a mixture of cobalt or nickel and zirconium oxide (CO-ZrO_2 or Ni-ZrO_2). The metal (Co or Ni) provides good conductivity and the entire cement mixture provides negative ion conductivity. The cathode (air electrode) is made of a mixture of ion and electronically conducting ceramic, typically strontium-doped lanthanum manganite (Sr-doped $LaMnO_3$).

SOFCs can use hydrogen as well as hydrocarbon gases as fuel, which can be obtained from readily available fuels like natural gas or methane. The schematic diagram of a SOFC is given in Fig. 3.6. When hydrogen is used as fuel, the chemical reactions in SOFCs (also shown at the anode and cathode in Fig. 3.6) are as follows, where water is produced at the anode, as opposed to PEMFC, where water is produced at the cathode.

$$H_2 + O^{2-} \rightarrow H_2O + 2e^- \text{ (anode reaction)} \quad 3.7$$

$$O_2 + 4e^- \rightarrow 2O^{2-} \quad \text{(cathode reaction)} \quad 3.8$$

$$2H_2 + O_2 \rightarrow 2H_2O \quad \text{(overall reaction)} \quad 3.9$$

SOFCs' high operating temperature makes them highly efficient (with efficiencies as high as 60%) and fuel flexible, and gives them the ability to use a wide variety of less expensive catalysts. This is because the chemical bonds of materials break at a much faster rate as temperature increases. The high-temperature operation also makes SOFCs attractive for combined heat and power (CHP) applications, producing electricity and/or heat, as in the case of hybrid system of SOFC/GT, with overall efficiencies as high as 75-80% [56].

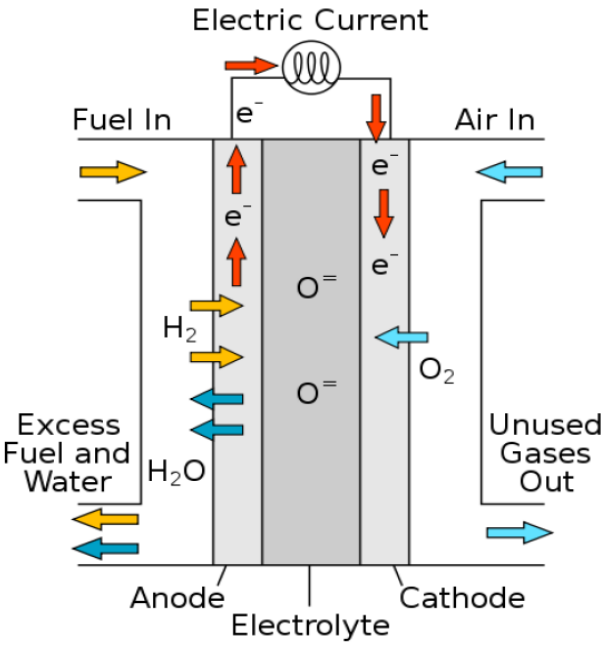

Figure 3-6: Schematic diagram of Solid Oxide Fuel Cell [56]

SOFCs have both a slow start up and thermal stresses due to their high operating temperature. However, they allow for internal reforming of gaseous fuel, which gives multi-fuel capability to SOFCs. Moreover, their solid electrolyte simplifies system design since the corrosion and management

problems related to liquid electrolyte are eliminated. These merits give SOFCs a high potential to be used in stationary applications.

In summary, the advantages of SOFC are fuel flexibility, inexpensive catalyst, solid electrolyte, and the availability of waste heat for CHP operation. Its disadvantages are operation at very high temperature, which leads to sealing issues.

3.3.4. Connecting individual SOFCs

Individual cells are linked with an inter-connect (typically a ferric stainless steel) in electrical series to increase voltage and power, forming a stack. As shown in Figure 3-7 below, the inter-connect electrically connects the anode of one cell (the lower cell in Figure 3-7) in series with the cathode of the adjacent, or upper cell in this illustration. This stacking arrangement forms the fuel channel for the lower cell and the air channels for the upper cell. Cells can be stacked in this manner until an optimal stack size is achieved. A number of stacks can then be arrayed in series and/or parallel to form an SOFC module. The size of the module to be developed depends on the capacity required and design limitation as to the number of stacks to be arranged to make a module [FC].

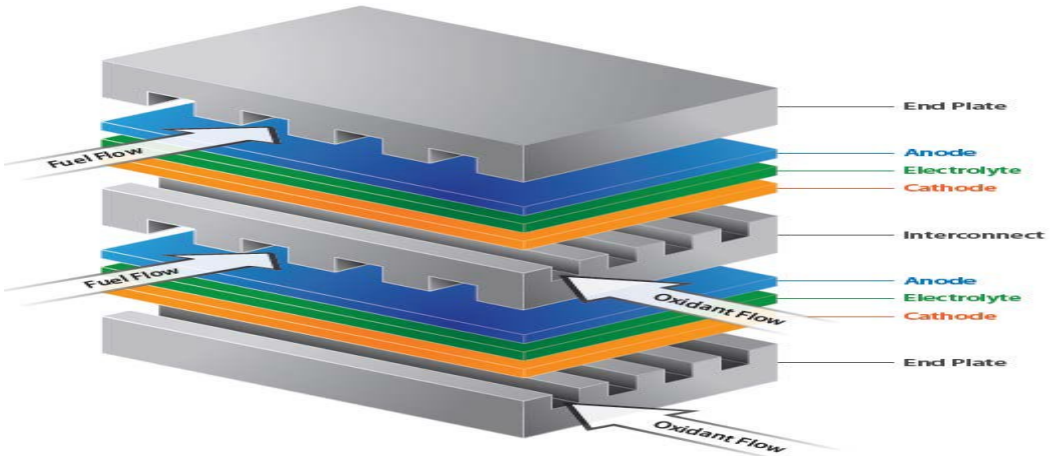

Figure 3-7: Planar SOFC (two cell array) [55]

3.3.5. Dynamic modelling of SOFC

As explained earlier the overall reaction in Solid oxide Fuel Cell is:

$$2H_2 + O_2 \rightarrow 2H_2O\ (g)$$

According to Nernst equation, the reverse potential of an individual SOFC is calculated as:

$$E_{cell} = E_{0,cell} + \frac{RT}{4F} \ln\left[\frac{(p_{H_2}^{ch})^2 \cdot p_{O_2}^{ch}}{(p_{H_2O}^{ch})^2}\right] \quad (3.10)$$

Where;

E_{cell} = SOFC open circuit voltage

$E_{O,\,cell}$ = SOFC standard reference potential

R = Universal gas constant

F = Faraday constant

T = Stack temperature

$P_{H_2}^{ch}$, $P_{O_2}^{ch}$ and $P_{H_2O}^{ch}$ are effective partial pressures of H_2, O_2 and H_2O in their respective channel respectively.

E_{cell}, calculated from (3-10), is the SOFC open-circuit voltage, which is both temperature and pressure dependent. When the fuel cell is under load, its output voltage is less than E_{cell} due to activation loss, ohmic resistance voltage drop and concentration overpotential. The SOFC output voltage can therefore be written as:

$$V_{cell} = E_{cell} - V_{act,\,cell} - V_{ohm,\,cell} - V_{conc,\,cell} \quad (3.11)$$

Where $V_{act,\,cell}$, $V_{ohm,\,cell}$ and $V_{conc,\,cell}$ are activation, ohmic and concentration voltage drops respectively.

The output voltage of the individual N cells connected in series can be lumped together to obtain the output voltage of a SOFC stack as follows:

$$V_{out} = N_{cell}V_{cell} = E - V_{act} - V_{ohm} - V_{conc} \quad (3.12)$$

The SOFC stack output voltage can therefore be calculated, once the voltage drops are calculated.

3.3.6. Steady state characteristics of SOFC

The steady-state terminal voltage versus current (V-I) characteristic curves of the SOFC stack model at different temperatures are shown in Fig. 3-8. In the low-current region, a voltage drop results due to an activation energy barrier that must be overcome before the chemical reaction starts inside SOFC. This voltage drop, called the SOFC activation voltage drop, dominates the total SOFC voltage drop at low currents.

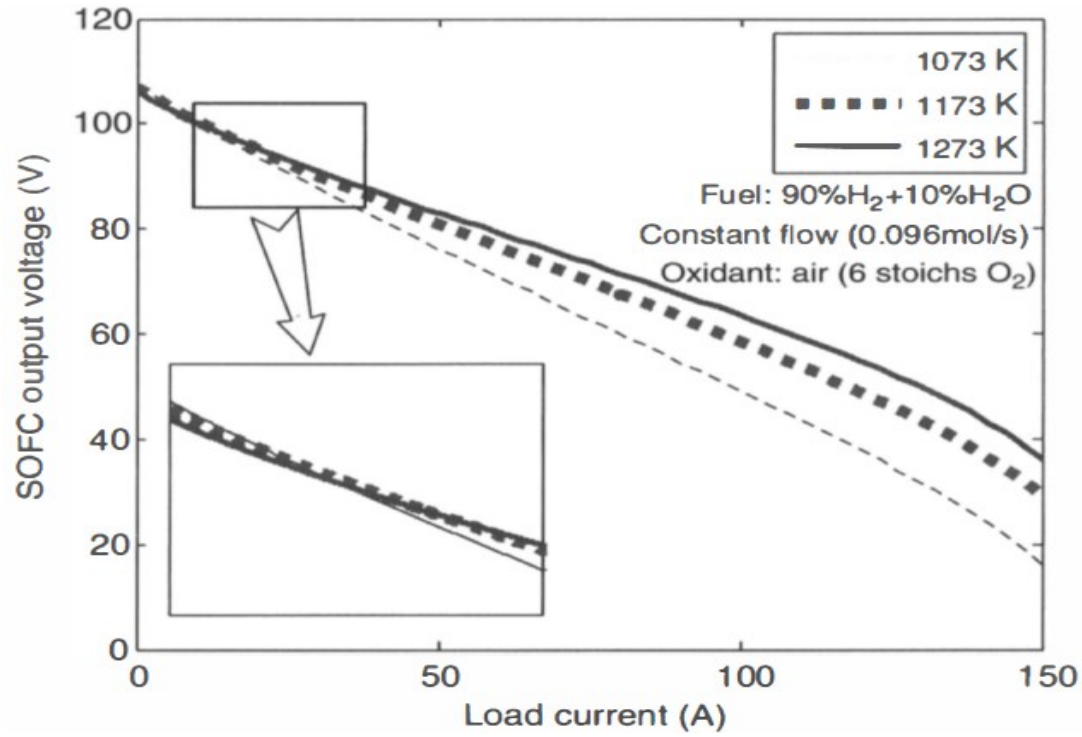

Figure 3-8: V-I characteristics of the SOFC model at different temperatures [57]

When the load current exceeds a certain (theoretical maximum) value, the SOFC output voltage and power delivering capability will drop sharply due to large ohmic and concentration voltage drops.

The output power versus current (P-I) curves of the model at different temperatures are shown in Fig.3.9. At higher load currents, higher output power can be achieved at higher operating temperatures. Under each operating temperature, there is a critical current, where the model output power reaches its maximum value.

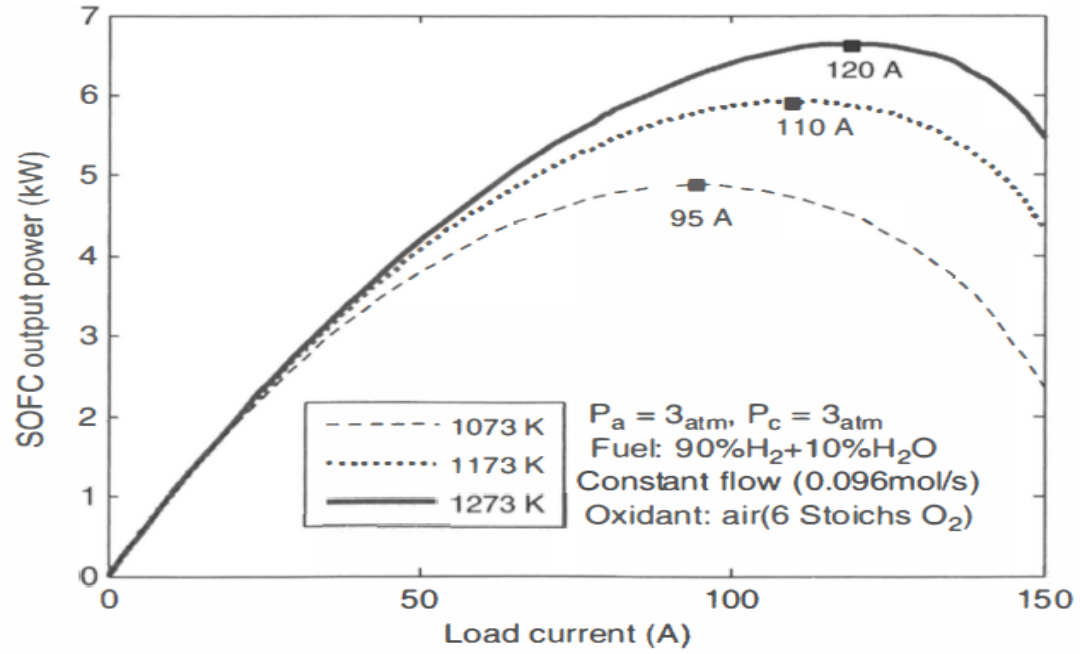

Figure 3-9: P-I characteristics of the SOFC stack model at different temperatures [57]

3.3.7. Integrated SOFC/GT system

The SOFC stack and GT can be integrated into a number of combinations of Integrated Fuel Cell Gas Turbine (IFCGT) power plants [26]. The basic idea is to combine them in such a way that the high temperature of the fuel cell exhaust gas is exploited to run the gas turbine. This can be accomplished using heat exchangers to transfer energy from one stream to another. One of the possible configurations used to establish Integrated SOFC/GT system is the one which applies Bryton cycle is demonstrated in the figure below.

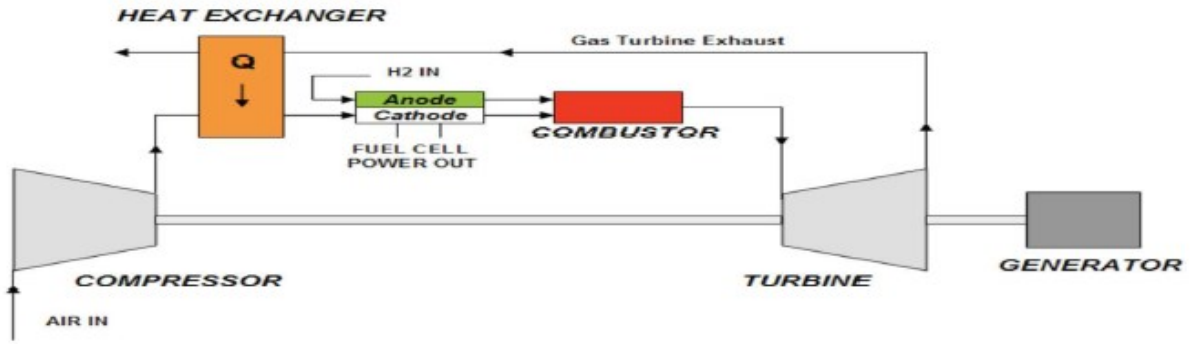

Figure 3-10: Main components of Integrated SOFC/GT (ISOFC/GT) system [56]

According to the above simplified layout of Integrated SOFC/GT system, external air is compressed approximately up to the SOFC operating pressure first. Then, air is preheated by the recuperative heat exchanger and enters the cathode compartment of the SOFC stack, where it participates in the electrochemical reaction. On the other side, fuel is compressed up to the SOFC operating pressure by the fuel compressor. Then, after possible preheating, the fuel enters the anode compartment of the fuel cell. Here, it is first reformed into a H_2-rich mixture and subsequently participates in the electrochemical reaction, producing electricity. Unreacted fuel and cathode exhaust air are burnt into the combustor, increasing the outlet temperature of the resulting stream. Such flow expands in the gas turbine, driving simultaneously the air compressor and the electrical generator, and producing additional power. Turbine exhaust gases are used to preheat air in the recuperative heat exchanger; finally, such exhausts are available for cogenerative purposes [56].

CHAPTER FOUR

Power Electronic Interface Design

4.1. Introduction

The micro-generators to be connected in the proposed Microgrid should supply their respective power through DC-AC converter (inverter).But there need be prior conversion stages using various power electronic interfaces (PEI) so as to facilitate the inversion stage to effect the required frequency and voltage level. The type of power electronic converter to be applied prior to inversion depends on the nature of the generation unit. If the generation unit produces DC power, first it has to be converted in to another appropriate DC level of a different magnitude which is regulated. This operation is performed by unidirectional DC-DC converter.

If the generation unit produces AC power before it is conditioned, the voltage has to be changed into a required level of standard frequency. For this operation to be performed, there are two standard options. The first one is to convert the AC power in to DC using a rectifier, and then into another DC voltage level using unidirectional DC-DC converter. Then the inversion process follows in similar way as in the case of the DC generator. The other option is to use an AC-AC converter so as to connect the unit directly into the grid. This option is easy but the supplied power cannot be regulated. So this study opts for the first option as it gives way to control the inverter.

4.2. DC-DC converter

Among the possible alternatives of DC-DC converters, this paper applies the boost converter with appropriate topology so that the process of inversion will be done easily. The dc-dc converter is connected to the respective microsource and the converter steps up the output voltage of the MS. This study assumes that the Photovoltaics array operates at its maximum power point and the SOFC array is also supplied with constant flow of air and fuel, so that the output DC voltage in both cases is constant in which case no regulation is required. The constant fuel and air supply of the SOFC is reflected on the

reliable production of high temperature steam which drives the GT so as to produce constant output power in its turn.

The proposed unidirectional DC-DC converter is a special type of boost converter in which stepping up of the DC input is carried out in two steps; so it is called two stage DC-DC boost converter. It has lower component count which leads to reduced losses.

4.2.1. Principle of operation of DC-DC boost converter

The schematic diagram of the elementary DC-DC boost converter is presented in Figure 4-1. The converter comprises a switch (mostly MOSFET) which operates using a pulse generator of appropriate duty cycle. When switch M_1 is closed for time t_1, the inductor current rises and energy is stored in it. If the switch is opened for time t_2, the energy stored in the inductor is transferred to the load through diode D_m and the inductor current falls. The input current now flows through L, C, load, and diode D_m. So the converter operates in two modes.

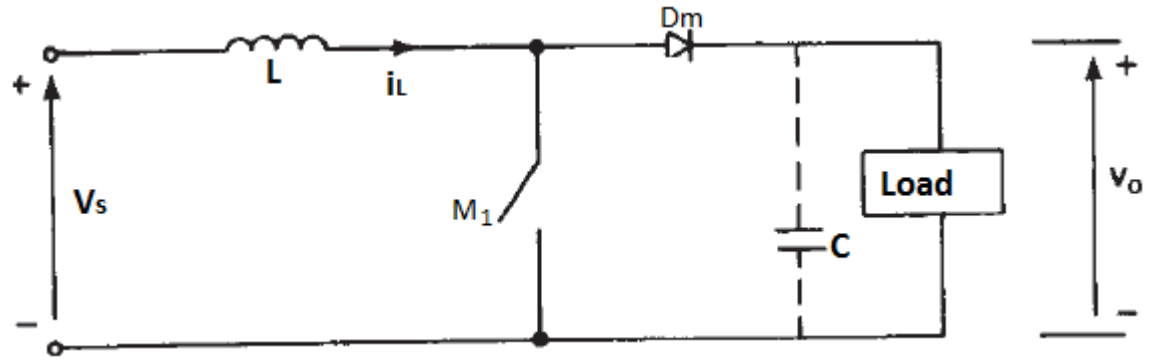

Figure 4-1: Schematic diagram of the boost DC-DC converter [29]

When the converter is turned on the voltage across the inductor is:

$$V_L = L\frac{di}{dt} \qquad (4.1)$$

And this gives peak to peak ripple current as;

$$\Delta I = \frac{V_S}{L} t_1 \qquad (4.2)$$

The instantaneous output voltage will be;

$$V_0 = V_s + L\frac{\Delta I}{t_2} = V_s\left(\frac{\Delta I}{1-K}\right) \qquad (4.3)$$

Where K is the duty cycle of the switch and t_2 the time in which it is switched off. If a large capacitor, C, is connected across the load, the output voltage will become continuous. The wave forms of the currents and voltages of the converter are shown below in figure 4-2.

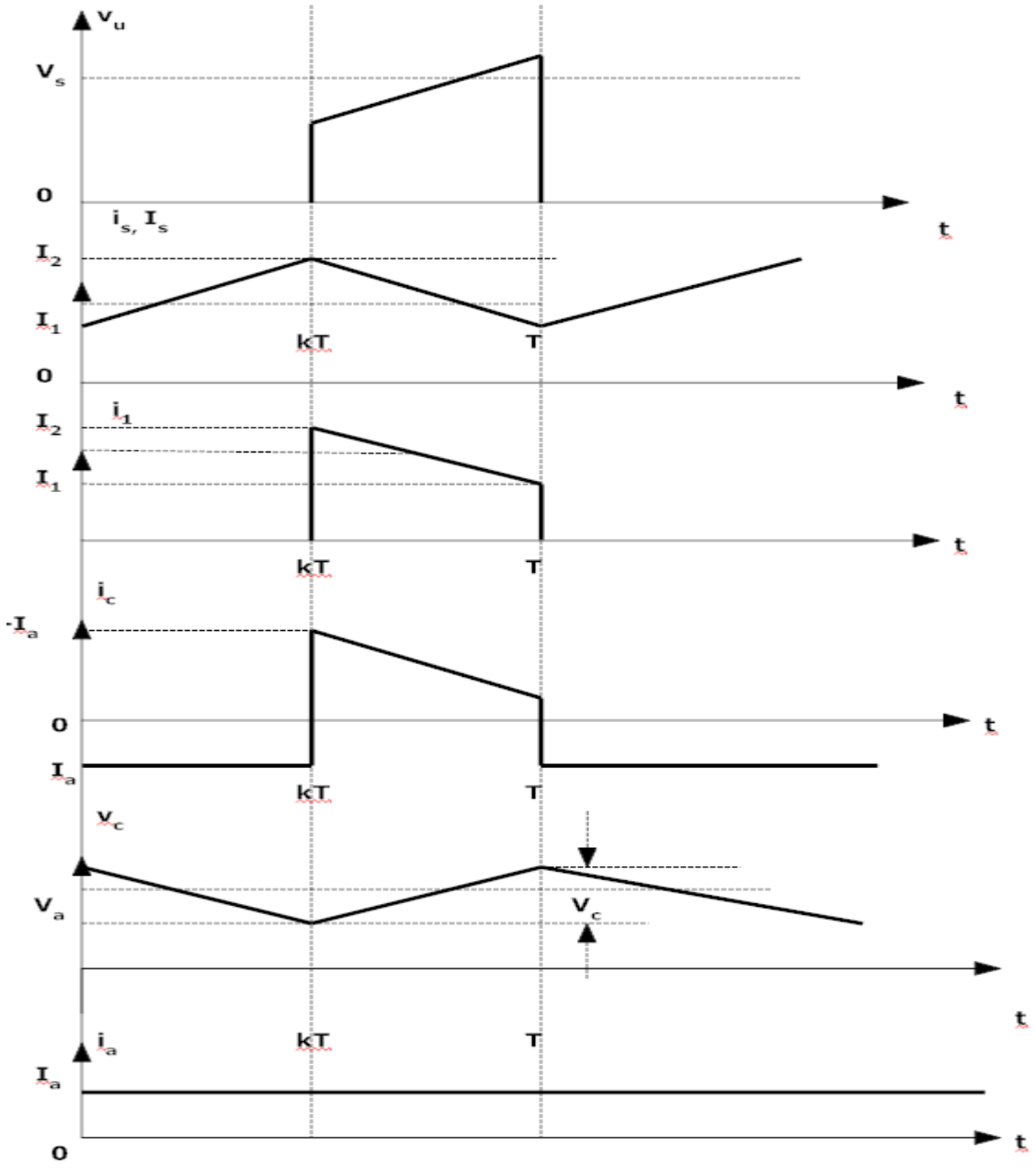

Figure 4-2: Principle of operation of the boost dc-dc converter [29]

According to [29] the duty cycle K, capacitor C size and inductor size L are calculated as:

$$K = 1 - \frac{V_S}{V_a} \quad (4.4)$$

So voltage transfer gain G can be calculated as:

$$G = \frac{1}{1-k} \quad (4.5)$$

Where V_s and V_a are input voltage and output average voltage respectively. Size of the inductor is calculated as;

$$L = \frac{V_S X\ K}{f\ X\ \Delta I} \quad (4.6)$$

Where: V_s, f and ΔI are input voltage, switching frequency and ripple inductor current, respectively. Size of the filter capacitor is calculated as;

$$C = \frac{I_a\ X\ K}{\Delta V_C\ X\ f} \quad (4.7)$$

Where I_a and ΔV_C are average output current and capacitor output ripple voltage, respectively. As can be observed from (4.6), the size of the inductor is directly proportional to the input voltage level. So the inductor will be large when we want larger output voltage. Therefore the stepping up of voltage should be done in multi-stage so that the size of the inductor we use will be reasonable. Plus in applying multi-stage DC-DC boost converter it is possible to reduce the size of the DC input further than the elementary converter. This study will consider using the two stage topology to design the boost converter which reduces the DC sources by half if the single stage would have been used.

4.2.2. Two stage boost converter

The two-stage boost circuit is derived from elementary boost converter by adding two diodes, an inductor and a capacitor. Its circuit diagram and equivalent circuits during switch-on and switch-off are shown in Figure 4-3.

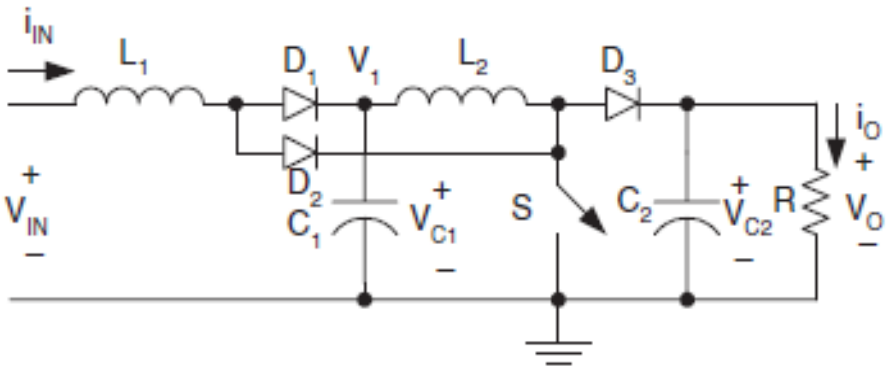

(a) Two stage DC-DC boost converter circuit diagram

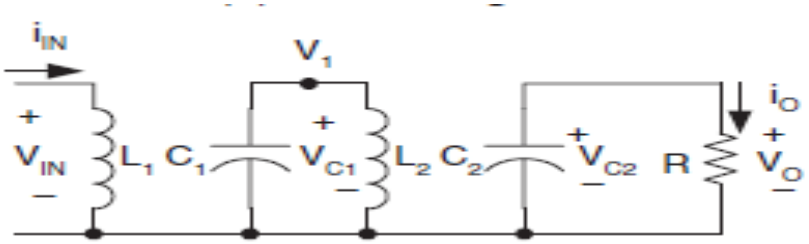

(b) Equivalent circuit during switching on

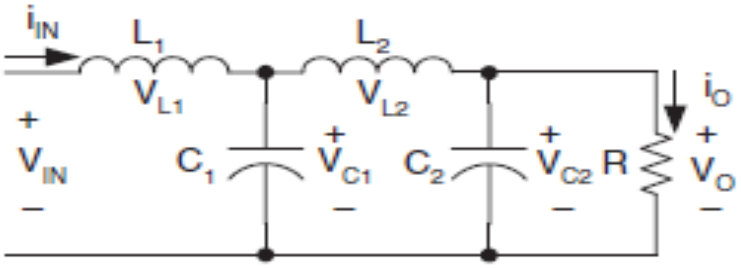

(c) Equivalent circuit during switching off

Figure 4-3: Two stage DC-DC boost converter [25]

Let the voltage across capacitor C_1 be $V_1 = V_{c1}$. As already described in the previous section the voltage across capacitor C_1 is:

$$V_1 = \frac{V_{in}}{1-K} \qquad (4.8)$$

The voltage across capacitor C_2 is charged to V_O. The current flowing through inductor L_2 increases with voltage V_1 during switching-on period KT and decreases with voltage ($V_O - V_1$) during switch-off period (1 –K)T. Therefore, the ripple of the inductor current is;

$$\Delta i_{L2} = \frac{V_1}{L_2} KT = \frac{V_O - V_1}{L_2} (1-K)\, T \qquad (4\text{-}9)$$

$$= \frac{V_O(1-K)K}{fL_2}$$

From the above equation it is possible to deduce that the current ripple is twice that of the elementary topology if the two inductors are equal. This relationship works to the capacitor too. So output voltage can be calculated as:

$$V_O = \frac{V_1}{1-K} = \left(\frac{1}{1-K}\right)^2 V_{in} \qquad (4\text{-}10)$$

The voltage transfer gain is;

$$G = \left(\frac{V_O}{V_{in}}\right) = \left(\frac{1}{1-K}\right)^2 \qquad (4\text{-}11)$$

Therefore for n stages DC-DC boost converter, the formulas will be derived from the elementary converter following the same pattern as in the case of two stages converters. The voltage gain is enhanced so that multistage DC-DC boost converter ensures the phenomena of not to use transformer in the DC-AC conversion.

4.3. Rectifier

Rectification of AC electric power in to DC form is one of the major conversions in a power system. The process helps either to supply DC power to electronic gadgets or to situate for further conversion into a voltage of required frequency. According to this study rectification helps to convert the high frequency output voltage in to DC so that the next step of DC-DC and DC-AC conversions are facilitated to get an output voltage of boosted magnitude with a frequency of 50 Hz. As already mentioned earlier the rectifier to be designed is used in the Gas Turbine unit which generate high frequency three-phase power. So the rectification involves converting the three phase voltage source in to DC one.

Generally there are two types of three phase rectifiers; controlled and uncontrolled rectifiers. The controlled ones are also divided in to line commutated (thyristor rectifiers) and forced commutated (PWM rectifiers). For the purpose of this study uncontrolled three phase bridge rectifier is used. Because there is no intention of controlling the DC level as it is assumed to be constant once conversion has taken place.

4.3.1. Three-phase bridge rectifier

The three phase bridge rectifier, shown in figure 4-4 below, is very common in high power application. It is a full wave rectifier. It can operate with or without a transformer and gives six ripples on the output voltage.

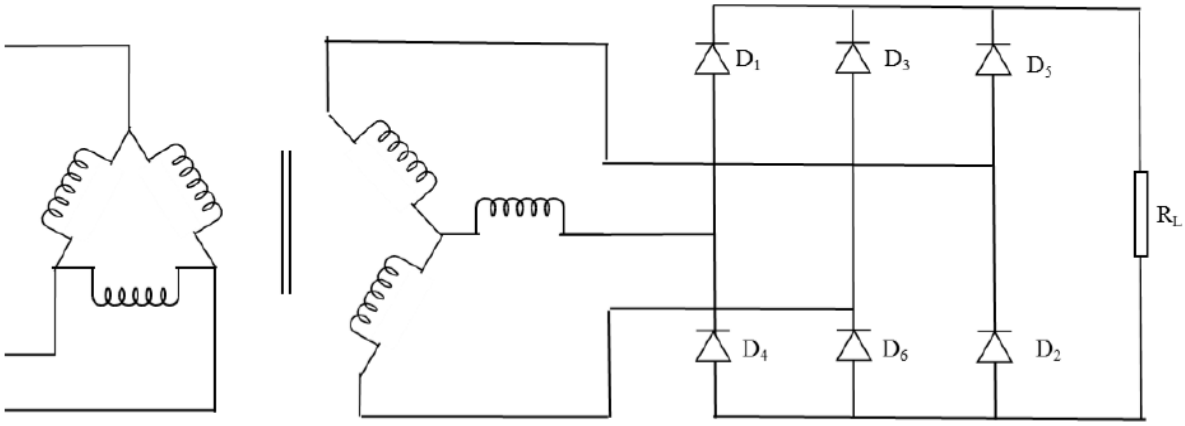

Figure 4-4: Three - phase full bridge rectifier [30]

The diodes are numbered in order of conduction sequences and each one conducts for 120^0. The conduction sequence for diodes is 12, 23, 34, 45, 56, and 61. The pair of diodes which are connected between that pair of supply line having the highest amount of instantaneous line-to-line voltage will conduct. The line-to-line voltage is $\sqrt{3}$ times the phase voltage of three phase source.

The average output voltage is found from;

$$V_{dc} = \frac{6}{\pi} \int_0^{\pi/6} \sqrt{3}\, V_m \cos \omega t \, d(\omega t) \qquad (4.12)$$

$$= \frac{3\sqrt{3}}{\pi} V_m = 1.6542\ V_m$$

Where, V_m is the peak phase voltage.

The output voltage needs to be filtered as to remove ripple voltage so that the next stage of inversion will not have significant distortion. A capacitor filter is proposed in this study. The size of the capacitor can be calculated using the following formula [31].

$$C = \frac{V_m}{2fR\Delta V_o} \qquad (4.13)$$

Where f, R, and ΔV_0: frequency of the input voltage, load resistance, and the output ripple voltage respectively. As the rectifier is to be designed for the Gas Turbine which produces high frequency voltage, the capacitor size should be very small so that the required rectification is achieved.

4.4. Inverter

In hybrid power system and Microgrid system the use of inverter is significant. In industrial applications, such as single phase and three Phase Induction Motor & other rotating machines, variable frequency &variable voltage supply is needed. To vary the supply frequency and supply voltage, voltage source inverter (VSI) is used. The voltage source inverters, where the independently controlled AC output is a voltage waveform, behave as voltage sources required by many industrial applications. While the single-phase VSIs cover low-range power applications, three-phase VSIs cover medium to high-power applications. Three phase VSI is used for the purpose of this study.

Modern power electronics have contributed a great deal to the development of new powerful applications and industrial solutions; but at the same time, these advances have increased the harmonic contamination present in line currents, which ends up distorting the voltage waveforms. The total harmonic distortion (THD) generated by the inverter is regulated by international standard IEC-61000-3-2 [8]. The total harmonic distortion (THD) of the voltage must be kept at minimum, and according to recommended limit by IEEE Standard 519-1992, has to be kept at less than 5% for harmonic spectra up to 49^{th} harmonic [21].

There are several switching techniques to control the VSI and for harmonic reduction. Pulse Width Modulation (PWM) technique is the best one among them. Till now, many types of modulating modes have been brought forward in motion control and power conversion, such as sinusoidal PWM, space vector PWM, current tracking PWM, harmonic elimination PWM and so on [28]. These methods have some advantages and disadvantages, but the most widely techniques used are the sinusoidal PWM and the space vector PWM. Sinusoidal Pulse Width Modulation (SPWM) technique of DC-AC conversion has been used widely for industrial and power generation purposes. This paper also considers as a best option to design such an inverter for the envisaged Microgrid. As already mentioned in the previous sections, the inverters to be designed will be applied in the SOFC, PV and Gas Turbine.

4.4.1. Components of inverter

There are five main groups of power semiconductors. They are: power diode, thyristor, power bipolar junction transistor (BJT), insulated gate bipolar transistor (IGBT), and static induction transistor (SIT). Figure 4-5 gives a picture of each.

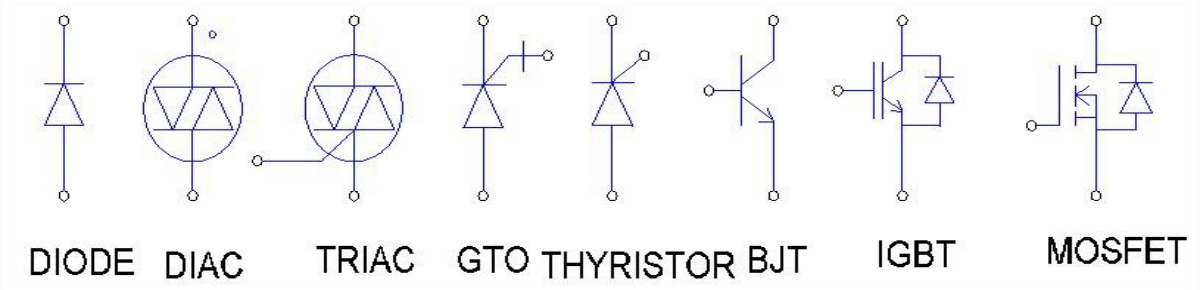

Figure 4-5: Different power semiconductor switches [21]

To assemble an inverter the MOSFET and IGBT are widely used power semiconductor devices. Power MOSFET can operate at somewhat higher frequencies (a few to several tens of kHz), but is limited to power ratings, usually 1000V, 50A. Insulated-gate bipolar transistor (IGBT) is voltage controlled power transistor that is used while voltage requirement increases and it also offers better speed than a BJT but is not quite as fast as a power MOSFET [20]. In higher switching frequencies MOSFET is superior to IGBT but higher switching operation of IGBT is feasible by employing soft switching power conversion [32]. Therefore, according to the requirements of the MG

MOSFET is chosen to design the inverter. Moreover power diode is used as freewheeling diode. A three phase PWM inverter is shown in Figure 4-6.

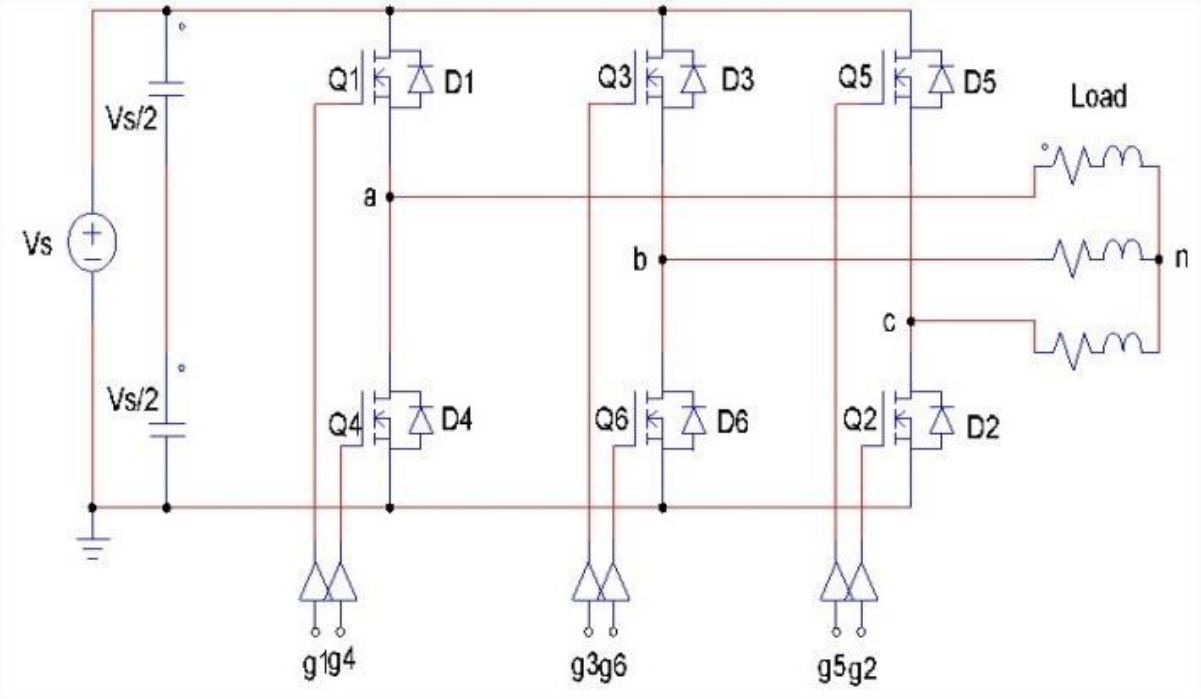

Figure 4-6: Three-phase voltage source inverter [24]

4.4.2. Sinusoidal Pulse Width Modulation (SPWM) technique

The voltage source inverter that use PWM switching techniques have a DC input voltage ($V_{DC} = V_S$) that is usually constant in magnitude. The inverter job is to take this DC input and to give AC output, where the magnitude and frequency can be controlled. There are several techniques of Pulse Width Modulation (PWM).The efficiency parameters of an inverter such as switching losses and harmonic reduction are principally depended on the modulation strategies used to control the inverter [24]. In this design the Sinusoidal Pulse Width Modulation (SPWM) technique has been used for controlling the inverter as it can directly control the inverter output voltage and output frequency according to the sine functions. Sinusoidal pulse width modulation (SPWM) is widely used in power electronics to digitize the power so that a sequence of voltage pulses can be generated by the on and off of the power switches.

SPWM techniques are characterized by constant amplitude pulses with different duty cycles for each period. The width of these pulses are modulated

to obtain inverter output voltage control and to reduce its harmonic content. In SPWM technique three sine waves and a high frequency triangular carrier wave are used to generate PWM signal [30-32]. Generally, three sinusoidal waves are used for three phase inverter. The sinusoidal waves are called reference signal and they have 120^0 phase difference with each other. The frequency of these sinusoidal waves is chosen based on the required inverter output frequency (50/60 Hz). The carrier triangular wave is usually a high frequency (in several KHz) wave. The switching signal is generated by comparing the sinusoidal waves with the triangular wave. The comparator gives out a pulse when sine voltage is greater than the triangular voltage and this pulse is used to trigger the respective inverter switches [30]. In order to avoid undefined switching states and undefined AC output line voltages in the VSI, the switches of any leg in the inverter cannot be switched off simultaneously. Also to avoid short circuit in the VSI, the switches of any leg should not be switched on at the same time. The phase outputs are mutually phase shifted by 120^0 angles.

The frequency-ratio between the triangular wave (f_c) & sine wave (f_s) must be an integer N, the number of voltage pulses per half-cycle, such that $2N= f_c/f_s$. Conventional SPWM signal generation technique for three phase voltage source inverter is shown in Figure 4-7.

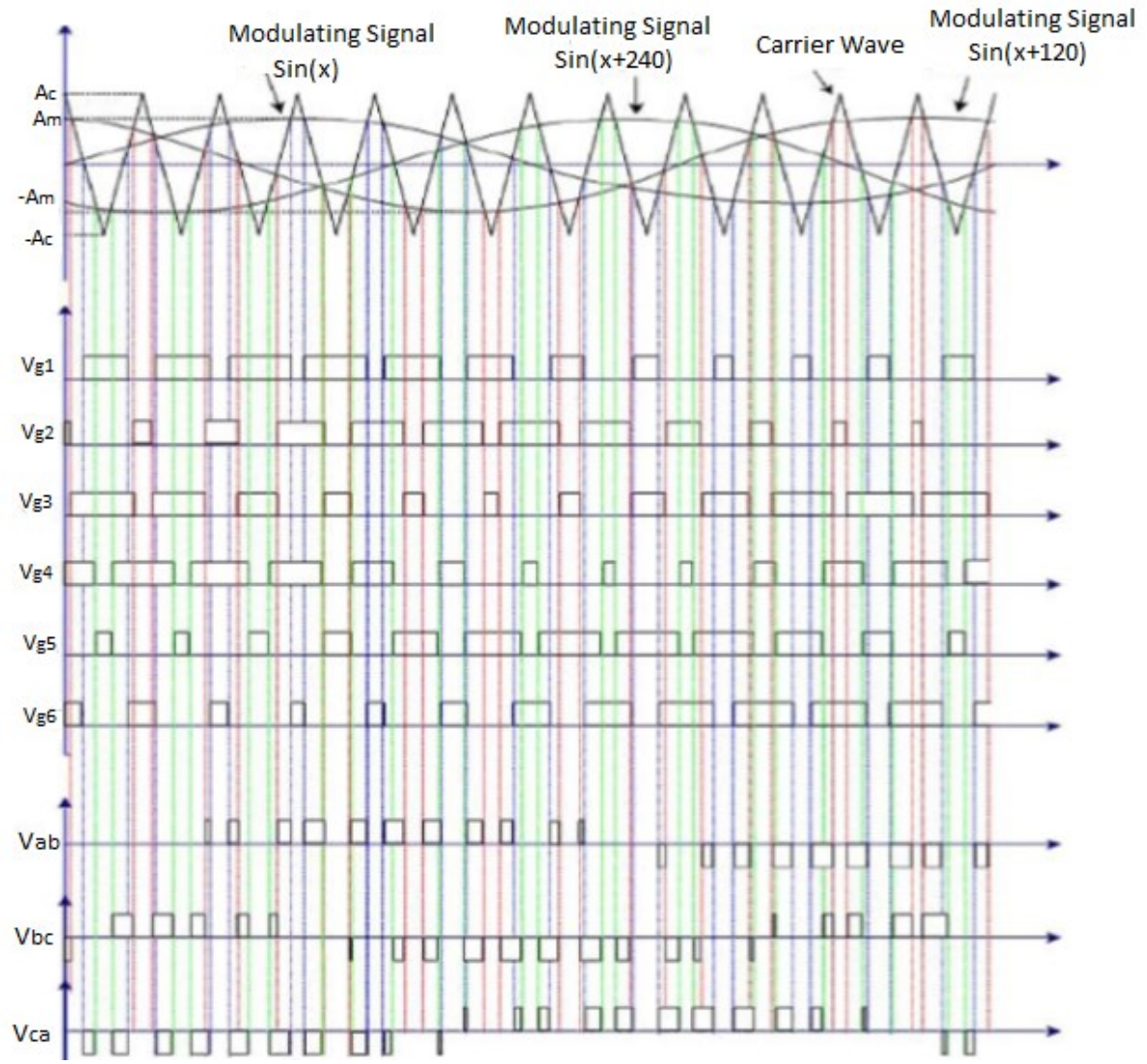

Figure 4-7: Conventional SPWM generation technique for three phase voltage source inverter [37]

Amplitude Modulation, $M_a = \frac{As}{Ac}$ (4.14)

Frequency Modulation, $M_f = \frac{fs}{fc}$ (4.15)

Where As, fs: Amplitude and frequency of the sine wave respectively

Ac, fc: Amplitude and frequency of the carrier wave respectively

The RMS output voltage can be varied by from 0 to V_s by varying the modulation index M_a from 0 to 1.

Total harmonic distortion (THD) is given by:

$$THD = \frac{V_h}{V_1} \quad (4.16)$$

Where: $V_h = \sqrt{(V_{out}^2 - V_1^2)}$

V_1 = fundamental component

4.4.3. Low pass filter

The outputs of an inverter contain large amount of harmonics. The VSI generates an AC output voltage waveform composed of discrete values; therefore, the load should be inductive at the harmonic frequencies in order to produce a smooth current waveform. Also a well-designed filter can attenuate switching frequency components.

To the low voltage power system like that of Microgrid, the inverter is used without transformer in most cases. This paper also opts for this option as it has the advantage of reduced power loses and cost. Harmonic attenuation can be achieved by several methods such as by resonating of the loads, by an LC filter, by pulse width modulation, by sine wave synthesis, by selected harmonic reduction and by poly phase inverters [32]. Apart from these in PWM technique, if the carrier frequency is increased, the harmonics components are reduced. A high-carrier ratio improves waveform quality by raising the order of the principle harmonics. At low fundamental frequencies, very large carrier ratios are feasible and resulting in near-sinusoidal output current waveforms account for one of the main attributes of the sine wave PWM inverter. However, there are different types of filtering circuits. RC & LC filters are the most used passive filters. One of the widely used types of filter used in DGs of Micro Grid is given in the figure below.

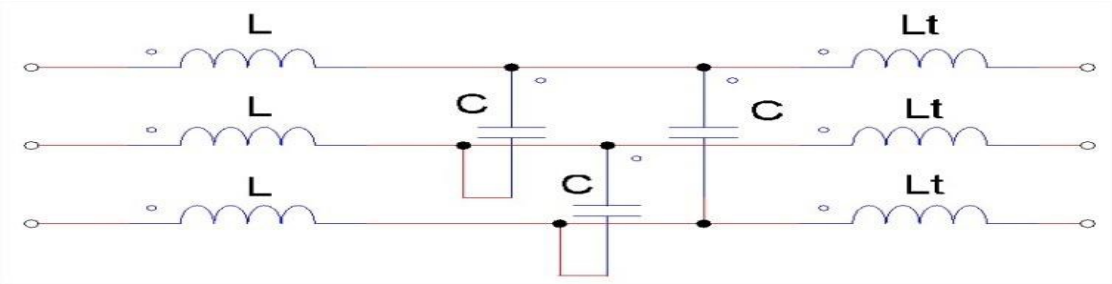

Figure 4-8: 3rd order LCL filter for three phase system [44]

With low inductance on the inverter side, it is difficult to achieve the required level reduced harmonic distortion. An LCL filter can achieve reduced levels of harmonic distortion with lower switching frequencies and with less overall stored energy [44]. In this system L_t is the coupling inductor of the inverter through which it is connected to the grid. After LC filter a coupling inductor is used and the LCL filter is formed. The coupling inductor has got two advantages. First it helps to decouple the active and reactive power components of the inverter so that they are controlled separately [19]. Secondly, it eliminates all high order harmonics from the output waveform of the inverter so that the output is 50Hz, low distortion, pure sinusoidal voltage wave. The cut-off frequency of the low pass filter is selected such that, total THD is less than 5%. The calculation is done by the following equation:

$$f_0 = \frac{1}{2\pi}\sqrt{\frac{L+L_t}{LL_tC}} \qquad (4.17)$$

4.5. PEIs Design and Simulation Scenario

As already mentioned three types of power electronic interfaces (PEI) have been used in the proposed MG to eventually connect a respective microsource to a corresponding feeder. The type of PEI used depends primarily on the nature of micro-generators. The appropriate PIEs applied in the microsources have been designed and simulated in MATLAB/SIMULINK. Prior to the design and simulation the estimated load of the proposed community, Black Lion Hospital, where there are sensitive loads which need continuous power supply without interruption should be mentioned so that the contribution from each microsource is set.

4.5.1. Load Estimation

The overall scheme of the PV-ISOFC/GT Microgrid in general, and the power electronic interfaces and Microsource controller in particular have been discussed as the theme of this paper. For the purpose of demonstration Black Lion Hospital is chosen as it harbours special types of sensitive loads – biomedical and analytical instruments. The non-sensitive loads are mostly ordinary types that can be found elsewhere; so no need of describing them. The following sensitive load types with their estimated power requirements

are those which are envisaged to be supplied by the proposed Microgrid. Each load type includes different specific instruments such as Electrocardiogram (ECG), X-ray machine, flame photometer, etc. So the loads described below are rooms which contain various instruments. Plus the oxygen supply for intensive care unit is centrally generated.

It is the sum of the power consumed by each specific electronic device in each load type (section) that is given in the table below. Detail description about specific load type is not given (available) on the devices except electrical quantities like voltage level and power consumption.

Table 4-1: Estimated loads

Sensitive Load types	Estimated power supply (KW)
Major Operating Theatres	9.5
Minor Operating Theatre	5
Intensive Care Units	11
Pathology Laboratory	8.5
Clinical Chemistry Laboratory	6
Total	40

The above load types can be accommodated fully by the three microsources, namely Solid Oxide Fuel Cell (SOFC), Photovoltaics (PV) and Gas Turbine (GT). The photovoltaics is assumed to operate at its maximum power point and at low solar irradiance the PV can be stopped to supply power and its share is compensated from the extra SOFC which can be considered as a spinning reserve. The GT is expected to generate steam or hot water, in addition to the electric power, for heating purposes like cleaning in the proposed community. Further analysis on the generated steam is not given in this study as it is not within its scope.

The amount of power to be delivered by each microsource is listed in the table below. The total sensitive load to be supplied by the microsources is estimated to be 40 KW. The supply from the SOFC considers 10 KW of spinning reserve when solar irradiation is low or absent for the PV to supply sufficient power. This is to mean that when power generation from PV becomes low due to time of a day or season of a year, the SOFC spinning reserve takes over the PV

generation share. The output steam from the SOFC is used to generate further electricity and heat in the GT unit.

Table 4-2: Microsource's power supply

Microsource	Power supply (KW)
Solid Oxide Fuel Cell	30
Photovoltaics	10
Gas Turbine	10
Total	50

4.5.2. PEIs for the SOFC

DC-DC boost converter and an inverter are used successively before the SOFC is connected to the Microgrid. The analysis and simulation are started with the inverter as the amount of enhanced DC level used in the inversion stage has to be determined first so that the required AC can be achieved.

Inverter

In designing an inverter, two important component parts play the major role; the switching devices and the low pass filter. Six MOSFETs are used as switching devices. The inductors and capacitor sizes of the low pass filter are calculated from equation (4.17). Components of the inverter and some important design specifications of the component parts are given in the following table.

Table 4-3: Components and design specifications of inverter for SOFC

Switching Device	Inductor L	Capacitor C	Inductor L_t	Input DC voltage	Output AC Voltage	Switching frequency	Cut-off frequency (f_0)
MOSFET	2 mH	5 mF	153.4 mH	632.27 V	380 V	20 KHz	50 Hz

Table 4-4: Specification of switching MOSFET for inverters

FET resistance	Internal diode resistance	Internal diode forward voltage	Snubber resistance
0.1 Ω	0.01 Ω	0 V	500 KΩ

In simulating the inverter in MATLAB/SIMULINK environment, two main subsystems are used; the switching bridge circuit which involves six power MOSFETs and the low pass filter. The required input DC source of 632.27 V, the SOFC, is obtained by tuning so as to get an output AC line voltage of 380 V. The bridge inverter subsystem is shown in figure 4-9 below.

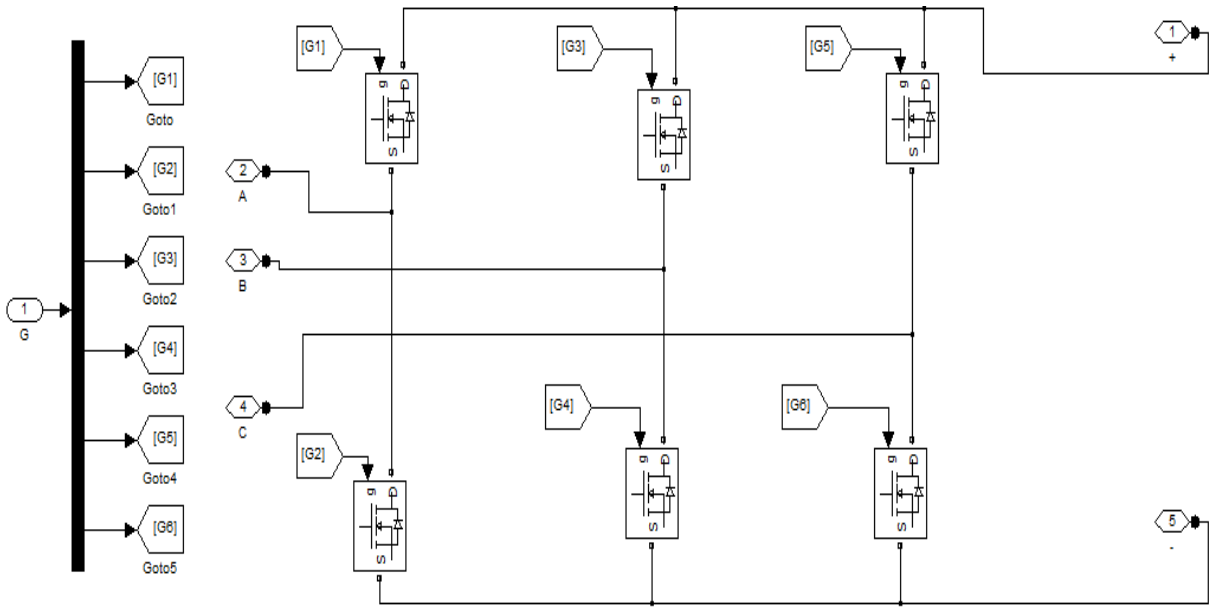

Figure 4-9: Bridge Inverter with switch gate signal

SPWM technique of switching to effect inversion is applied with PWM generator tool in which the modulating sine wave and carrier wave are generated with modulating index (M_a) of 0.75.

The other main subsystem unit of the inverter to be simulated is the low pass filter where harmonics of higher frequency are avoided. The parameters of the components of the filter are given in Table 4-3. The model from SIMULINK is shown in the figure below.

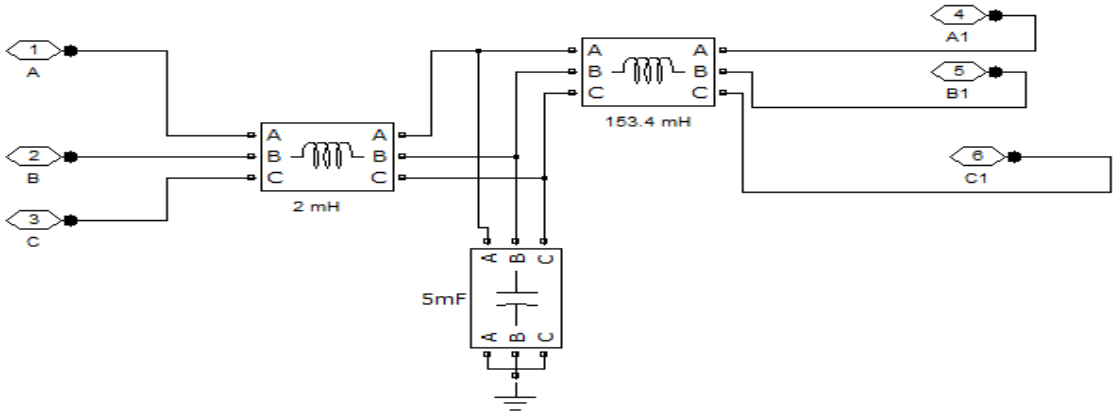

Figure 4-10: SIMULINK model of LCL filter

The overall SIMMULINK model of the inverter is shown in figure 4-11 below:

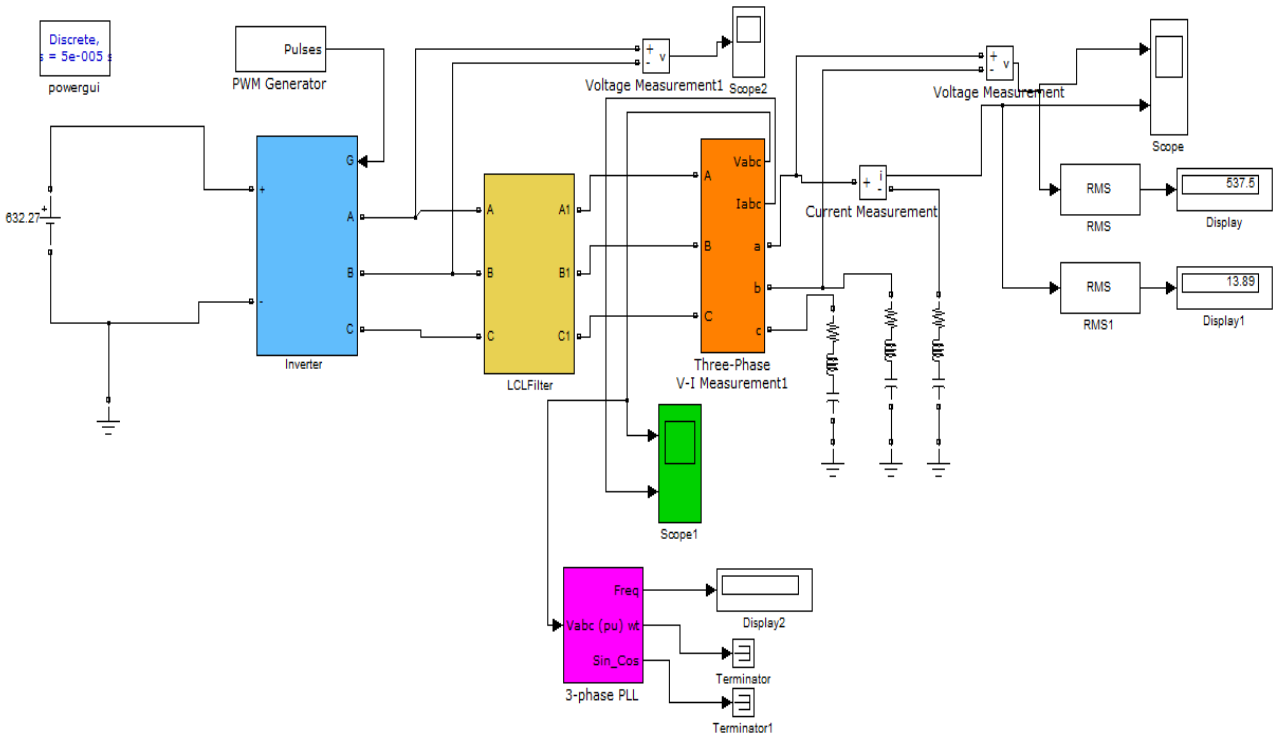

Figure 4-11: The overall SIMULINK model of the inverter with measuring units

The simulation results of the output wave forms of the three phase inverter are shown below.

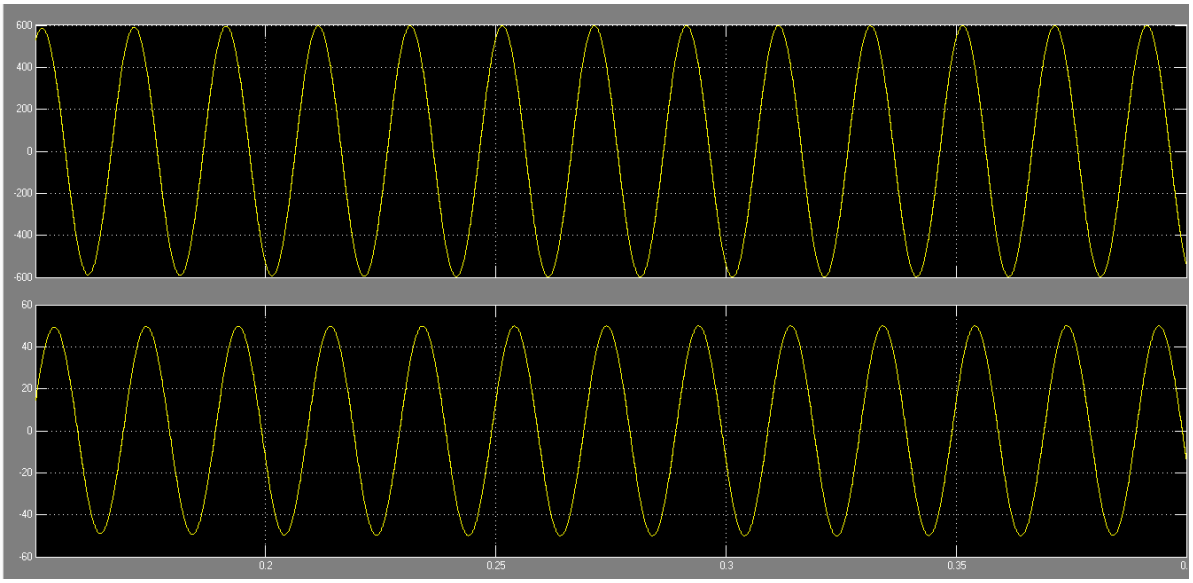

Figure 4-12: A Phase to phase AC output voltage and current

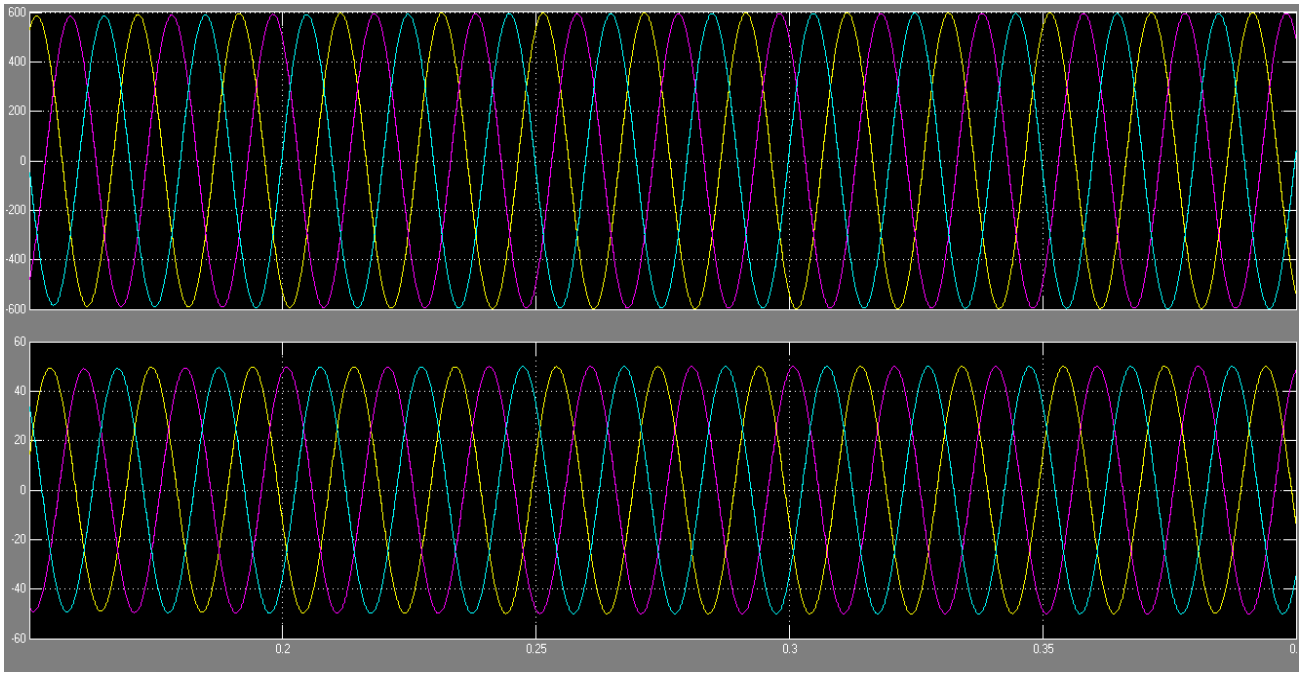

Figure 4-13: Three phase output voltage and current wave form for SOFC

DC-DC Boost converter

In designing a two stage DC-DC boost converters the important design specifications are the sizes of two inductors and two capacitors, switching frequency of the MOSFET switch, input voltage and output voltage. The DC-DC inverter for SOFC microsource is required to boost its DC output voltage level which avoids exaggerated cost of the fuel cell and the use of transformer. Again it is possible to reduce the size of the SOFC further by applying two-stage DC-DC boost converter. The specification of the two stage DC-DC boost converter is given in the table below. First the size of C_1 and L_1 are calculated according to the formula (4.6) and (4.7); then for the second stage twice of the size of C_1 and L_1 is calculated as the values of C_2 and L_2.

Table 4-5: Design Specification of two stage DC-DC boost converter for SOFC

Inductor L_1	Capacitor C_1	Inductor L_2	Capacitor C_2	Switching Frequency	Input DC voltage	Output Dc voltage
6.96 mH	8 mF	13.96	16 mF	25 KHz	79.33 V	632.3 V

Table 4-6: Specification of diodes used in the DC-DC boost converters

Resistance	Inductance	Forward Voltage	Snubber resistance	Snubber Capacitance
0.001 Ω	0 H	0.8 V	500 Ω	250 nF

Specification of the MOSFET switch used in the DC-DC converter is the same as that used in the inverter.

The SIMULINK model for the two stage DC-DC boost converter is shown in figure 4-14 and the wave form of the output voltage in figure 4-15.

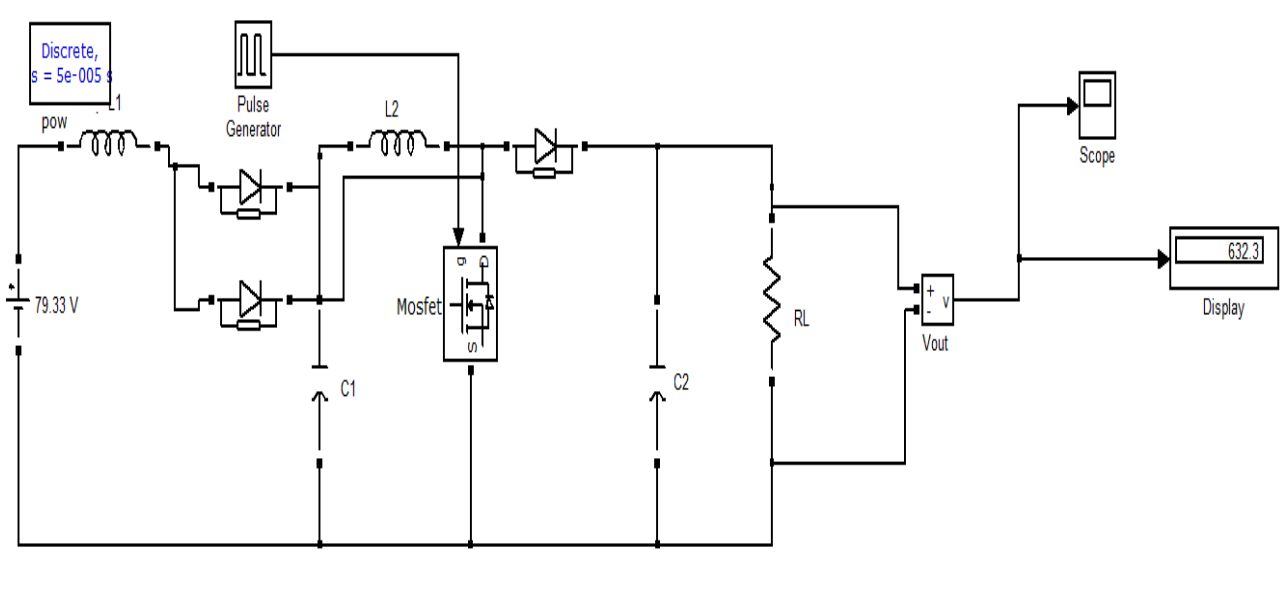

Figure 4-14: SIMULINK model of the two stage DC-DC boost converter

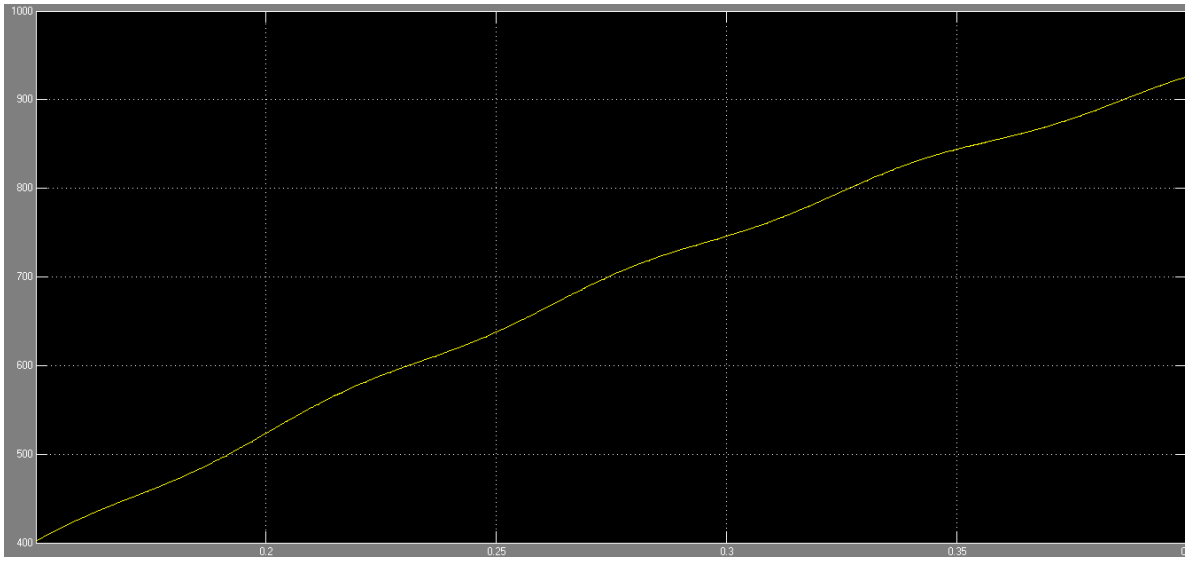

Figure 4-15: The output voltage wave form of the DC-DC boost converter

4.5.3. PEIs for the Photovoltaic

The photovoltaic arrays have DC output voltage. In order to be connected to the MG, the DC voltage has to be boosted and inverted like that of the SOFC.

Inverter

As usual the design starts with the inverter as it determines the DC voltage to be stepped up. For the 10 KW supply from the PV source, a Power Factor (PF) of 0.95 is assumed like the SOFC. And except the load, the DC level applied to the inverter and the type of microsource, the other parameters and the design topology are the same. The input DC voltage from the PV arrays is 324.2 V which gives an output AC line voltage of 380 V. The DC supply is almost half of the supply from the SOFC which is the reflection of the difference in the original power supplies, 20 KW from the SOFC and 10 KW from the PV. The SIMULINK model and the output voltage waveforms are shown in the figures below. The design specification of the inverter and low pass filter is same as that of the SOFC.

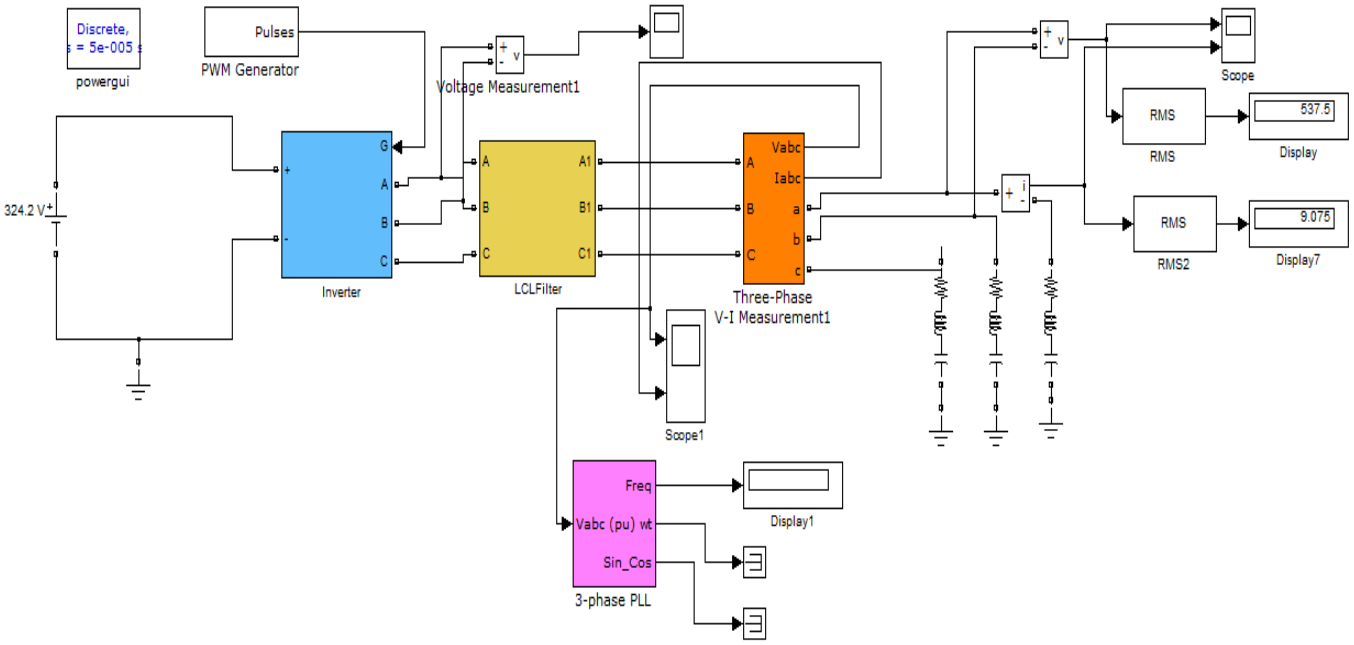

Figure 4-16: SIMULINK model of the inverter with measuring units for the PV

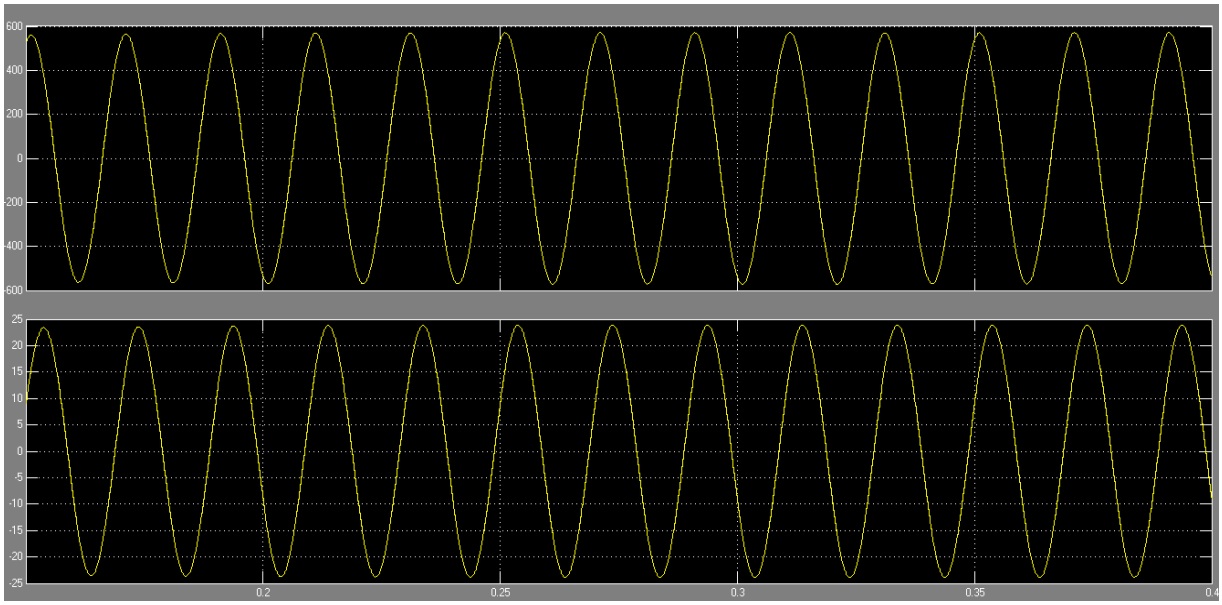

Figure 4-17: Inverter phase to phase output voltage and current for PV

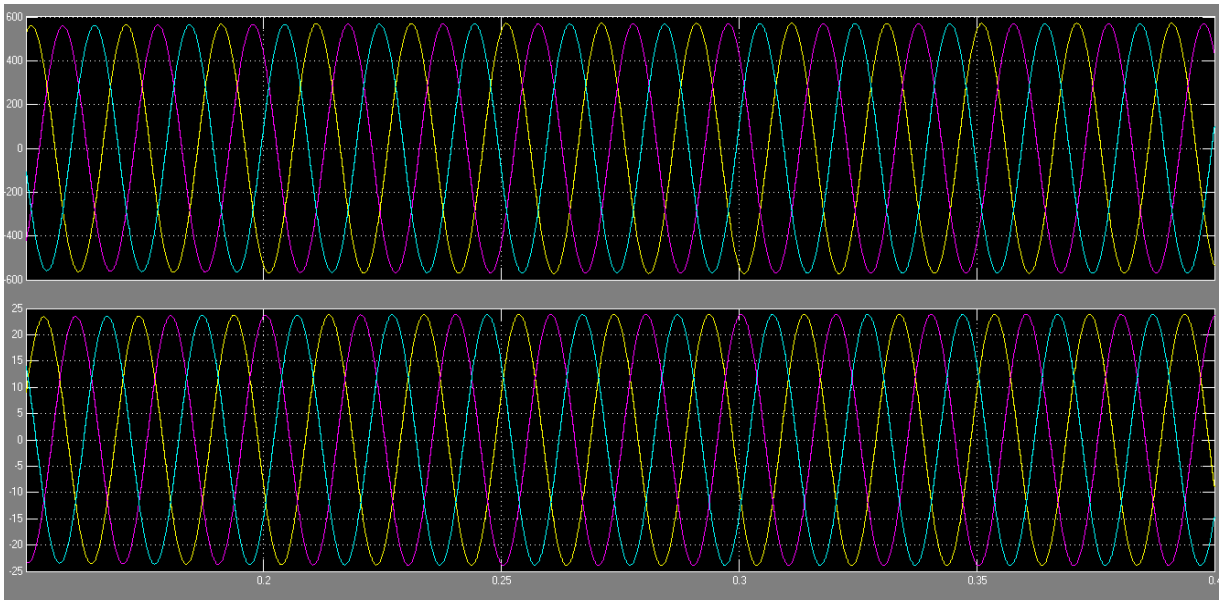

Figure 4-18: The three phase output voltage and current for PV

DC-DC boost converter

The DC voltage from the PV source is to be boosted to the required level so that inversion is realized. The appropriate topology to be applied for the DC-DC conversion is the two stage boost converter for the same reason as stated earlier. The differences with that of the SOFC are the size of the two inductors, capacitors and the input DC voltage from the PV array. The specification for the

design of two stage DC-DC boost converter for PV is described in the table below.

Table 4-7: Design specification of two stage DC-DC boost converter for PV

Inductor L_1	Capacitor C_1	Inductor L_2	Capacitor C_2	Switching Frequency	Input DC Voltage	Output DC Voltage
2.32 mH	8.15 mF	4.64mH	12.29 mF	25 KHz	40.42 V	324.2 V

The design specification for the diodes and the switching MOSFET is the same as those used in the SOFC.

The SIMULINK model of two-stage DC-DC boost converter for PV and its output voltage waveform are shown in the figures below.

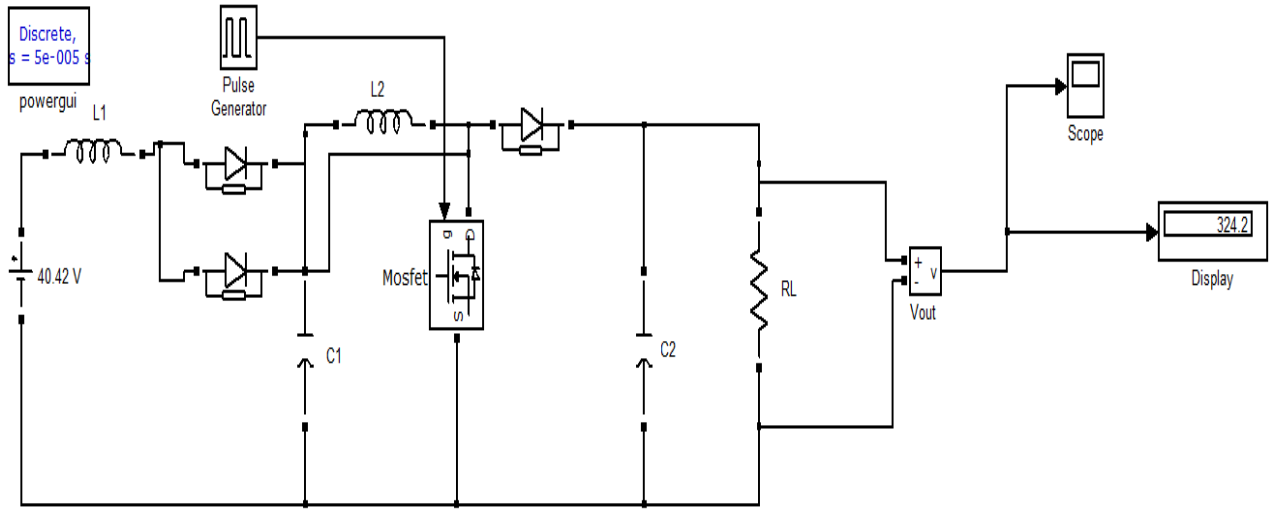

Figure 4-19: SIMULINK model of two stage boost converter for PV

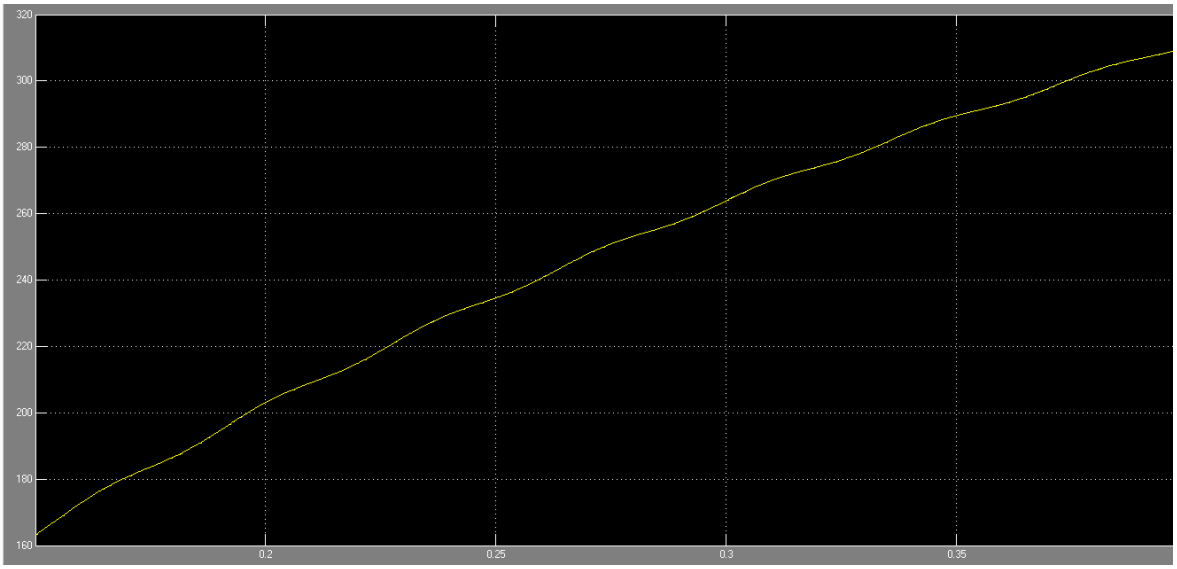

Figure 4-20: Output voltage waveform of the two stage DC-DC boost converter

4.5.4. PEIs for Gas Turbine

The Gas Turbine generates high frequency AC voltage. So first of all it has to be rectified so that the required nominal frequency can be achieved from the rectified DC voltage. Therefore three types of PEIs are required before the GT is connected with the MG.

Rectifier

The rectifier changes the high frequency AC output voltage of the GT in to DC. Different topologies have been applied. For the purpose of this study the uncontrolled diode bridge rectifier type will be designed. AS the power supplied by the Gas Turbine is the same as that of the PV, the rectifier design reflects the DC level to be boosted to the level as that of the PV too. So the designed rectifier for the GT is tuned to produce a DC output of 40.42 V so that it would be stepped up to 324.2 V DC using the two stage DC-DC boost converter. Therefore, the DC-DC converter and the inverter design is the same as that of the PV ones. Then there is no need of indicating here the design of the two PEIs as the design procedures are the same. The following figures show the SIMULINK model for the rectifier design and the output DC waveform only.

Table 4-8: Design specifications of rectifier for GT

Input AC Voltage	Input AC Frequency	Filter capacitor (C)	Output Voltage	Diode VF	Diode Snubber R
200 V	3000 Hz	272 µF	40.43 V	0.8 V	500 ohm

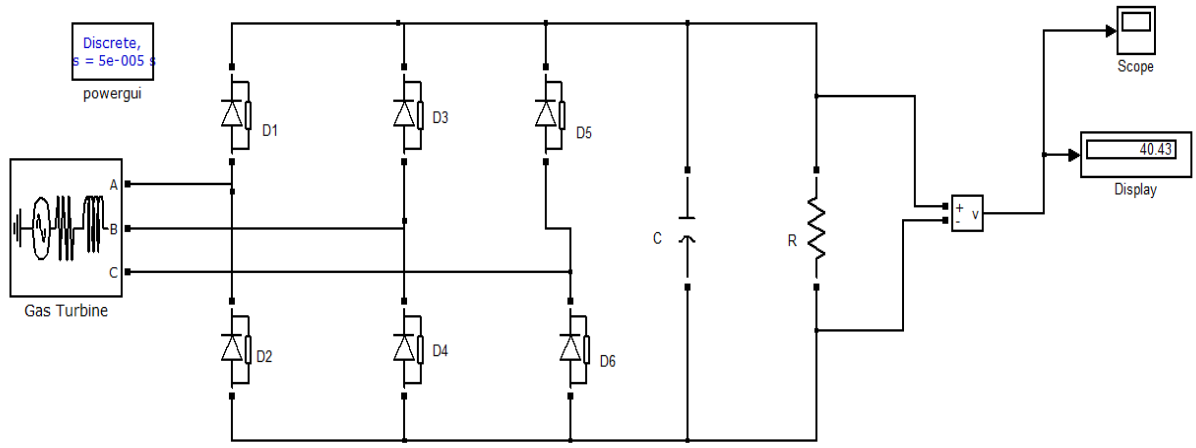

Figure 4-21: SIMULINK model of rectifier for the Gas Turbine.

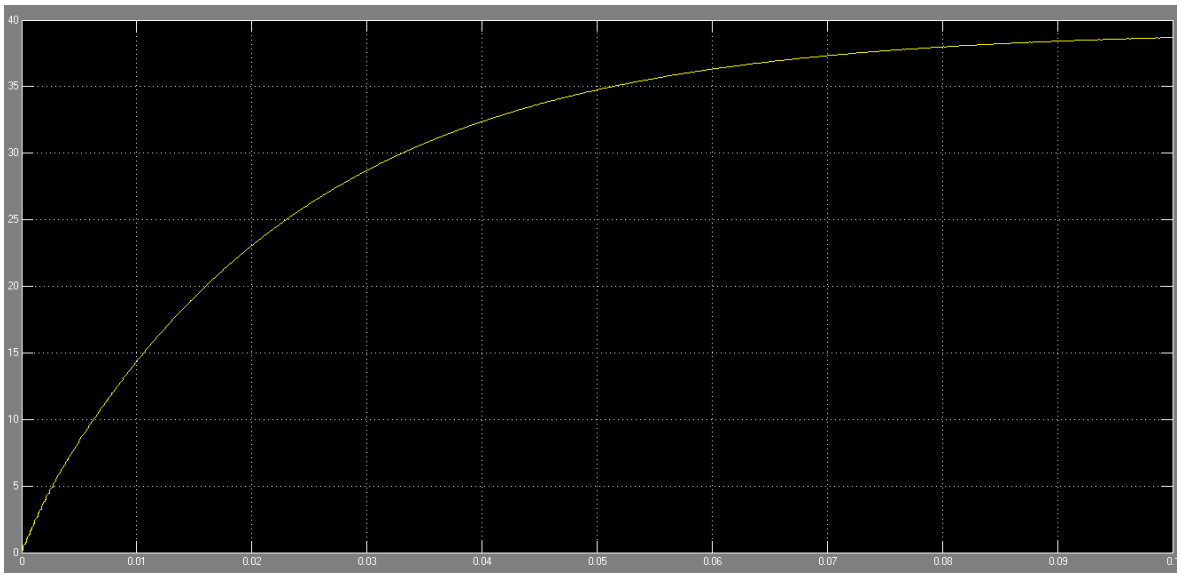

Figure 4-22: Waveform of the rectifier output DC voltage for the GT

CHAPTER FIVE

Microsource Controller Design

5.1. Introduction

The fundamental of Microgrid (MG) control is basically concerned with power sharing control on one hand and voltage and frequency control on the other hand. This is to mean that the controller which is installed into each microsource has the main duties of regulating its generated power and voltage; that is the general control philosophy within a microgrid is that sources must rely only on local information, yet must cooperate with other sources. In both cases the major concern is when the MG is in islanding mode of operation. In grid-connected mode the only control is that of unit generation as far as this thesis is concerned with. Two options can be raised regarding this mode of operation; i.e. either the controller regulates a unit output or it controls a feeder flow. This study concerns with controlling unit power output. This is to imply that a microsource (MS) is controlled to supply a constant power while importing the rest from the host grid in interconnected mode. But during islanding power is shared among microsources of the Microgrid as per their individual ratings through droop control mechanism. Here while sensitive loads are fully supplied the non-sensitive ones ride through grid power interruption.

With regard to the architecture of a MG control, two very distinctive opposite approaches can be identified: centralized and decentralized. A fully centralized control relies on the data gathered in a dedicated central controller that performs the required calculations and determines the control actions for all the units at a single point, requiring extensive communication between the central controller and controlled units. On the other hand, in a fully decentralized control each unit is controlled by its local controller, which only receives local information and is neither fully aware of system-wide variables nor other controllers' actions.

This thesis work opts to design a decentralized type of microsource controller system for the following reasons. The first one is centralized controlling requires communication infrastructure which is cost incurring and unreliable as it may fail so that the system of the Microgrid collapses. The other one is the decentralized type of controlling which has the privilege of 'plug-and-play' way of configuration in which a generation unit can be added anywhere within a Microgrid (MG) without any kind of reengineering while the centralized one does not allow such a privilege. In being so, a phenomena known as 'peer-to-peer' relationship emerges among the microsources whereby there is no any master generator to set reference control variables to the rest of generators to be considered as slave ones.

The well-known type of decentralized Microsource controller is Droop Controller. Droop controller is a controller in which power sharing of each microsource of a MG is determined in terms of its rating while controlling the frequency and voltage level in island mode of operation, and active and reactive power in grid-connected mode. In grid-connected mode voltage and frequency are measured, and active and reactive powers are controlled. Whereas in island mode, active and reactive powers are measured as voltage and frequency are controlled.

During islanding the droop controller of each microsource causes voltage magnitude and frequency deviation to realize the active and reactive power sharing among the microsources. And yet there are sensitive loads which can be affected by those deviations. So both the frequency and voltage should be regulated to the nominal values. Then the droop control system need to an embedded PI controller which can restore the voltage and frequency deviations during islanding. This operation helps seamless resynchronization of the Microgrid and the proper operation of sensitive instruments.

5.2. Control functions of Microsource controller

Microsource Controller (MC) may operate with or without any intervention of the Microgrid Central Controller (MGCC). However this thesis only deals with those MC which operates without the intervention of MGCC. MC functioning depends greatly on the power electronic interfaces provided in the microsources and storage devices. MC ensures: (i) new microsources can be

added to the system without modification in the existing Microgrid configuration, (ii) Microgrid can connect/disconnect itself to/from the utility in a rapid and seamless fashion, (iii) active and reactive power can be independently controlled, (iv) voltage sag and system imbalances can be corrected, (v) faults can be handled without the loss of stability and (vi) Microgrid can meet the requirements of load dynamics of the power utility.

The built in control features of the Microsource Controller includes:

1. Active and reactive power control
2. Voltage and frequency control
3. Load sharing of microsources through P-f and Q-V droop control
4. Voltage magnitude and frequency restoration after islanding

The Microsource Controller should ensure that the microsources rapidly pick up their share of load when the Microgrid disconnects itself from the utility using droop controller. And MC should also enable the seamless transition of the Microgrid from grid-connected to stand-alone mode and vice versa with minimum disturbance to both systems using voltage and frequency restoration mechanism. During grid connected mode, the MG uses utility voltage and frequency as reference values. So inverters of the MG only control the active and reactive power to be delivered by the respective microsource to the MG loads in addition to that of the utility. In general the microsource controller includes PQ droop controller, V-f droop controller, and Phase Locked Loop (PLL) to synchronize the MG inverters with the main grid.

Microgrid controlling is mainly concerned with regulation of electrical parameters of a MG when it is either in grid connected mode or islanding mode. In grid connected mode, the MG is supposed to control the active and reactive power generated (contributed) by the MG while voltage and frequency are synchronized with the main grid. In the islanding mode voltage and frequency are controlled by P-f and Q-V droop control mechanism while active and reactive power demand are dictated by the loads in the MG.

5.3. Droop V-f control

When a MG operates in island mode the only parameters to be controlled are frequency and voltage level, whereas the active and reactive powers are dictated by the total sensitive loads in the MG. To get an independent controllability of frequency and voltage in the VSIs of the proposed MG, it is necessary to get two control variables for each. Dq0 transformation (Park transformation) units for both voltage and current outputs are required to facilitate the measurement of active and reactive powers so that frequency and voltage level are controlled.

5.3.1. Dqo transformation

Dq0 transformation is used to transfer three phase voltage or current sequence to a two axis (I_d, I_q) rotating coordinate system and it consists with two transformation steps, namely Clark transformation and Park transformation. For balanced symmetric three phase systems, dq0 transformation can be simplified to dq transformation and zero current or voltage component can be neglected.

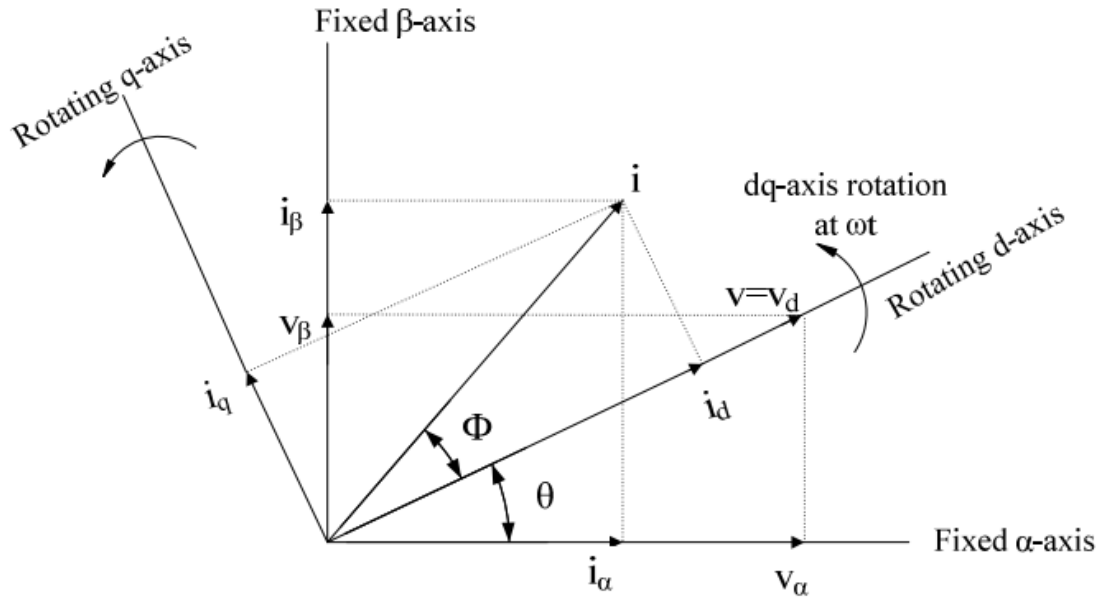

Figure 5-1: Clark and Park Transformations [51]

Clark transformation

Clark transformation helps to transform 3 phase voltage or current sequence (V_{abc} or I_{abc}) to stationary voltage or current reference frame (V_α, V_β or I_α, I_β). Mathematically this process can be shown as following.

$$\begin{bmatrix} V_\alpha \\ V_\beta \end{bmatrix} = \frac{2}{3}\begin{bmatrix} 1 & -\frac{1}{2} & -\frac{1}{2} \\ 0 & \frac{\sqrt{3}}{2} & -\frac{\sqrt{3}}{2} \end{bmatrix}\begin{bmatrix} V_a \\ V_b \\ V_c \end{bmatrix} \qquad (5.1)$$

Park transformation

Park transformation is used to transform stationary voltage or current reference frame (V_α,V_β or I_α,I_β) to a rotating voltage or current reference frame (V_d,V_q or I_d,I_q) and mathematically shown in the following equation.

$$\begin{bmatrix} V_d \\ V_q \end{bmatrix} = \begin{bmatrix} cos\ \Theta & sin\ \Theta \\ -sin\ \Theta & cos\ \Theta \end{bmatrix}\begin{bmatrix} V_\alpha \\ V_\beta \end{bmatrix} \qquad (5.2)$$

Considering symmetrical phase system;

$V_a = V \cos \Theta$, $V_b = V \cos (\Theta - 2\pi/3)$, $V_c = V \cos (\Theta + 2\pi/3)$

Then by applying Clark and Park transformations;

$$\begin{bmatrix} V_\alpha \\ V_\beta \end{bmatrix} = \frac{2}{3}\begin{bmatrix} \frac{2}{3}V cos\ \theta \\ \frac{2}{3}V \sin\theta \end{bmatrix}, \qquad \begin{bmatrix} V_d \\ V_q \end{bmatrix} = \begin{bmatrix} V \\ 0 \end{bmatrix} \qquad (5.3)$$

Here $V_d = V$ and V_q is zero.

5.3.2. Independent measurement of Active and Reactive Power

Consider a three phase VSI system, where DC power is converted to AC and transferred to infinite AC bus. Each IGBT transistors are controlled by a PWM system to generate the required AC waveform.

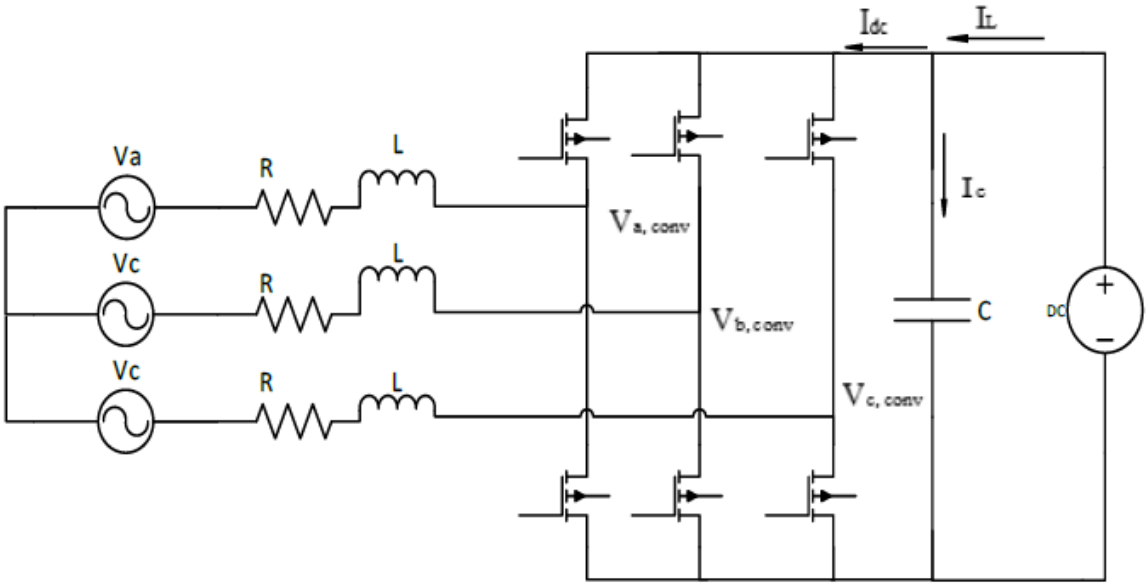

Figure 5-2: Basic VSI converter system [51]

The voltage balance equation (Consider current flow DC side to AC) for above system can be written as;

$$V_{abc,\,conv} = V_{abc} + R\,i_{abc} + L\frac{di_{abc}}{dt} \tag{5.4}$$

$$\begin{bmatrix} V_{a,conv} \\ V_{b,conv} \\ V_{c,conv} \end{bmatrix} = \begin{bmatrix} V_a \\ V_b \\ V_c \end{bmatrix} + R \begin{bmatrix} i_a \\ i_b \\ i_c \end{bmatrix} + L\frac{d}{dt}\begin{bmatrix} i_a \\ i_b \\ i_c \end{bmatrix}$$

From dq transformation;

$$V_{d,\,conv} = V_d + Ri_d + L\frac{di_d}{dt} - \omega L i_q \tag{5.5}$$

$$V_{q,\,conv} = V_q + Ri_q + L\frac{di_q}{dt} + \omega L i_d \tag{5.6}$$

Considering dc voltage side;

$$I_L = C\frac{dV_{dc}}{dt} + I_{dc} \tag{5.7}$$

The power balance equation is given by;

$$V_{dc}I_{dc} = \frac{3}{2}(V_d\,I_d + V_q I_q) + \frac{3}{2}(V_q I_d - V_d I_q) \tag{5.8}$$

But V_q is zero. Considering grid voltage along d axis V_d, the instantaneous active power p and reactive power q will be;

$$P = \frac{3}{2}(V_d I_d) \quad (5.9)$$

$$q = -\frac{3}{2}(V_d I_q) \quad (5.10)$$

This means active and reactive power can be measured and controlled independently with i_d and i_q current components respectively [51].

After the active and reactive power are measured from dq values of the current and voltage levels in accordance with equations (5.9) and (5.10), the P and Q values are passed through V-f droop controller unit to get the actual values of frequency and voltage so that they are regulated using PI controller to their respective nominal values. This is done according to the droop characteristic equations: $\omega = \omega_0 - m(P - P_0)$ and $V = V_0 - n(Q - Q_0)$, as already mentioned in the previous sections. The relationship between power and frequency (phase) is shown in the characteristic curve below.

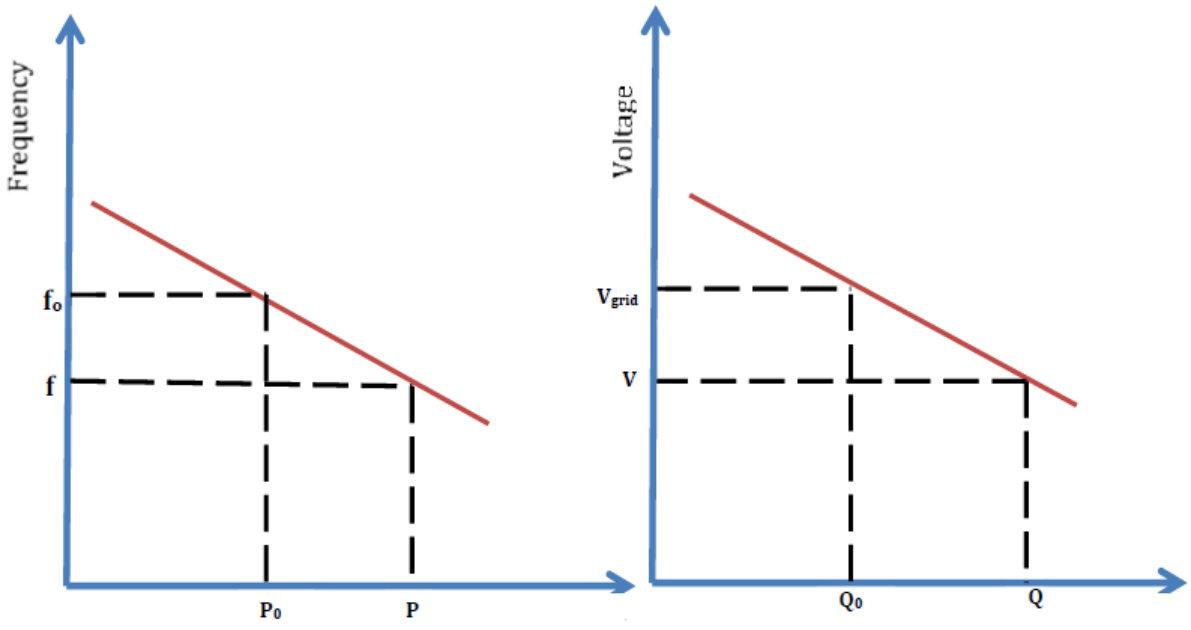

(a) Frequency droop characteristic (b) Voltage droop characteristic

Figure 5-3: Droop characteristic curve of a microsource [51]

Then the regulated voltage wave from with regulated voltage and frequency values are fed in to the PWM generator so as to generate SPWM signal for the

inverter switching. Finally the voltage and frequency of the individual inverters are restored to standard levels. The overall scenario of V-f droop control technique is described in the following figure:

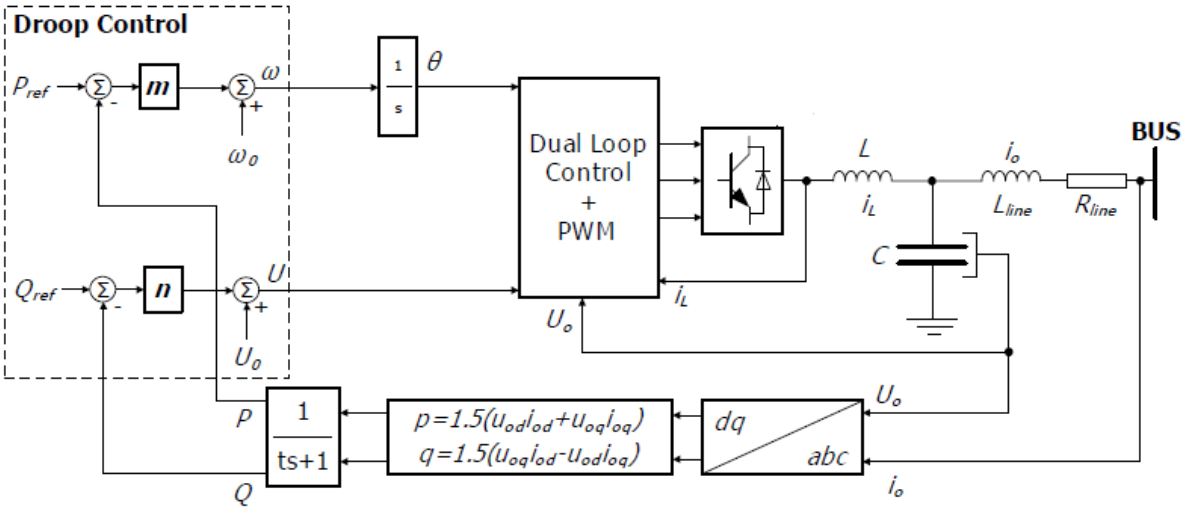

Figure 5-4: V-f droop control system schematic [22]

5.4. P-Q Droop control

In this study power flow in the MG is controlled by controlling the currents I_d and I_q as mentioned above. That is dq0 transformation and its associated I_d and I_q current components are used for power flow control. There can find many implementation methods in this category. But in all inverters, internal current control method and grid synchronization with PLL are common, while other external control designs modified according to the nature of microsource used. This is to mean that the design of the external control unit depends on whether the microsource is intermittent or not. For instance the system used in figure 5-5 can be used for grid connected intermittent microsource-inverter in which output DC voltage regulation is required. However, output DC voltage regulation is not within the scope of this study. So the control system to be designed more or less looks the schematic described in figure 5-6.

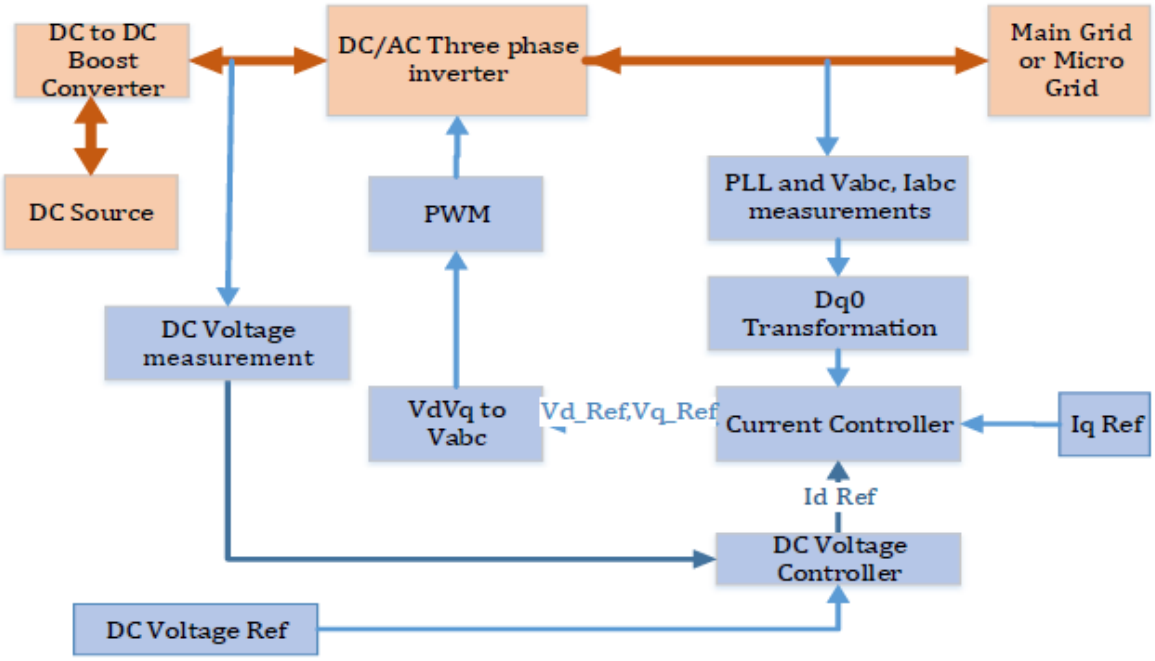

Figure 5-5: Current mode control for intermittent renewables [51]

When this system uses solar inverter, PV array work as DC current source and DC to DC boost converter should work in maximum power point tracking mode by controlling its output voltage [51]. The objective of DC voltage controller is maintaining the constant DC bus voltage by controlling its active power output (I_d current component).

Here it is worth mentioning again that the DC sources in all DGs of the proposed MG are assumed to have stable and regulated output, ready to be used by the DC-AC converter. The control of the DC source will not be discussed. So the current mode power flow control system to be considered in this study is more or less described in the following schematics. Constant DC voltage is assured by boost converter. I_d and I_q can be control as active and reactive power requirements respectively.

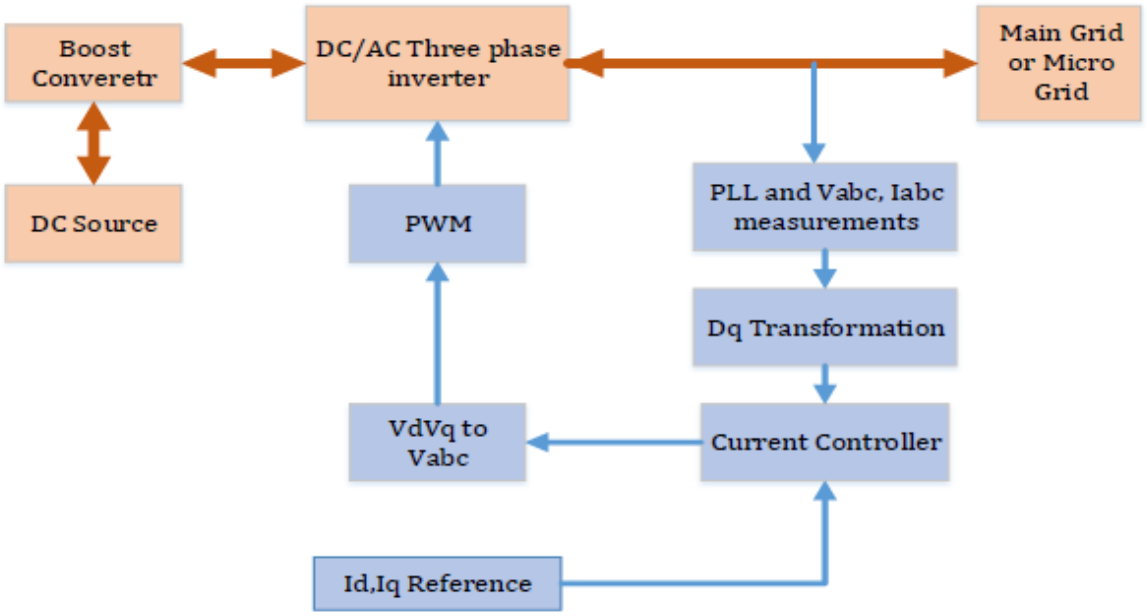

Figure 5-6: Current mode power flow control for dispatchable sources [51]

5.4.1. PQ control scenario

According to this thesis active and reactive power control are carried out by measuring frequency using Phase Locked Loop (PLL) and voltage using voltmeter. Then the measured values are fed in to PQ droop controller whose outputs are respective active and reactive power magnitudes as per the droop characteristic equations. Then the two parameters are passed through PI controller which gives reference voltage magnitude and phase angle. These reference values are fed in to standard voltage generator whose output wave is passed through PWM generator so as to provide SPWM signals to an inverter.

5.5. Power sharing control

In most cases of power sharing control, Microgrids use drooping technique to compensate power whenever there is change in load or mismatch. Droop methods originate from the principle of power balance of synchronous generators in large interconnected power systems. An imbalance between the input mechanical power of the generator and its output electric active power causes a change in the rotor speed which is translated into a deviation in

frequency. Similarly, output reactive power variation results in deviation in voltage magnitude. The frequency-power droop control method is inherent to the steady-state operation of conventional DG units such as synchronous generators, and it can be artificially crafted for electronically interfaced DG units through droop control technique.

Power sharing controllers are responsible for the adequate share of active and reactive power mismatches in the Microgrid, whereas inverter output controllers should control and regulate the output voltages and currents. Also power sharing is performed without need for communication by using active power-frequency and reactive power-voltage droop controllers that emulate the droop characteristics of synchronous generators.

If the slope of a P-f and Q-V control is chosen in such a way that;

$$m_1P_{1r} = m_2P_{2r} = \ldots\ldots\ldots\ldots\ldots\ldots = m_NP_{Nr} \text{ and}$$

$$n_1Q_{1r} = n_2Q_{2r} = \ldots\ldots\ldots\ldots\ldots\ldots = n_NQ_{Nr} \qquad (5.11)$$

Where Nr indicates the rated amount of n^{th} microsource, then the microsources share the total load in the MG in proportion with their power rating. This study also considers this approach to design the droop controller.

5.6. Design and Simulation of MS Droop controller

In implementing the design of droop controller the following procedures (algorithm) are followed:

1. Droop coefficients for frequency and voltage control are calculated from droop characteristic equations. So the frequency and voltage droop coefficients, m and n respectively, are calculated as follows:

$$m = -\frac{\omega_0 - \omega_{min}}{P_{max} - P_0} \qquad (5.12)$$

The nominal frequency is 50 Hz; the minimum allowable frequency at the time islanding occurs is assumed to be 49.5 Hz for the SOFC. The rated power P_{max} and the power that a microsource supplies during grid connected mode P_0 varies according to the capacity of microsources. And the voltage droop coefficient is calculated as:

$$n = -\frac{V_0 - V_{min}}{Q_{max} - Q_0} \qquad (5.13)$$

The nominal voltage is 380 V; the minimum allowable frequency at the time islanding occurs is assumed to be 378 V for the SOFC. So for each microsource the calculated frequency droop coefficient m and voltage droop coefficient n are given in the following table. First the m and n values of the SOFC are calculated from (5.12) and (5.13). Then the values for the PV and GT are calculated from the relation in (5.11).

Table 5-1: Summary of microsources data

Microsource	V_{rated} (phase) [V]	P_{rated} [KW]	Q_{rated} [KVar]	m [rad/KW]	n [V/KVar]	Frequency Hz
SOFC	380	20	6.574	-π/10	-0.61	50
PV	380	10	3.287	-π/5	-1.22	50
GT	380	10	3.287	-π/5	-1.22	50

The rated reactive power for each microsource is calculated assuming that all sources operate at power factor of 0.95.

2. Transform the three phase voltage into the dq0 form which helps to calculate the active and reactive power of a microsource, and also it helps also in voltage and frequency regulation. The design is developed from models derived from Park transformation. The SIMULINK model of abc to dqo transformation is shown below.

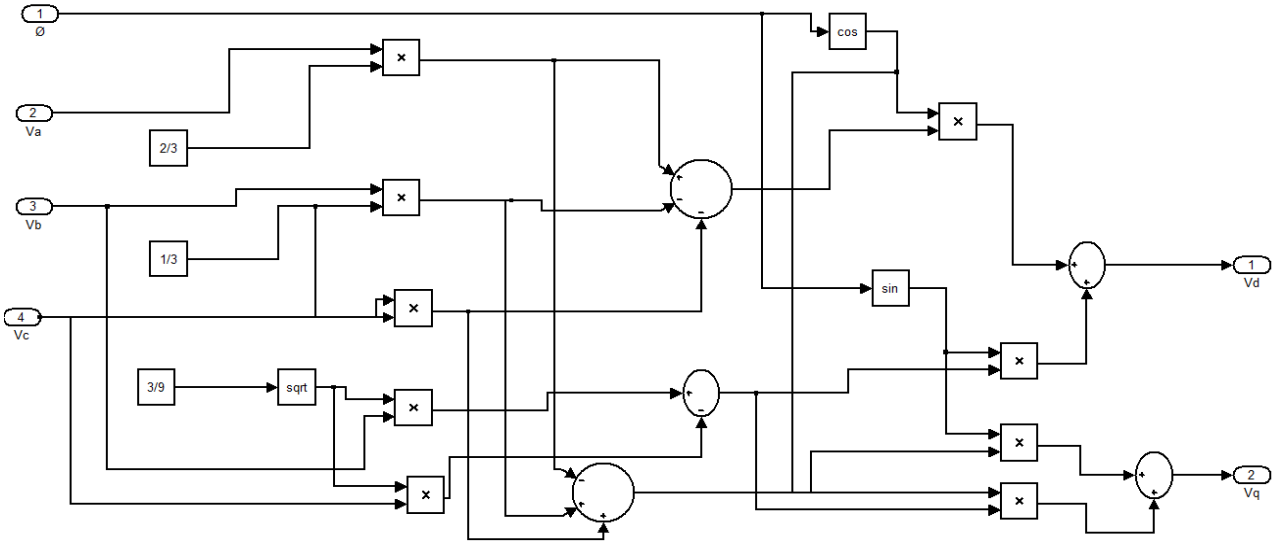

Figure 5-7: SIMULINK model of abc-dqo converter

3. Power calculation is done in the unit designed from Park transformation model for three phase voltage and current. The process is done in two steps. The first is Park transformation and the second one active and reactive power calculation. The power calculation unit is developed in SIMULINK as follows:

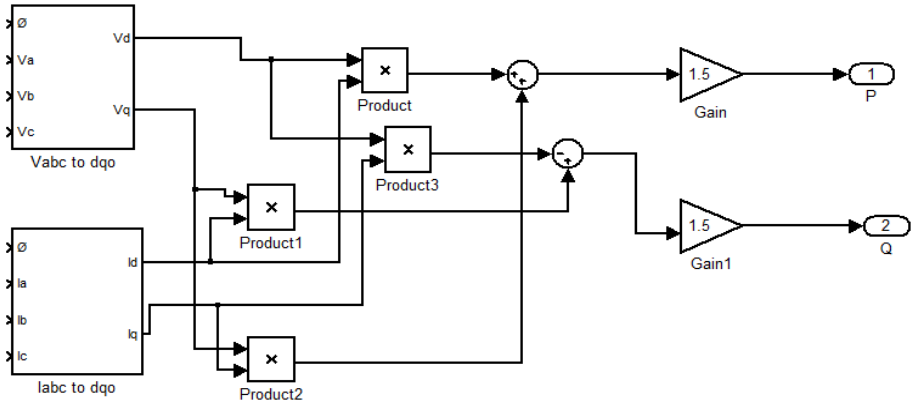

Figure 5-8: Active and reactive power calculation unit in SIMULINK

The subsystems V_{abc} *to dq0* and I_{abc} *to dqo* receive their inputs from the respective inverter.

4. The next important unit is droop control unit. The main part of the system is designed based on the droop characteristic model. The output voltage and phase angle (Ø) are fed into the respective PI controllers.

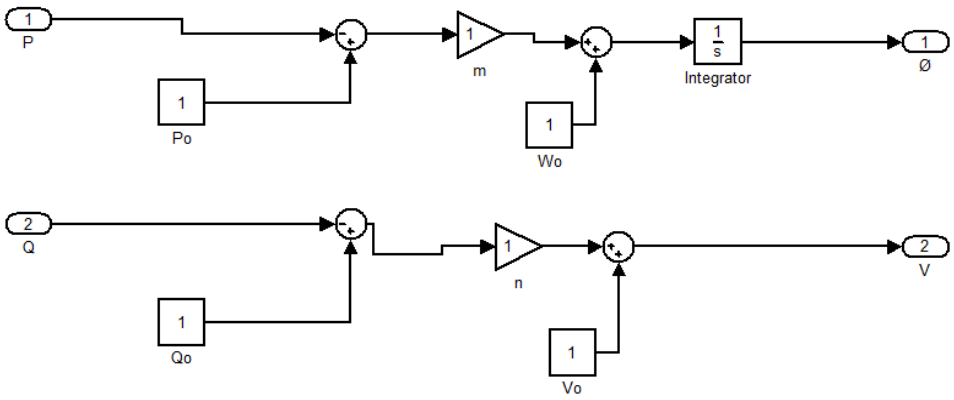

Figure 5-9: Frequency and voltage droop control unit in SIMULINK

The parameters P_0, Q_0, V_0 and ω_0 are nominal values when an inverter is connected to the main grid.

5. The outputs of the droop control unit, ø and V, are compared with reference signals and fed into PI controller. Then the PI controller output is fed in to sine wave generator to generate a modulating signal for the PWM unit so that SPWM signals are generated to switch the MOSFETs of an inverter. The above sequence of events is implemented in SIMULINK.

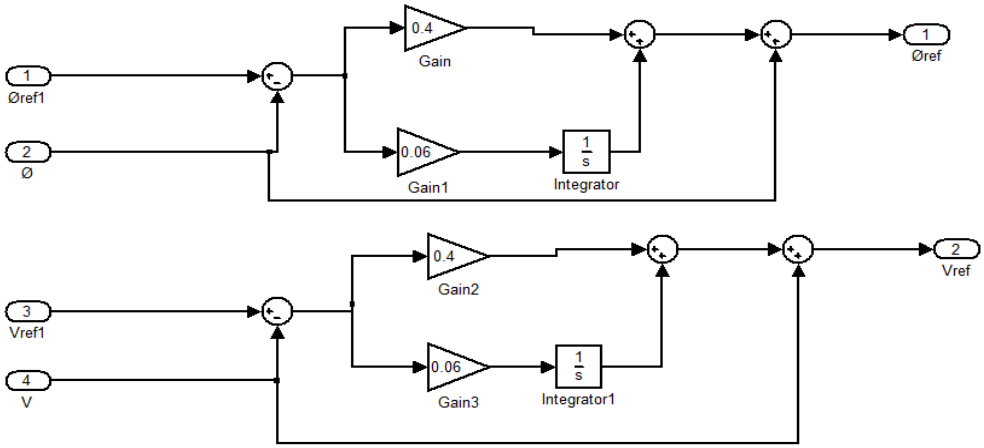

(a) PI controller for reference voltage and phase generation

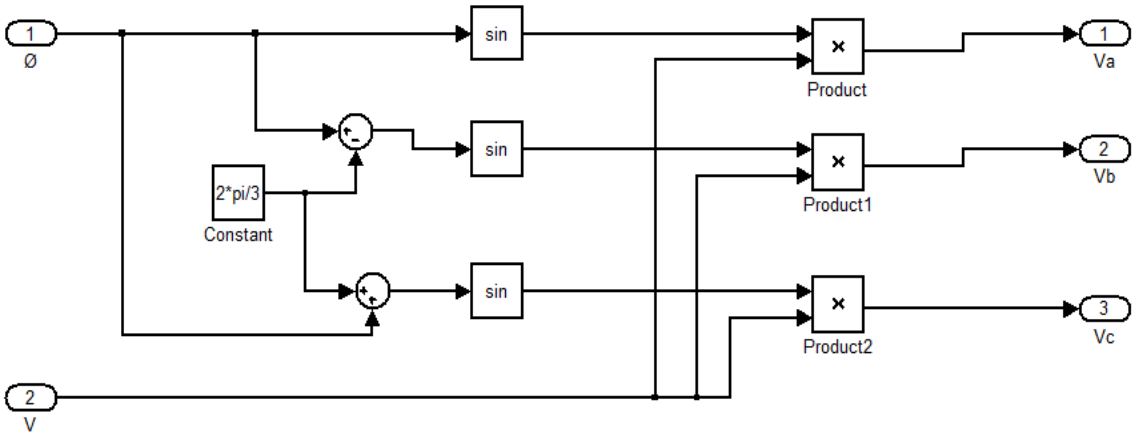

(b) Sine wave generator for PWM unit

Figure 5-10: Modulating signal generation unit

6. Then overall MS droop controller in island mode (V-f) controller and in grid-connected mode (PQ) controller are designed.
   (a) The SIMULINK model of V-f droop controller in island mode is shown below:

;

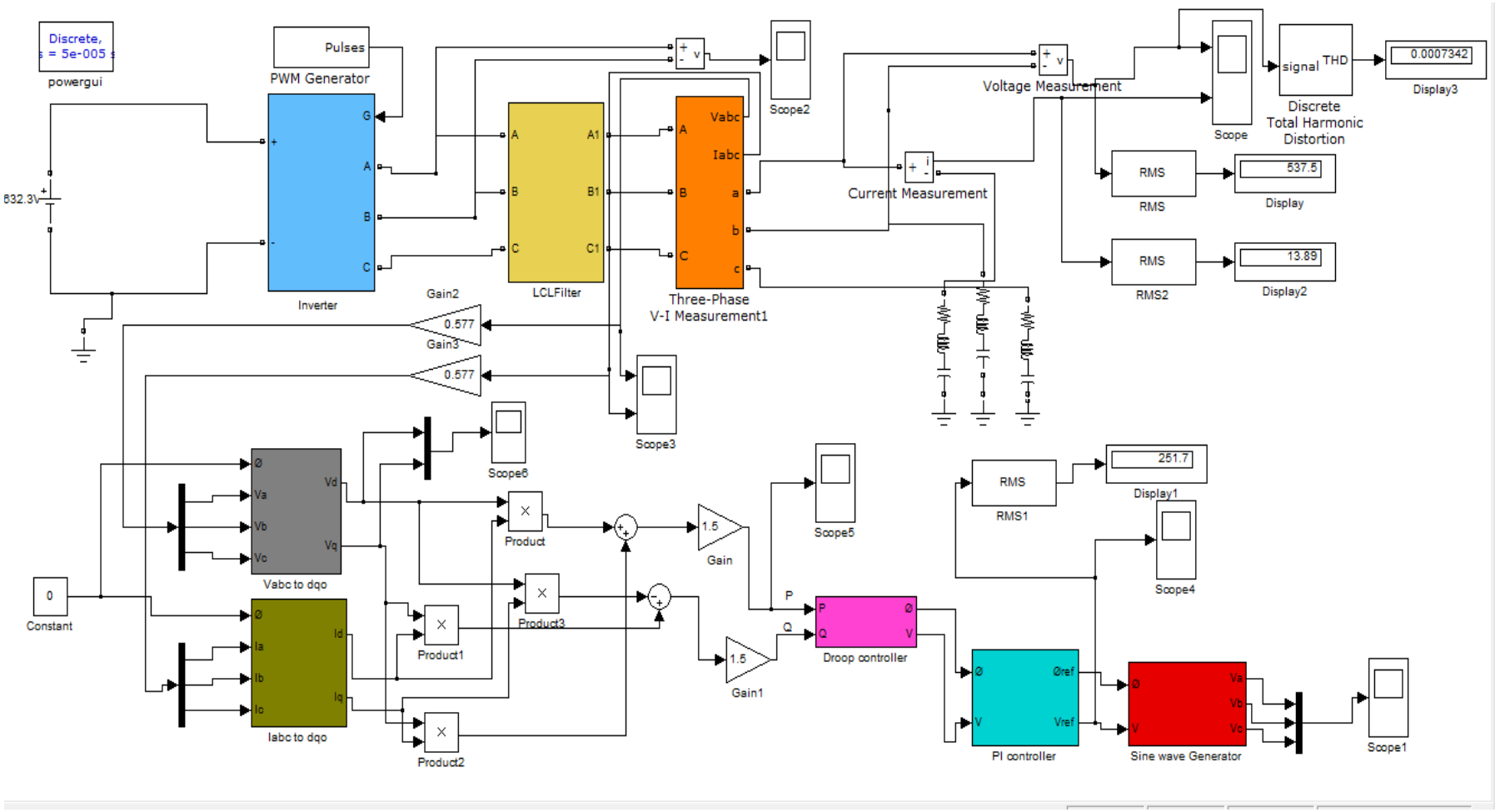

Figure 5-11: Complete features of MS controller during islanding in SIMULINK

The microsource used to test the MS controller is the SOFC unit; all the parameters given are that of SOFC. It is assumed that during islanding a voltage deviation of 2V and frequency deviation of 0.5 Hz were allowed. There is some deviation in the magnitude of the output voltage wave form of the MS controller which is used as modulating signal to the PWM generator. This is believed to be due to some harmonics generated by the source. According to [38] abc to dqo transformation is only possible if only the phases are symmetric. So if there is a distortion in Park transformation stage, it will be reflected on the upcoming processes. The following is the final output voltage wave form to be applied in to PWM unit.

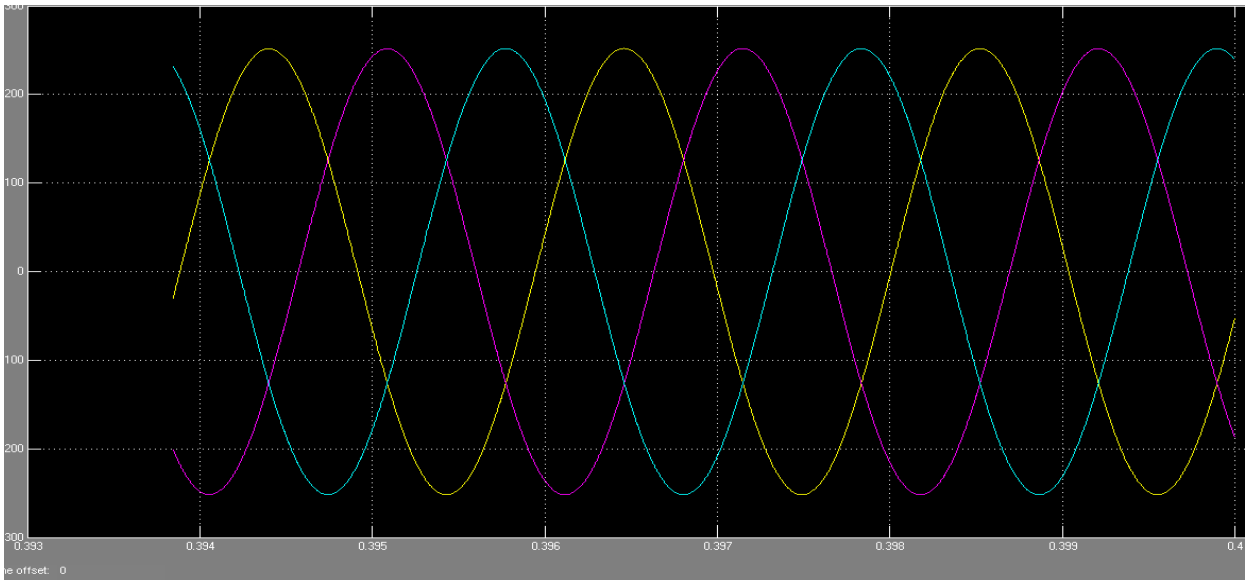

Figure 5-12: The output voltage wave form of MS controller during islanding

Therefore this voltage generated from the controller may not be applied to the PWM unit. As a solution a standard wave generator and a selector switch can be included in the MS controller design so that the standard wave is selected if the controller output is not up to expectation. Then the selected wave from is applied in to PWM unit so that voltage and frequency restoration and seamless transition are ensured. The standard wave form is shown below.

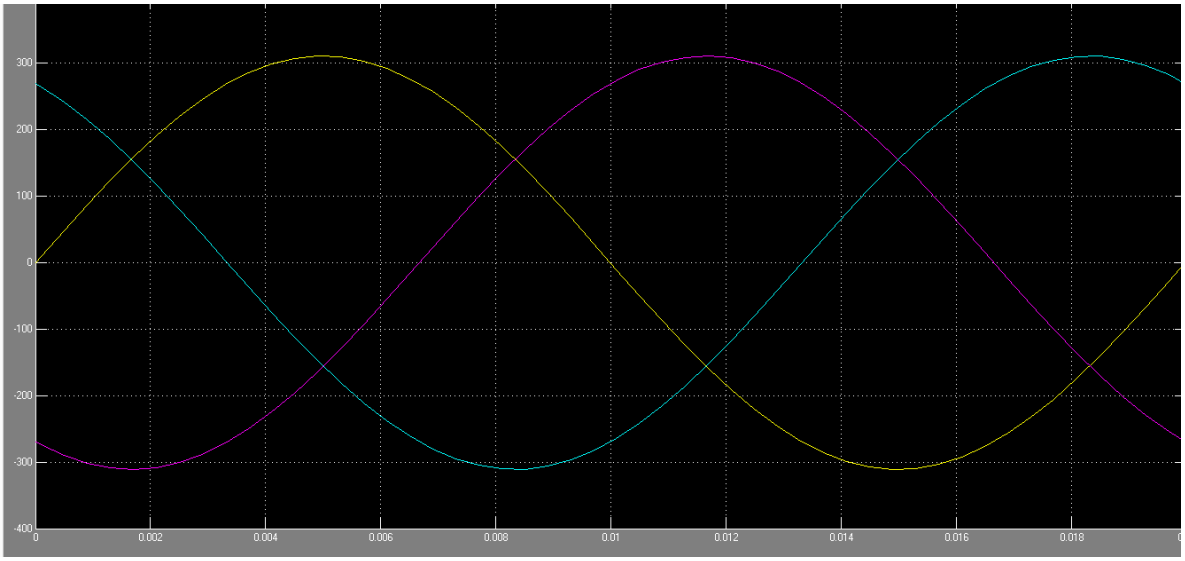

Figure 5-13: Standard wave form generated from sine wave generator

(b) The SIMULINK model of PQ droop controller in grid-connected mode is shown below:

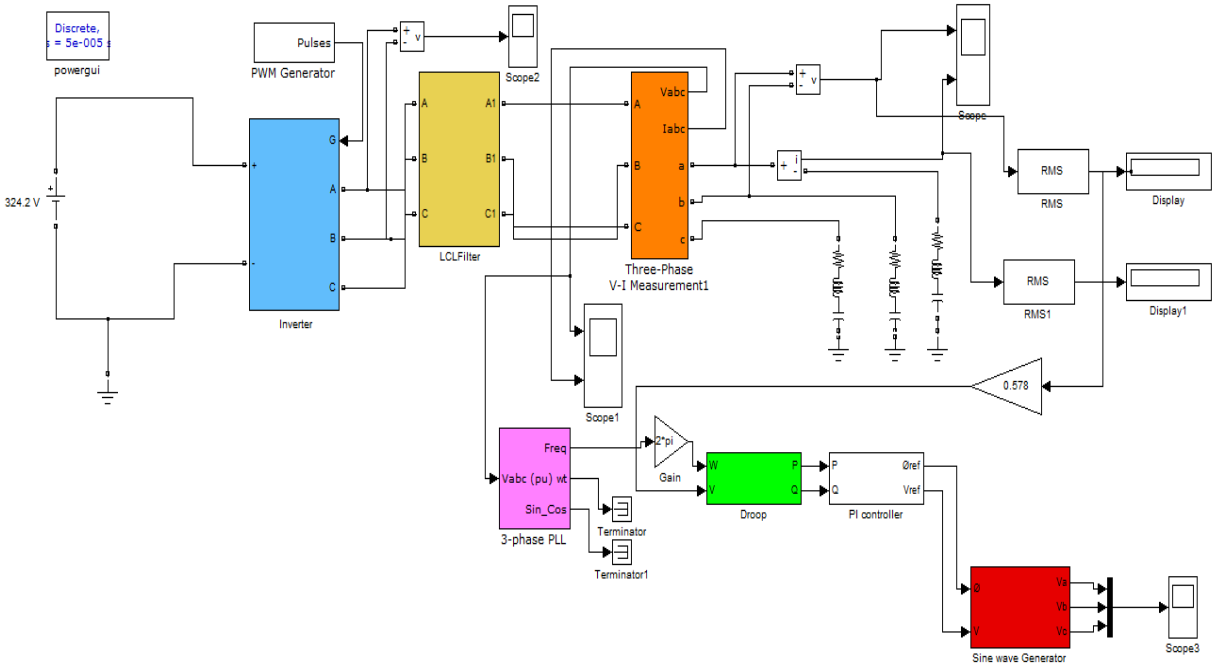

Figure 5-14: SIMULINK model of PQ droop controller

In PQ control the droop technique is not suitable in SIMULINK model as the zero crossing is more than two, which is not appropriate for frequency measurement. So for the PQ control method the non-droop control technique is applied. The only difference is the calculated active and reactive power from park transformation unit is fed in to the PI controller out of which a reference phase and voltage magnitude are provided to the sine wave generator. The PQ controller model and the standard sine wave output are demonstrated in SIMULINK below.

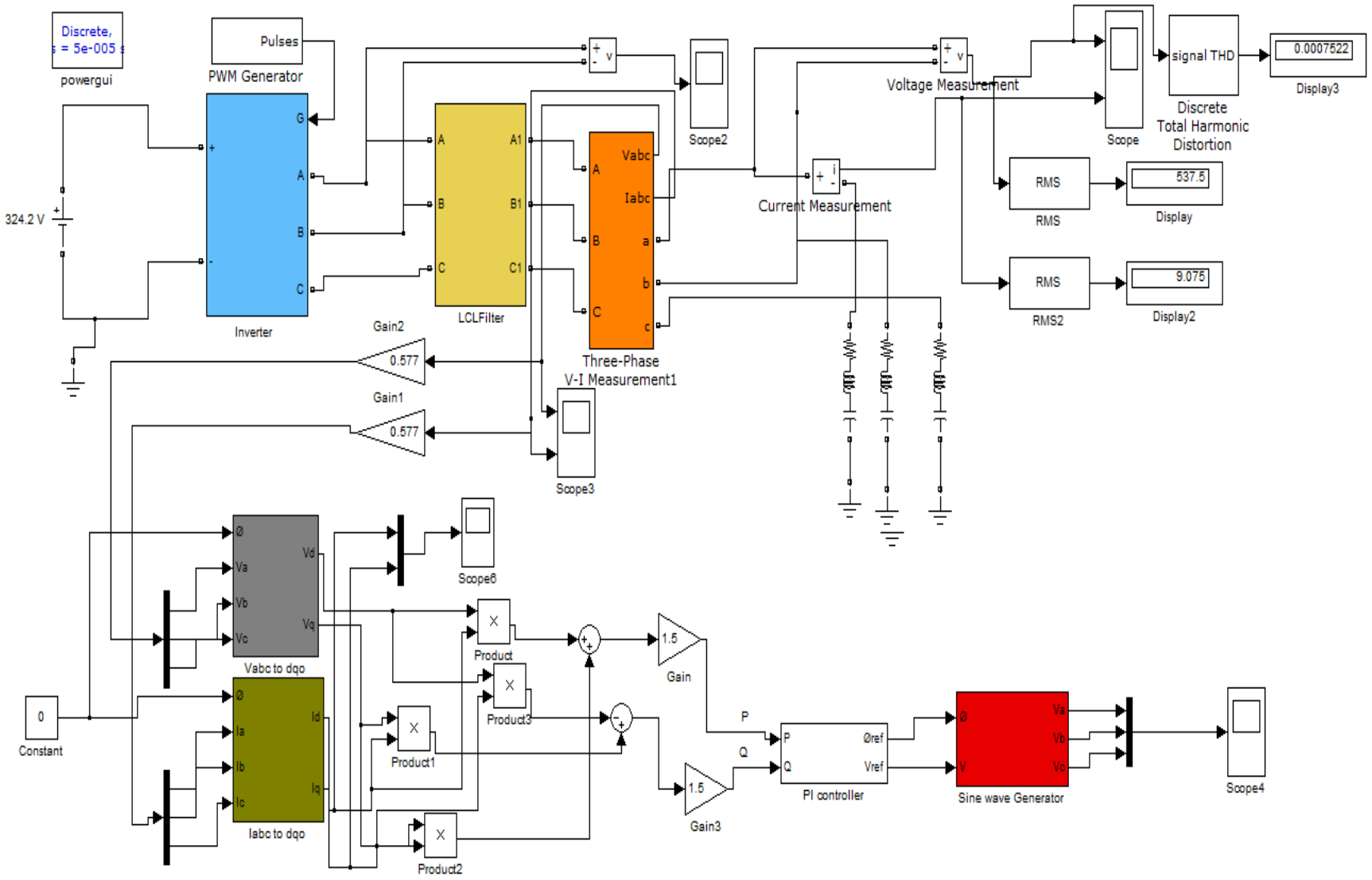

Figure 5-15: Non-droop PQ controller in grid connected mode for PV

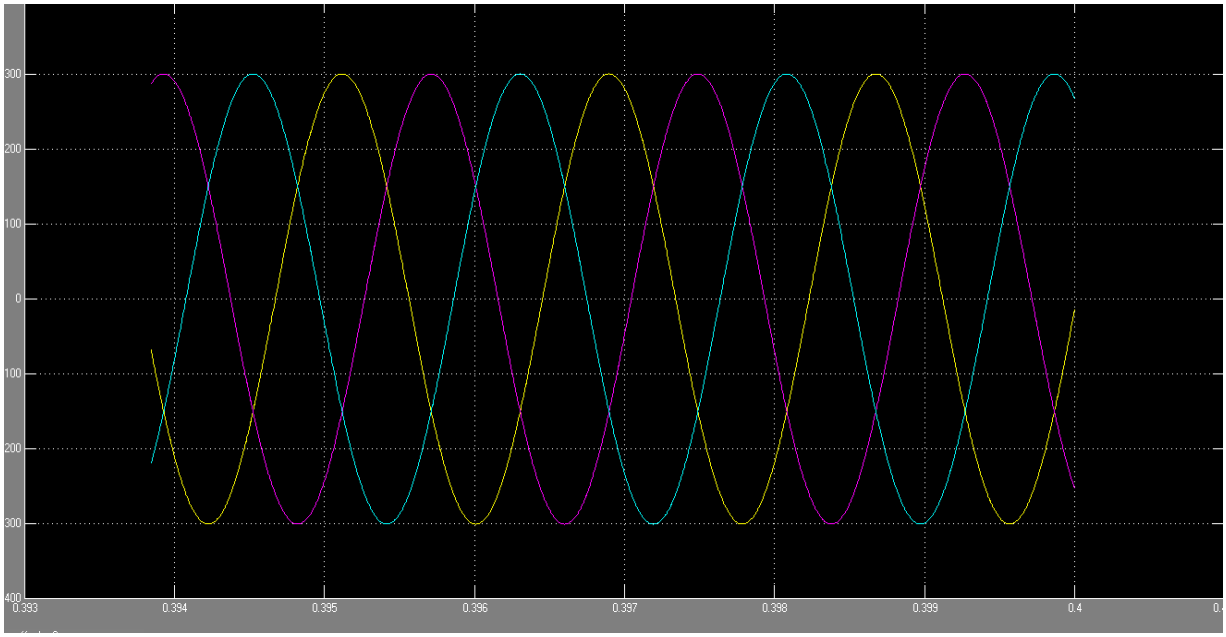

Figure 5-16: Output voltage wave form of the PQ controller

5.6.1. Power sharing simulation

The load sharing in the Microgrid is carried out in proportion with the rating of each microsource. The proportional power sharing is according to the droop control technique whereby the P-f and Q-v droop coefficients are calculated, and the load sharing is calculated from equation (5.11). The load sharing scenario is simulated with all microsources and their respective droop controllers participate in both grid-connected and island mode of operation of the Microgrid. The change in power generation from individual microsource during load change due to switching between islanding and grid connected mode will be demonstrated in SIMULINK too.

The algorithm of connecting the microsources and their corresponding Microsource controller (MC) in SIMULINK environment for power sharing control mode is described as follows;

1. The three phase voltage and current from the corresponding microsource subsystem which contains the micro-generator, inverter and filter are facilitated for connection with droop controller subsystem in the following way;

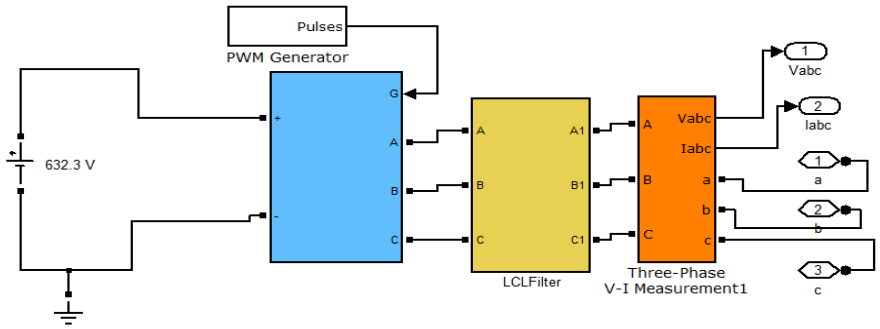

Figure 5-17: SOFC subsystem

2. Each microsource subsystem is connected to the corresponding microsource droop controller subsystem. The droop MC contains park transformation units which convert the three phase voltage and current waveform in to dqo form and the droop controller unit. The subsystem is shown below;

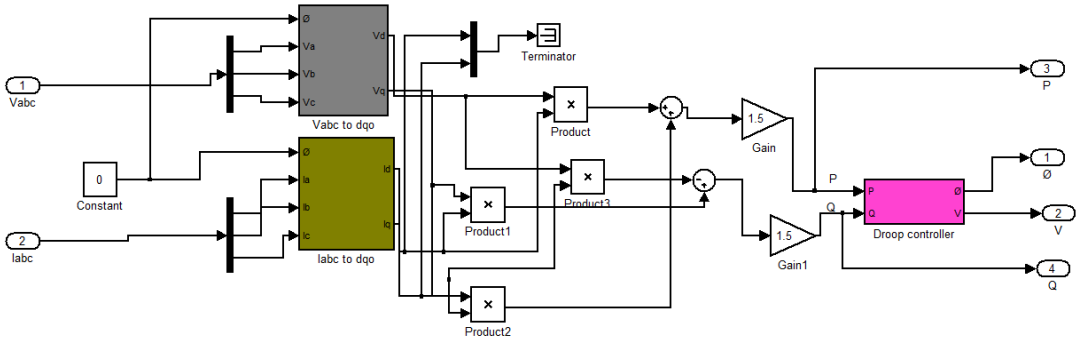

Figure 5-18: MS droop controller subsystem

3. All the three microsources with their corresponding controller are connected at a common AC bus point at which the estimated loads are connected.
4. The estimated load is subdivided in to two equal parts so that they are connected to the microsources through clocked circuit breaker which represent the STS in the real MG. Half of the load is connected when the clock is low (off) to disregard the other half to simulate the grid-connected mode of operation of the MG.
5. The total load is connected to the MG when the clock of the circuit breaker is high (on) to simulate the island mode of operation of the MG.
6. The power sharing status of each microsource can be checked through the scope connected at the outputs of the corresponding droop controller.

The following is a flow diagram which demonstrates the operation of the proposed MG.

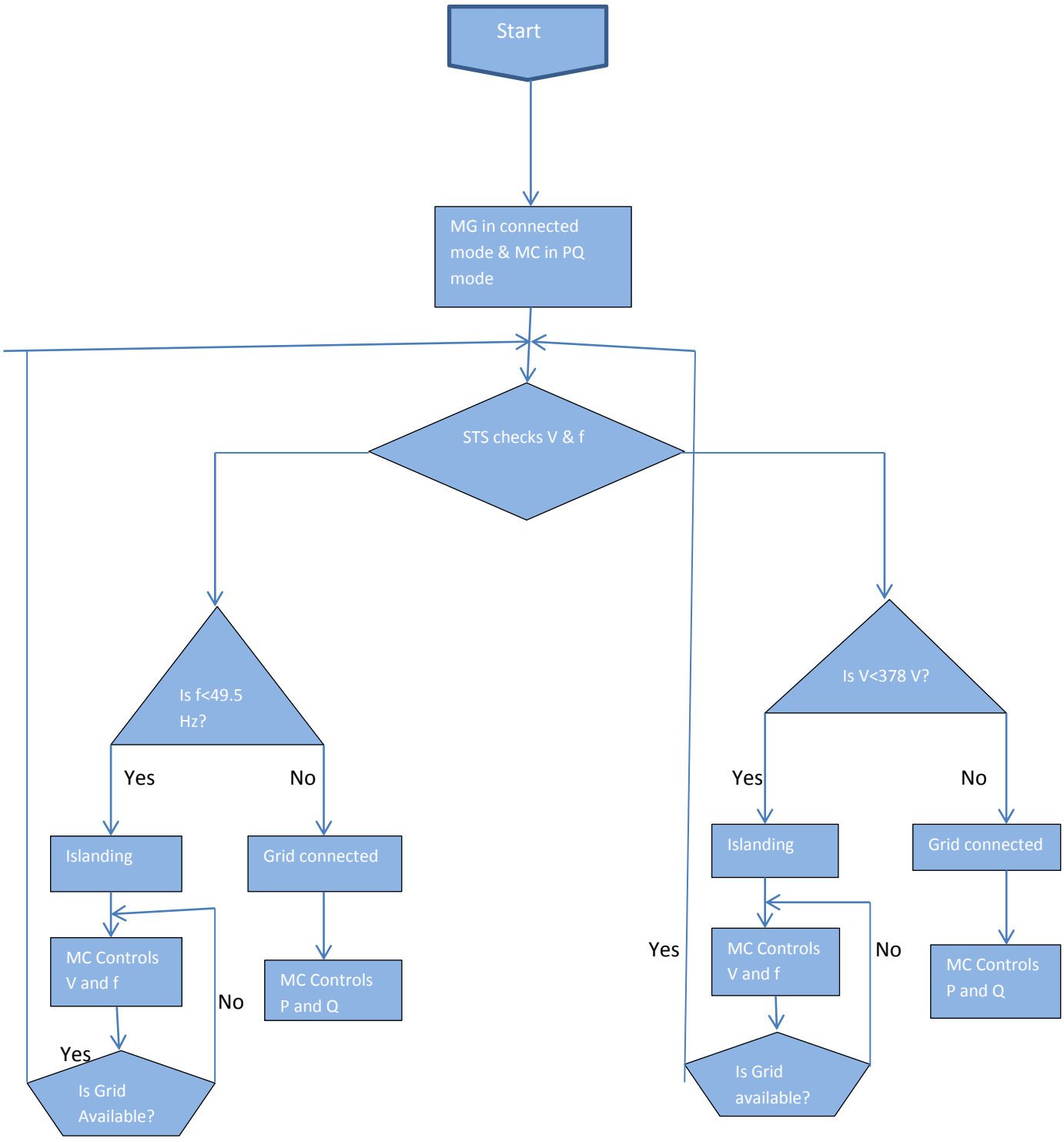

Figure 5-19: Flow diagram of modes of operation of the Microgrid

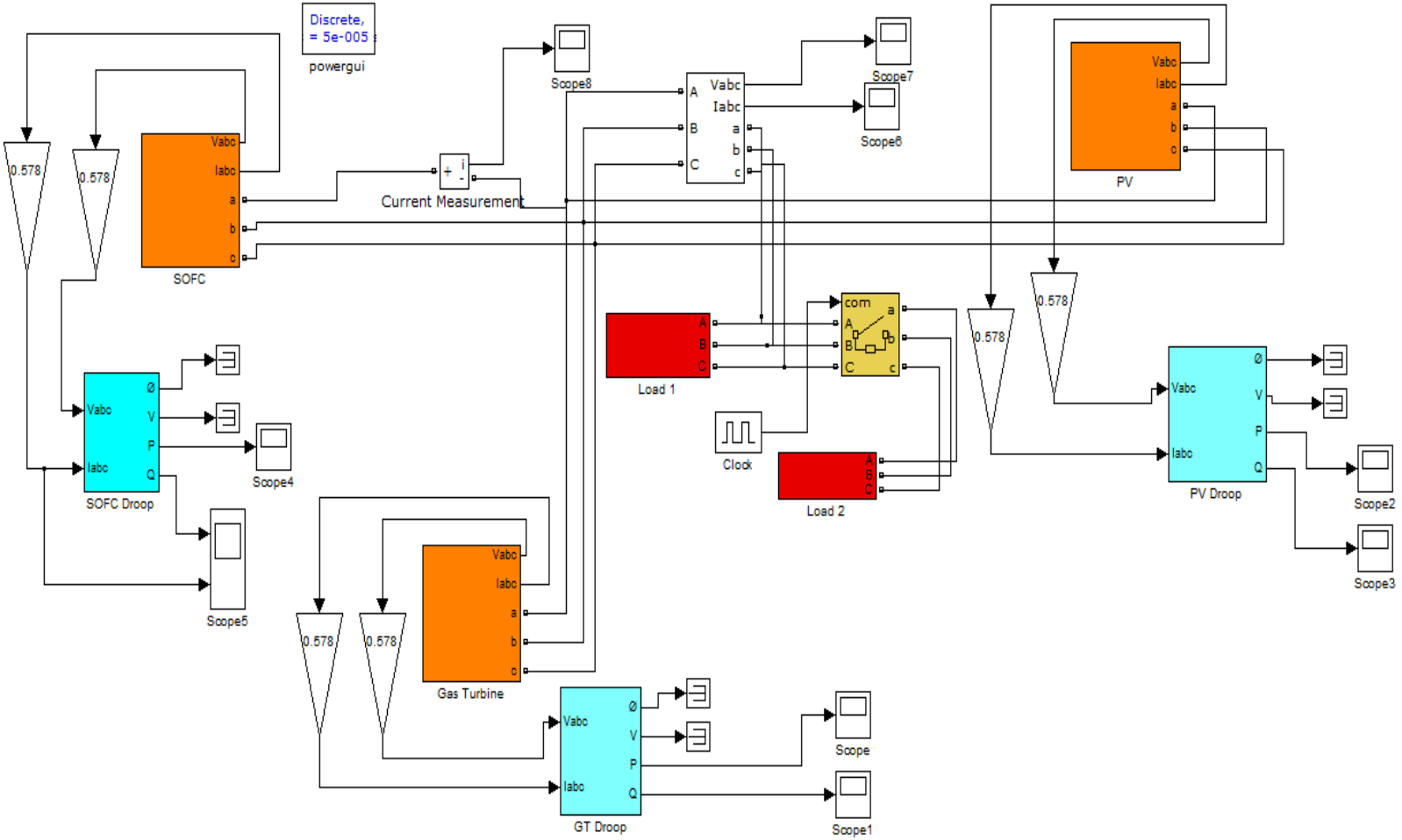

Figure 5-20: Power sharing simulation model of the Microgrid in SIMULINK

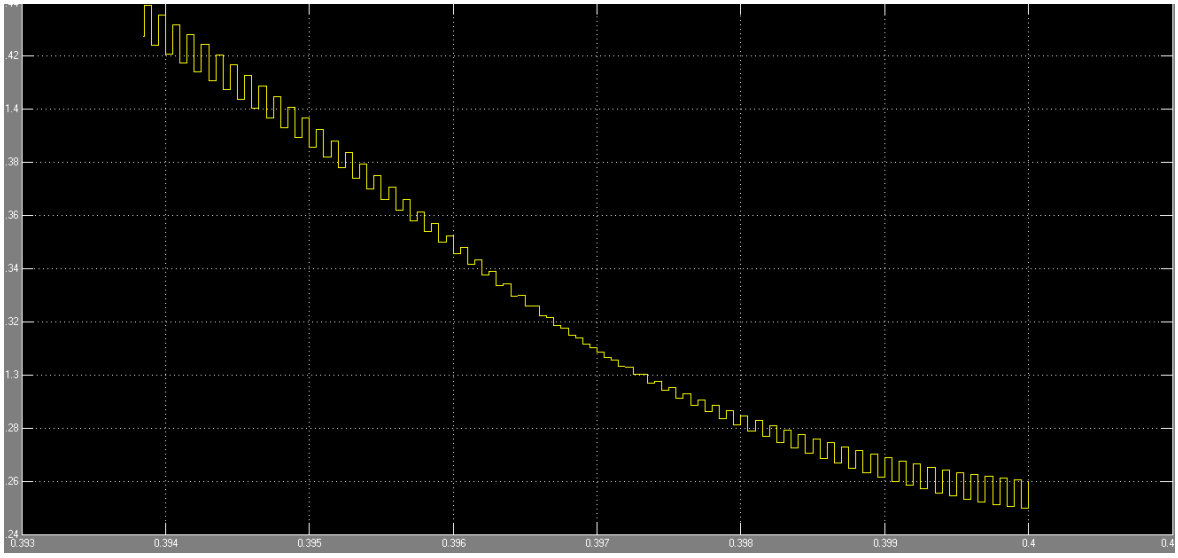

Figure 5-21: Active power output of the SOFC in Grid-connected and islanding modes

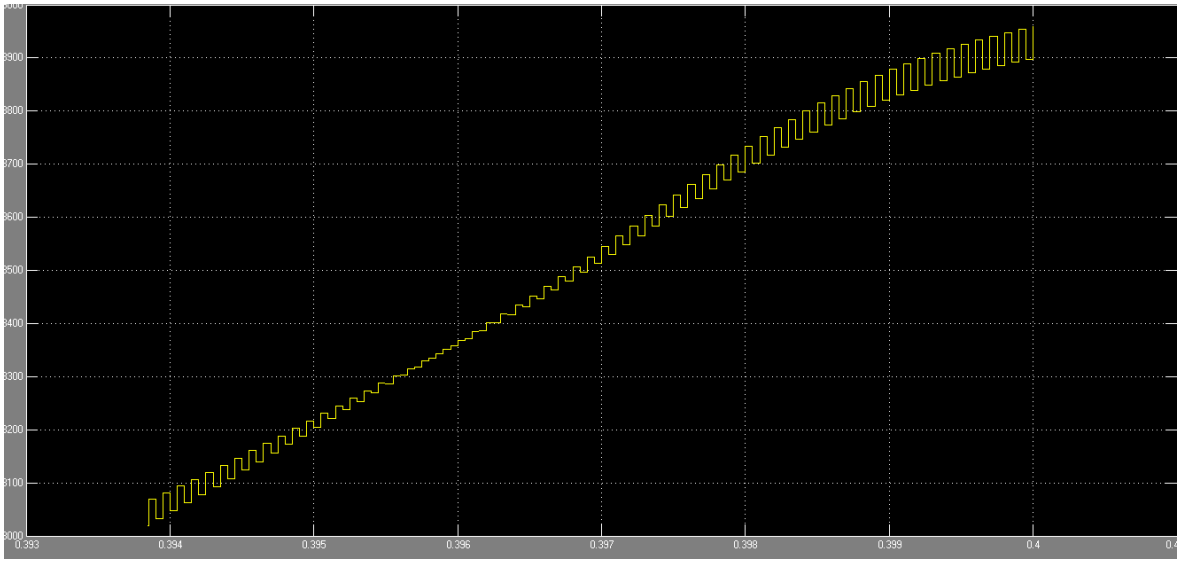

Figure 5-22: Active power output of the PV in Grid-connected and islanding modes

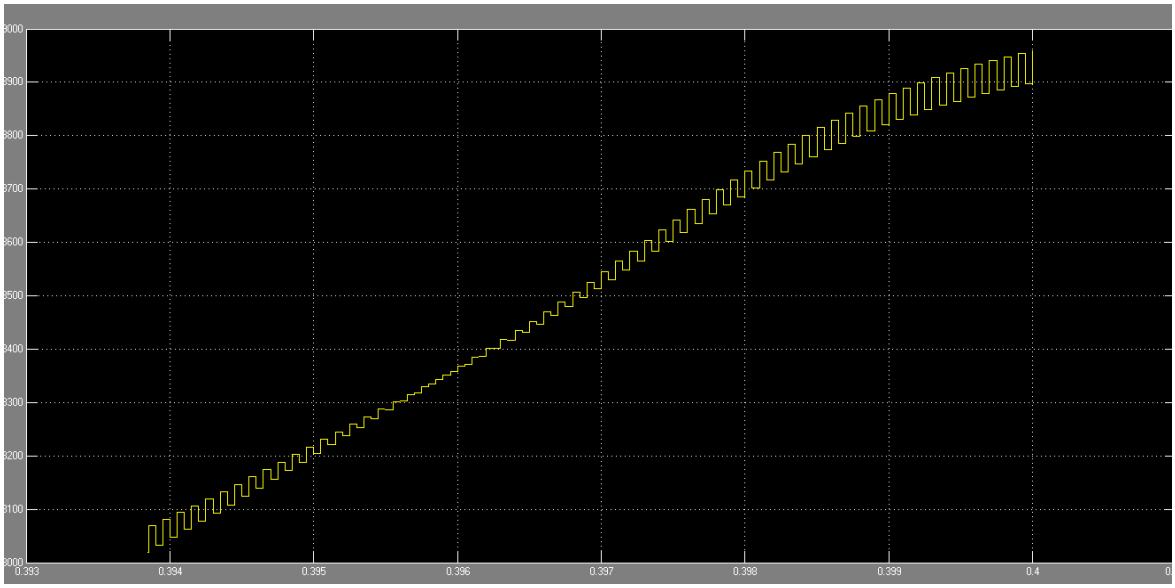

Figure 5-23: Active power output of the GT in Grid-connected and islanding modes

CHAPTER SIX

Results and Discussion

6.1. Introduction

In the previous two chapters the details of designing Power Electronic Interfaces (PEIs) and Microsource controller for ISOFC/GT have been discussed. The designed PIEs and MS controller has been tested through simulation in MATLAB/SIMULINK. There are satisfactory and bad results obtained from the simulations. In this chapter, detail investigation will be given under each design. In doing so detail parameters of individual design together with mathematical analysis will be also given to show the discrepancy between the real design and the theoretical background.

6.2. Power Electronic Interfaces

6.2.1. Inverter

The design of PEIs has been started with that of inverter for the SOFC microsource. The mathematical relationship between the input DC source and the phase to phase AC output voltage is not reflected on the real design. According to [28] the mathematical relation is given as;

$$V_{ab} = \frac{4V_S \cos 30}{\sqrt{2}\,\pi} \qquad (6.1)$$

This mathematical relationship considers that only the fundamental component is filtered out. So for the relationship to be realized a DC source of 487.4 V is required to get an output of 380 V phase to phase AC voltages. But in our case an input DC voltage of 632.27 V is required in the case of SOFC source to supply a load of 20 KW with 0.95 Pf. This is because the theoretical relation doesn't consider the amount of power that a load consumes. There is no mathematical formula applied which correlate the input DC source, the output AC voltage and the load. So manual tuning was used to match the required inverter output AC voltage with the input DC source while simulating in SIMULINK.

The output voltage has good sinusoidal wave form and its frequency is 50 Hz. It also looks like that there is no any harmonics. When the Total Harmonic Distortion (THD) is measured, it is almost zero. But when it is converted in to dqo form, the output results are not typical DC; rather they somehow oscillate. The resulting wave form of the dqo conversion is shown below.

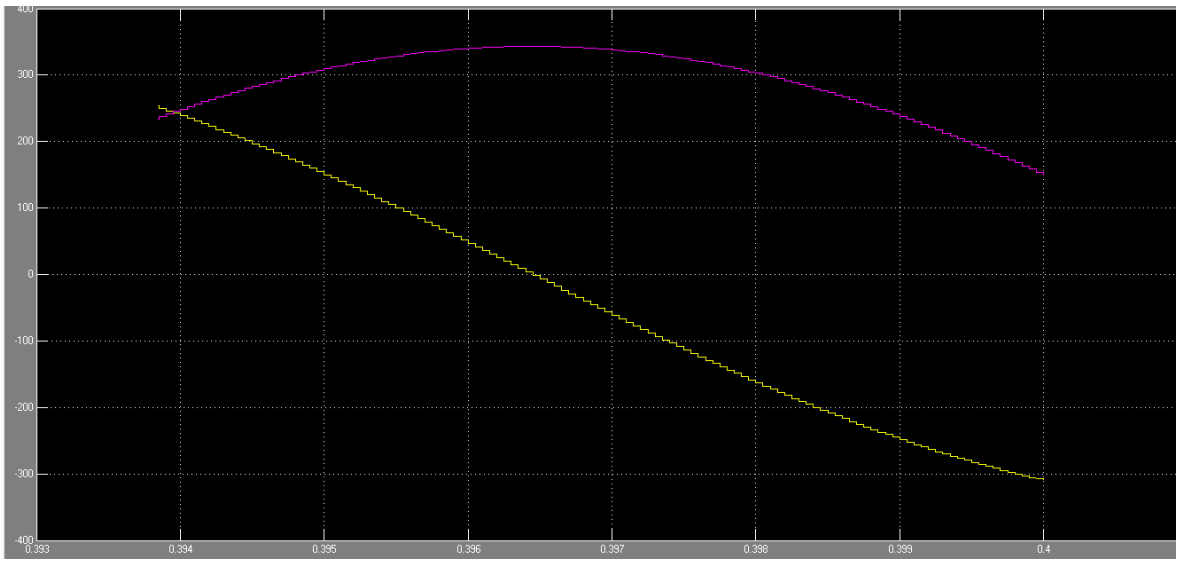

Figure 6-1: dqo output wave form of the AC voltage from inverters

From the SIMULIK simulation result it is possible to conclude that the output AC voltage from the designed inverters are not harmonic free and symmetric as they seem to be.

As far as designing of the low pass filter is concerned, two scholarly papers [33&34] claim that it possible to get good filtering using different approaches of their own. The first approach uses the following formula to select the appropriate inductor and capacitor:

$$f_0 = \frac{1}{2\pi\sqrt{LC}} \qquad 6\text{-}2$$

According to the formula an inductor size of 2 mH and a capacitor size of 5 mF were obtained to get a frequency of 50 Hz. The other option uses the formula already used in this paper. The simulation result of the first technique shows that there is distortion in output wave forms. So the

second technique is considered as a better option. The size of the additional inductor is chosen based on the first method sticking to the formula $f_0 = 1/2\pi * \sqrt{L + L_t / LCL_t}$. Where, L_t is the additional inductor to the components in the first technique. The simulation results of the two techniques are shown below.

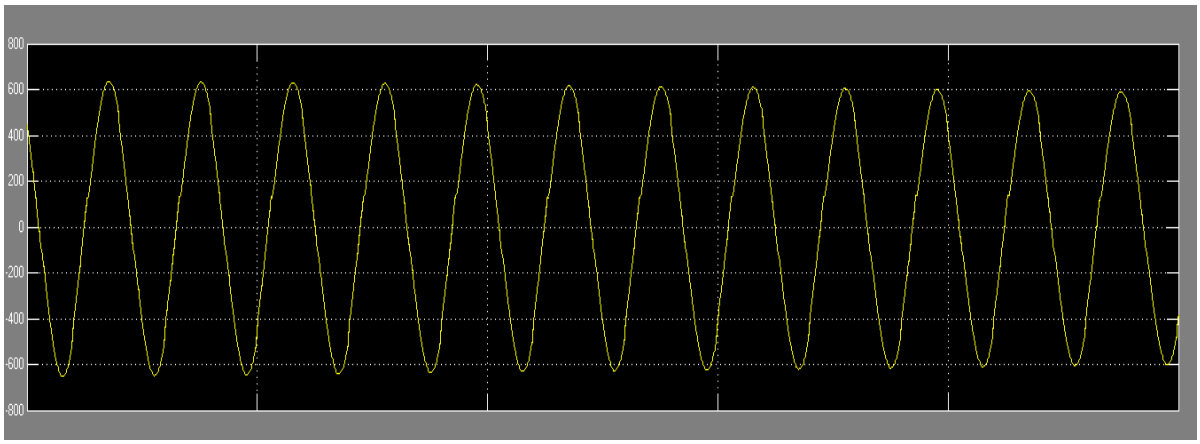

(a) Wave form obtained from LC filtering method

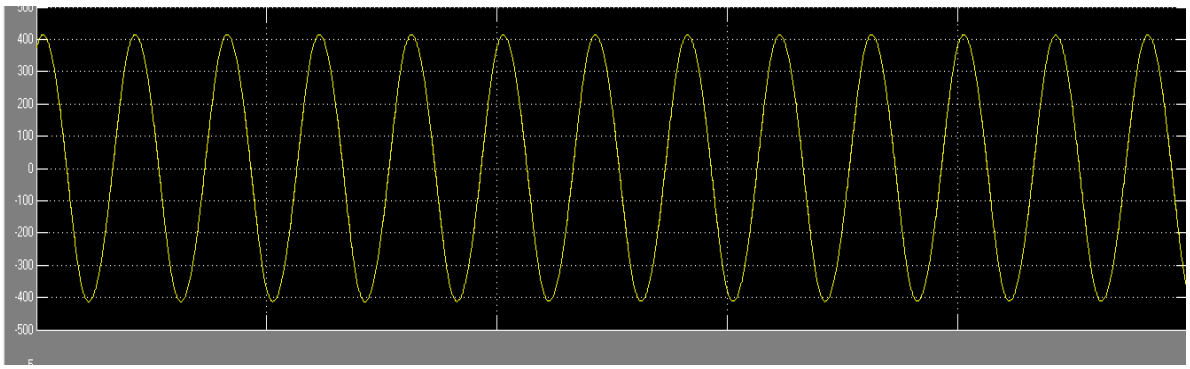

(b) Wave form obtained from LCL filtering method

Figure 6-2: Simulation results of LC and LCL filtering techniques

As observed from the simulation results the LCL filtering method is better than that of LC. Plus it contributes for the total output impedance of the inverter to be inductive so that the droop character equation holds. And the decoupling of the active and reactive power will be realized too.

6.2.2. DC-DC boost converter

From the DC source input of inverters it is possible to decide what kind of DC-DC converter to be used so that the required voltage level is achieved. As already mentioned the intention in this paper is to avoid use of transformer and reduce the size of the generating unit in terms of the DC voltage magnitude to be introduced in to the DC-DC boost converter so cost of micro-generator is reduced. The kind of DC-DC converter which meets the two themes is the two stage DC-DC boost converter.

As already mentioned in the previous chapter, the following are common parameters used in designing the two stage DC-DC boost converters:

Switching frequency = 25 KHz

Pulse width used for switching = 75%

Pulse amplitude = 2 V

The duty ratio of the switching pulse determines the output of the converter. In this paper the duty ratio is 0.75. So the output of the single converter would be four times the input according to equation (4.8). Following the mathematical relationship between the input and output voltages stated in equation (4.10), the magnitude of the output is eight times that of the input one. The other determining factor for the converter is the sizes of the inductor and capacitor selected based on the mathematical model already mentioned previously so that the inductor current and capacitor voltage should have minimum ripples. The inductor current ripple is chosen according to frequent practices in different studies (0.3-0.5 A), and that of the ripple voltage is set by tuning so that the main mathematical models will not be violated, plus it should be too small.

The following are the parameters used for each sources.

SOFC

Source voltage 79.33V

L_1 = 6.96 mH

C_1 = 8 mF

L_2 = 13.92

C_2 = 16 mF

Output Voltage = 632.27 V

As we can see from the parameters given above, the mathematical relationships given in the previous chapter are maintained except few deviations due lack of exactness in the size of capacitors and inductors. The input voltage is stepped up eight times. The sizes of inductor and capacitor of the second stage (see fig. 4-14) has doubled from the first stage. In the simulation result the output voltage seems to increase linearly with time. But it will settle slowly to the final value. This scenario can be demonstrated by increasing the sample time from 50 µs to 500 µs in discrete mode of the SIMULINK simulation. But in doing so the mathematical basic is violated. This is shown in the simulations below.

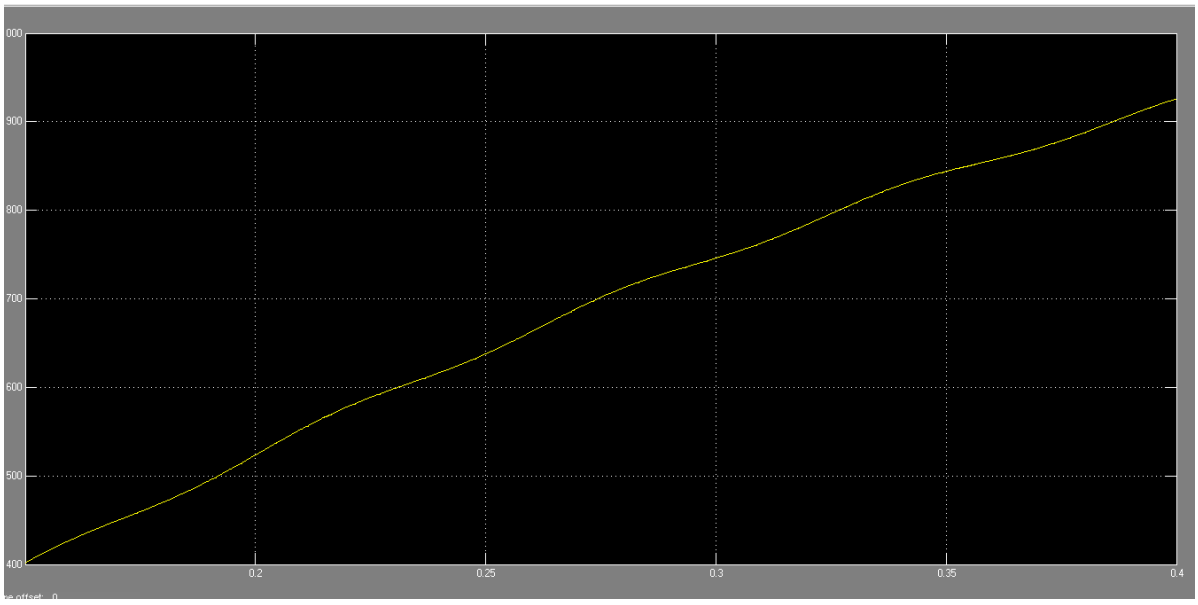

(a) Output DC voltage at 50 µs sample time

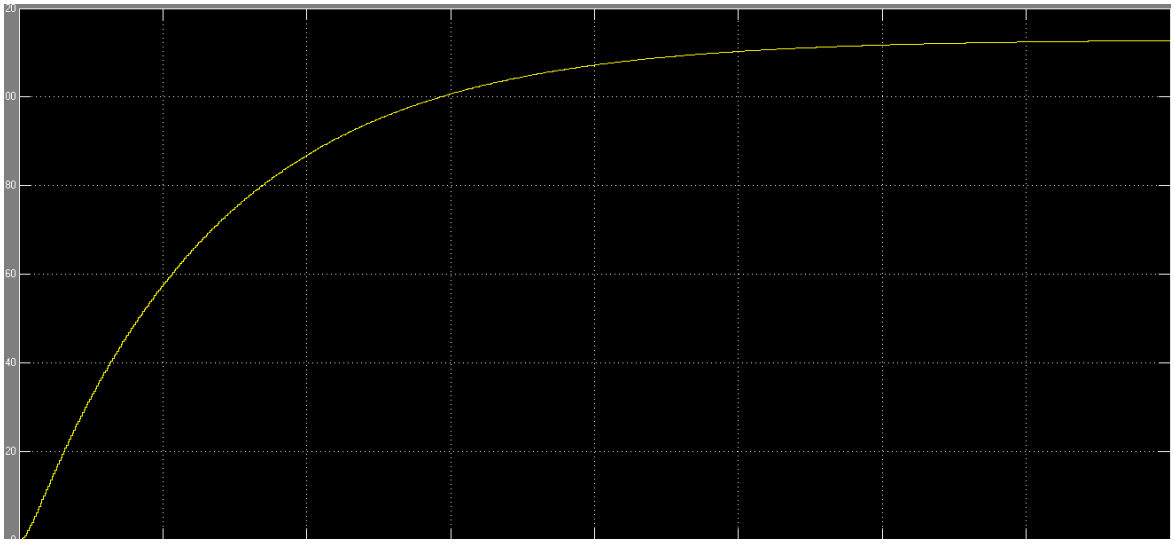

(b) Output DC voltage at 500 µs sample time.

Figure 6-3: Output voltage response change Vs change in sample time

PV and GT

Since both the PV and GT are assumed to supply equal amount of power, the design parameters are all the same in DC-DC conversion. Plus all the mathematical relationships described in the SOFC case are also maintained here; also the change in output response due to change in sample time is also reflected here.

6.2.3. Rectifier

The GT microsource to be included in the proposed MG needs a rectifier so that the high frequency output voltage is changed to DC form followed by DC stepping up and inversion. It could have been possible to use double shaft GT equipped with gearbox which helps generation of AC voltage with required frequency (50 Hz). Though it eliminates the need for PEIs, it can't be controlled electronically to involve in a MG operating in grid-connected and island mode. To facilitate the GT with control unit, to make compact in size and eliminate the gearbox, this study opts for the high speed single shaft GT. The output of the rectifier has to meet the need of the DC-DC boost converter as per the intent of this study. SO care was taken in determining the rating of the gas turbine. The design parameters of the rectifier are described below:

Phase to phase input source voltage (rms) = 200 V

Filter capacitor = 0.27 mF

Output DC voltage = 40.42 V

Frequency of the input AC source = 3000 Hz

The selection of the filter capacitor was carried out by tuning so that reduced ripple of output DC voltage is obtained. As the size of the capacitor is reduced, the ripple level increases, the response is fast and there is transient. So the design considers less ripple voltage, no transient and also reasonable response. These events are shown in the simulation results below.

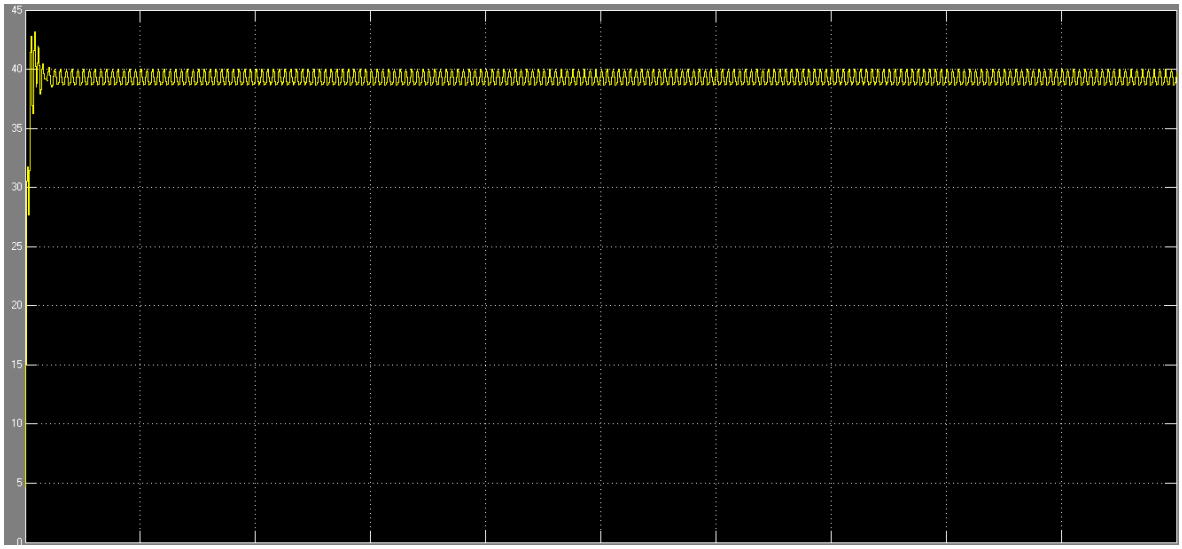

(a) Output voltage response with 2.7 µF filter capacitor

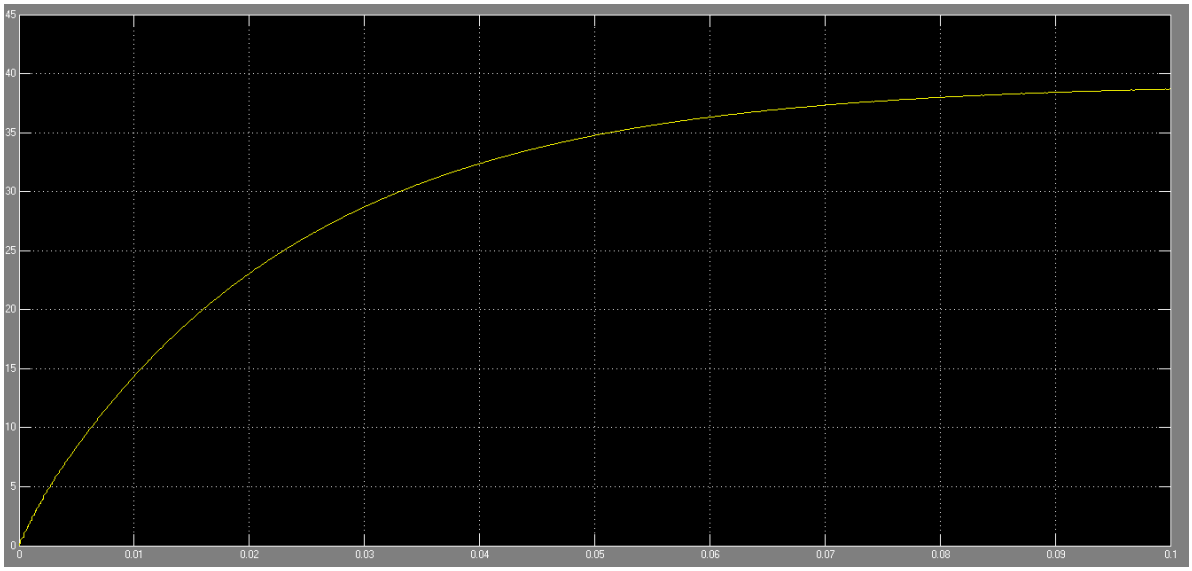

(b) Output voltage response with 0.27 mF

Figure 6-4: Change in ripple content and response of output voltage

6.3. Microsource Controller

Controlling microsources of a Microgrid is based on the two modes of operation that dictates the change in active and reactive power and the change in voltage and frequency of the microsources. In grid-connected mode of MG operation the MS controller unit controls the power flow so that each microsource contributes a certain level of power while the voltage and frequency level are controlled with the grid voltage as a reference. In island mode of operation, the MS control unit controls the voltage and frequency of the microsource inverter whereas the power flow is dictated by the loads in the Microgrid. Both types of control are carried out by droop control techniques; which are specifically known as PQ droop control and V-f droop control.

6.3.1. V-f droop controller

According to the results obtained in simulation, some deviation in the output voltage magnitude of the v-f droop controller was noticed. So it may not be appropriate to provide this voltage wave form to the PWM generator as far as generating good quality voltage in terms of its magnitude and frequency. So switching to a standard sine wave generator is considered as an option in this study when the v-f droop controller out is not up to expectation.

6.3.2. PQ droop controller

In designing the PQ droop controller, proper technique was used so that frequency and voltage output of the inverter are measured to control its active and reactive power. But unfortunately the expected results were not obtained during simulation. The only suspected cause is the incompatibility of the frequency and voltage measurements. Frequency measurement in SIMULINK needs only two zero crossings so that error is displayed before the assigned simulation time is elapsed. The PQ control design in SIMULINK which does not give the required AC output voltage is shown in figure 5-14, and its corresponding simulation result is shown below.

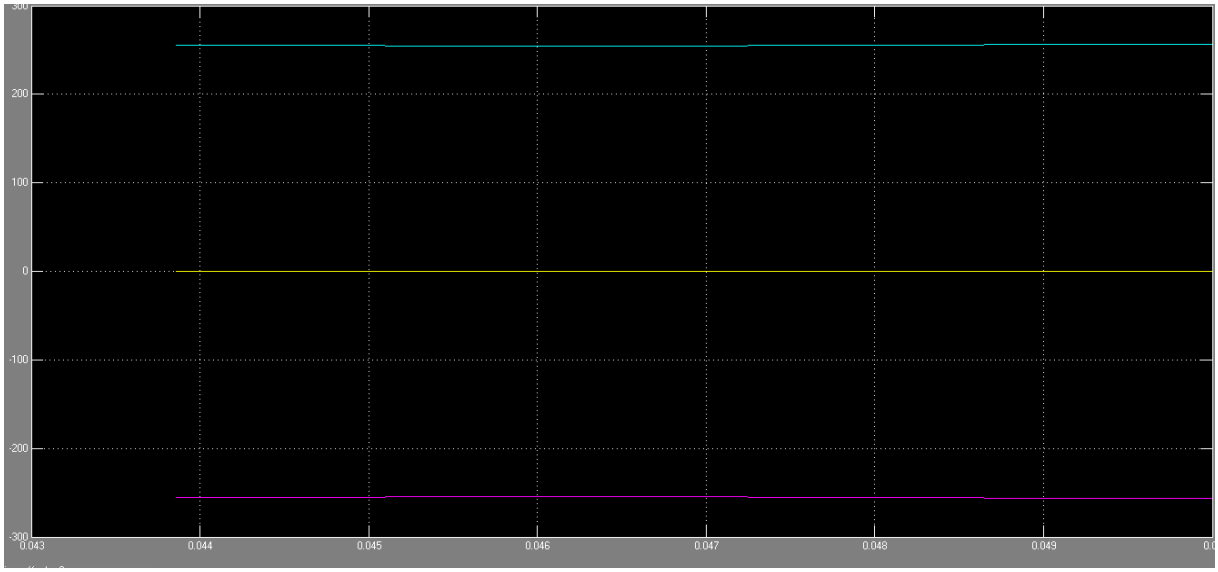

Figure 6-5: The simulation result of PQ droop controller

The expected output result is AC voltage waveform. Therefore as an alternative option, a controller which does not require droop controller is designed and tested on SIMULINK and a satisfactory result was obtained. But this design change can't be considered as a violation as far as the theme of this study is concerned.

6.3.2. Power sharing

Proportional power sharing among the microsources is the important feature of MS droop controller. According to the mathematical model described in equation (5.11), the maximum and minimum power sharing that a microsource can contribute depends on its rating and the respective

droop coefficients. According to the results obtained from the SIMULINK model (see fig. 5-21 to 5-23), the output active power from each microsource fluctuates and seems to settle at a certain value. This is due to the fact that the switching of operational modes simulated with clocked three-phase circuit breaker. The deviation from the real world experience is that bus bar, to which sources are connected and from which loads tap their power need, cannot be simulated in MATLAB. May be this and other deviation contribute to the oscillation of the microsources output power.

The other major issue to be raised is the response of the total current when there is change in load in the MG. There is change in the total current flow whenever load changes in the MG. But the change in current flow is not in proportion with the change in load. When load increases or decreases twice of the previous value, the total current doesn't do so. Transients were also observed subsequent to mode changes. These two events are shown in the simulation result below.

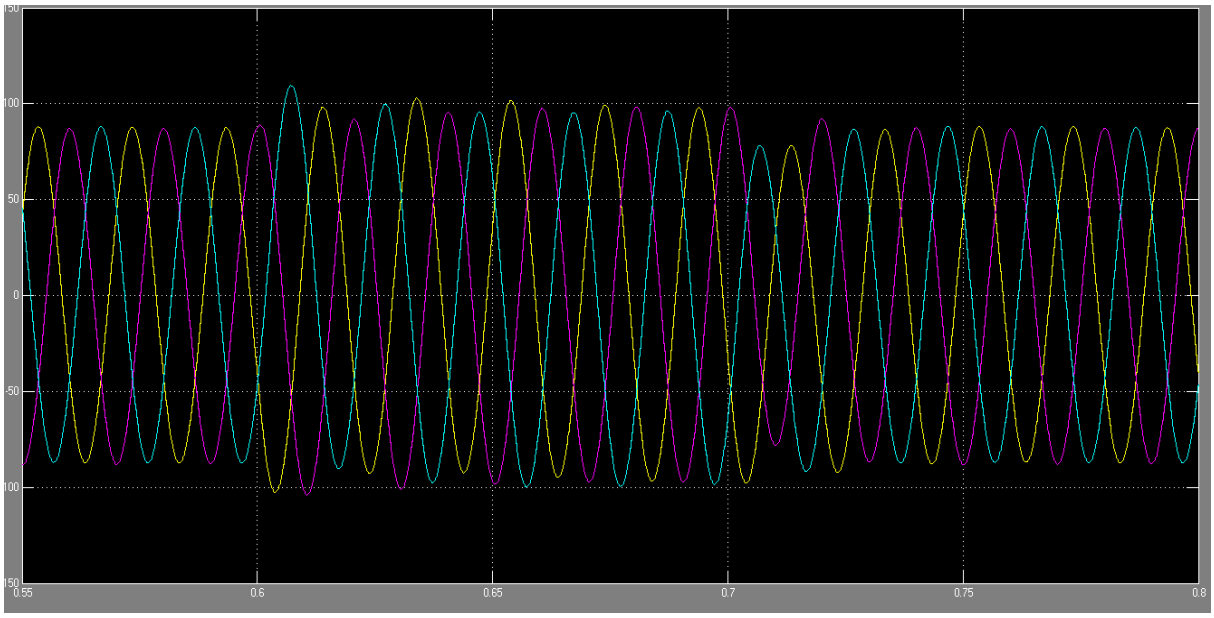

Figure 6-6: Total current response to change in load

6.4. Transition mode of MG operation

There is transition when a Microgrid switches between the two modes of operation. The special event considered in this study is that when there is fault in the utility the MG separates itself automatically from Static Transfer Switch. The moment the MG islands, the microsources like SOFC do not respond immediately to compensate for the utility supply due to lack of inertia and nature of the micro-generators. Till the microsources respond fully to the load changes the storage unit takes over the shortage of power supply. For the purpose of transition power shortage coverage this paper considers using a flywheel as a storage unit. As the inverter design for the flywheel can't be that much different from those already used for the microsources, there is no need to include the design process here.

The other important issue to be raised here is the resynchronization process when utility power supply is back to normal. STS checks whether the utility supply is up to the expectation in terms of voltage magnitude and frequency. But the problem is whether the restoration of the utility sustains so that unnecessary re-interruption will not occur immediately after the STS reclose. This study would like to propose a logical system which does check the sustainability of power restoration so that the reclosure at PCC and STS ensures reliable transition. The proposal recommends the use of two PLLs; one for each inverter and one for the main grid to measure the respective frequency and phase angle. The mechanism of STS without transition can be simulated in SIMULINK in the following way.

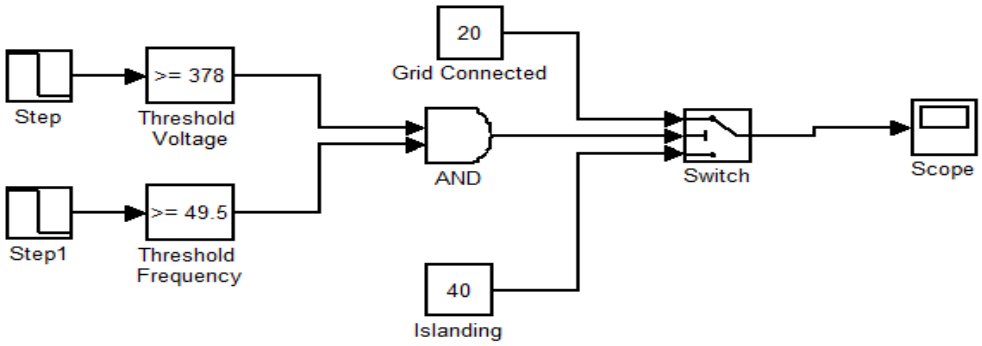

Figure 6-7: STS mechanism of operation in SIMULINK

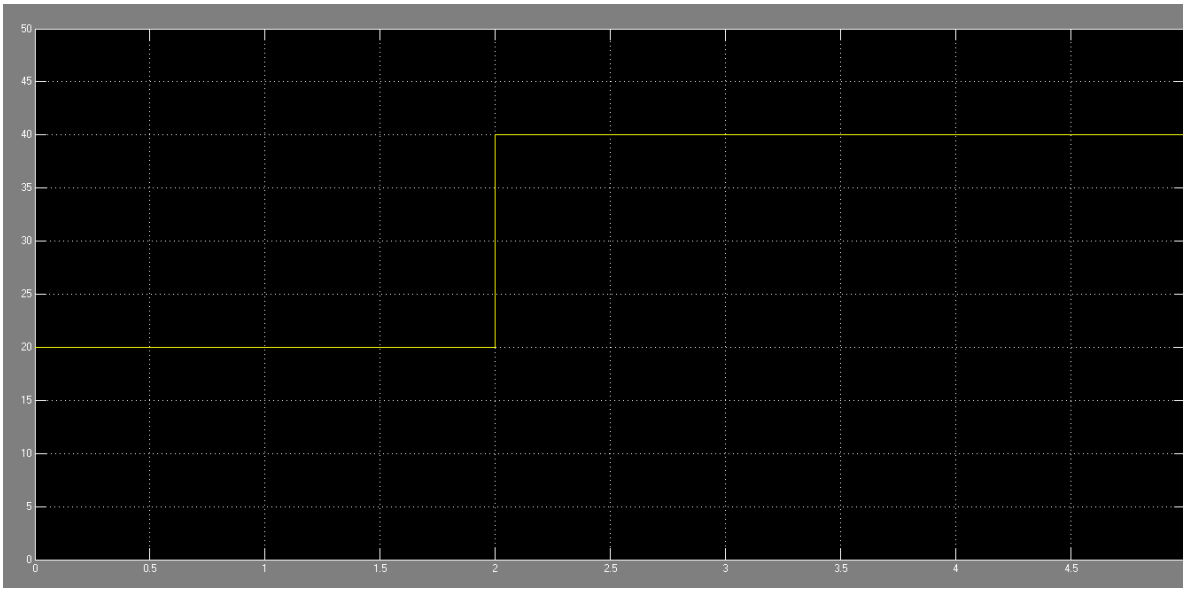

Figure 6-8: The switching of STS from Grid connected mode to Islanding.

The following flow chart demonstrates the application of the proposed logical system used in reclosure during resynchronization.

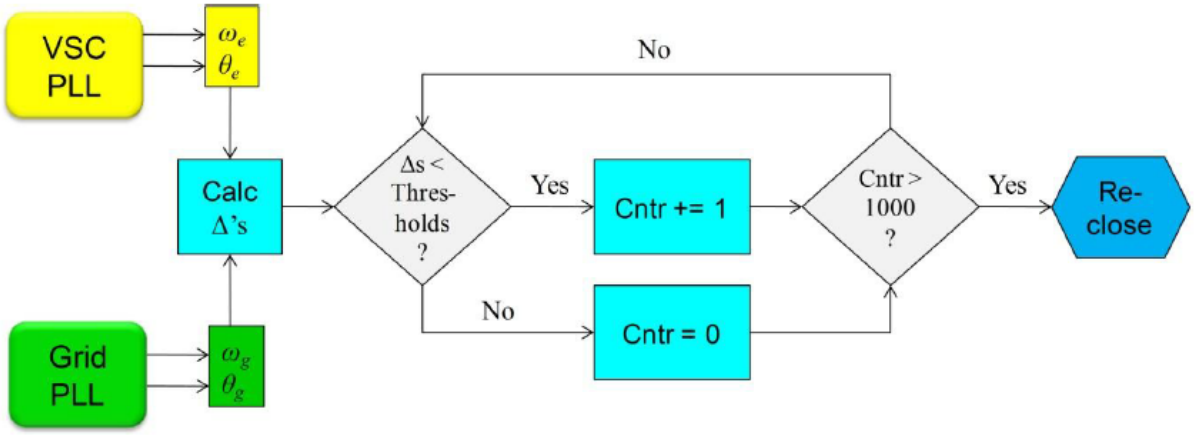

Figure 6-9: Logic Flowchart for Synchronization Determination.

The flowchart in Figure 6-9 outlines how the reclosure parameters are used; essentially, from the two PLLs, the frequencies and phase angles are compared against the limits set according to certain requirements, and if they are within the acceptable range, a counter is started. The counter must reach 1000 (three 50 Hz line-cycles assuming 20 kHz switching frequency) before the actual reclosure process can begin. If at any time, the compared values violate the limit restrictions, the counter is reset to zero. This allows

for an enforcement of the three line-cycles of synchronized operation before reclosure can take place.

6.5. PV without Battery

As already mentioned in previous chapters the PV microsource is supposed to operate without battery of its own. The intention of this thesis is that to switch to a reserve SOFC whenever power supply from the PV unit is decreased from a certain level during night time or when solar irradiance is low. This can be done by connecting a current sensing relay switch which can sense the decrease in current or power so that the supply is switched to the reserve SOFC. For this purpose this study has already assigned a reserve of 10 KW SOFC power supply which is equivalent to the rating of the PV. The proposed relay switch is connected to the two sources in such a way that it selects the SOFC when power supply from the PV is less than 10 KW. In other words the current sensing relay switch monitors the current of the PV circuit and switches the SOFC in case of an under current condition.

CHAPTER SEVEN

Conclusion

This thesis work has tried to show the design process of Power Electronic Interfaces (PIEs) and Microsources controller using droop control technique for PV-ISOFC/GT Microgrid. In the PEIs design the study has already shown the satisfactory results obtained through simulations. The intention of designing the PEIs is to generate AC voltage with frequency of 50 Hz and magnitude of 380 V in reliance with the standard in our country. The intended results were obtained starting with the two stages DC-DC boost converters in the case of SOFC and PV, and rectifier in that of the GT. This voltage level is supposed to be generated for the estimated loads of 40 KW; i.e. 20 KW from the SOFC, 10 KW from the PV and 10 KW from the GT. And considering the intermittent nature of the PV 10 KW of extra power supply from SOFC is allocated as a spinning reserve.

Also the design of microsource controller operating in grid-connected mode to control active and reactive power, and in island mode to control voltage and frequency has been demonstrated in SIMULINK. Although some deviations were noticed in the design of microsource controllers, either alternative design approach has been followed to come up with a design of some modification but for the same purpose. In the V-f droop controller design it was possible to control both voltage magnitude and frequency of the MG in the islanding mode. This result was confirmed with the output voltage waveform to be used as a modulating signal in PWM generator. In the PQ droop controller case, it was not possible to generate standard sine wave as a confirmation of the right controlling mechanism. Actually in PQ control mode it is possible to use the voltage waveform from the main grid as a modulating signal. Any how an alternative design which could give reliable results has been recommended.

The study could also provide a proposal for a better performance of a MG during transition mode when it resynchronizes with the grid after the fault

is cleared. Now it is time to conclude on the study based on the research questions raised in the thesis.

7.1. Contributions

Conventional way of power generation is being criticized as it is one of the main causes of global warming and environmental pollution; it is costly in terms of infrastructure, inefficient in power generation, not reliable in terms of power quality, disrupts the existing ecosystem during construction, etc. Developing a Microgrid is one of the solutions in reducing and eliminating the impacts caused by the above consequences. Power electronic interfaces and microsource controller are among the key element in a MG. So this study has paid contribution in its own way by designing these two important systems for a model MG.

7.1.1. Power Electronic Interfaces

In this thesis three major PEIs have been designed. In all the three designs significant achievements have been made. The following are the achievements that this study has contributed in designing the PEIs:

1. In designing the inverters, it is possible to have a design whose output AC voltage has the minimum harmonics that the Total Harmonic Distortion (THD) for all the inverters is at its lowest level.
2. In designing the DC-DC boost converters, two major contributions have been made. The first one is it was possible to avoid the use of transformer after inversion by carefully tuning components in the DC-DC converter and inverter too. The second one is the two stage DC-DC conversion technique can bring a huge stepping up in voltage level so that the size or amount of the micro-generator is reduced when compared to a single stage DC-DC converter would have been used. Therefore, by doing so it is possible to achieve a significant reduction in the cost of generation.
3. The rectifier design could make the output voltage from Gas Turbine controllable.

7.1.2. Microsource Controller

The designed microsource controller in this study has also achieved significant contributions in terms of the power quality, reliability, cost and the ease of controlling each microsource in self-contained manner. Each microsource in the MG has its own controller which operates independently of any other microsource in both grid-connected and island mode of operation. This scenario avoids using communication facilities to connect with central controller so that reliability is increased. In both modes of operation it is possible to control voltage magnitude and frequency, and active and reactive power using the droop technique. Though some unexpected outputs, like the oscillation of output power in power sharing control using droop control technique, were achieved possible remedies and causes has been mentioned for the better design of microsource controller. So it is possible to conclude that the designed controller can perform in an intended way.

7.2. Future Duties

The designed PIEs and MS Droop controller have not been tested in a laboratory or practical environment. This thesis would like to propose the designed systems have to be practical and tested so that the drawbacks and strengths of the designed systems can be identified for the better of the devices which leads to its practical implementation beyond the simulations. Even practical tests may indicate ways as to how the problems which have manifested in this study can be tackled. I hope there will be, or there is underway, a study which will include the practical undertakings of the designed PIEs and MS Controller so that the drawbacks of this thesis work and its improvement will be realized.

7.3. Recommendations

The proposed Microgrid, PV-ISOFC/GT, is envisaged to be efficient and reliable in terms of enhanced dispatchablity and minimum energy wastage. This thesis work has developed important devices, Power Electronic Interfaces and Microsource Controllers, for the Microgrid. These designed devices have been demonstrated using Black Lion Hospital as a community which needs continuous power supply for its sensitive loads. Therefore this study would like

to recommend for the application of the proposed Microgrid with its designed PEIs and MS Controllers so that it can be used as a model to other Microgrids to be developed for the intended purpose of reliable power supply to sensitive loads. It is also possible to develop other type of comprehensive Microgrid with a different combination of microsources using the developed PEIs and MS Controllers as a reference. Also it is possible to develop a Microgrid to support all loads of a community whenever power from the utility is interrupted.

REFERENCES

1. Nikos Hatziargyriou, '' **Microgrid Architecture and Contro**l'', IEEE, John Wely and Sons Ltd., 2014.
2. S. Chowdhury, S.P. Chowdhury and P. Crossley, '' **Microgrids and Active Distribution Networks**'', The Institution of Engineering and Technology, UK, London, 2009.
3. XueSong Zhou, Tie Guo and YouJie Ma, **'' An Overview on Operation and Control of Microgrid**'', International Conference on Manufacturing Construction and Energy Engineering, 2016.
4. Robert H. Lasseter and Paolo Piagi, **''Control and Design of Microgrid Components**'', University of Wisconsin-Madison, 2006.
5. Robert H. Lasseter and Paolo Piagi, **''Autonomous Control of MicroGrids**'', IEEE, Montreal, 2006.
6. Prabath Janaka Binduhewa, ''**Microsource Interface for a Microgrid,**'', University of Manchester, 2010.
7. Robert H. Lasseter, Paolo Piagi, '' **Control and Design of Microgrid Components**, '' Power Systems Engineering Research Centre, University of Wisconsin-Madison, 2006.
8. Robert Lasseter, Abbas Akhil, Chris Marnay, John Stephens, Jeff Dagle, Ross Guttromson, A. Sakis Meliopoulous, Robert Yinger, and Joe Eto, ''**The CERTS MicroGrid Concept**'' Consortium for Electric Reliability Technology Solutions, 2002.
9. R.H. Lasseter, "**MicroGrids**," IEEE Power Engineering Society Winter Meeting, 2002, Vol. 1.
10. C.E. Jones, C. Fitzer, and M. Barnes, "**Investigation of Microgrids**," The 3rd IET International Conference on Power Electronics, Machines and Drives, 2006.
11. L. Yunwei, D.M. Vilathgamuwa, and L. Poh Chiang, "**Design, analysis, and real time testing of a controller for multi-bus microgrid system**," IEEE Transactions on Power Electronics, vol. 19, 2004.
12. N. Pogaku, M. Prodanovic, and T.C. Green, "**Modelling, Analysis and Testing of Autonomous Operation of an Inverter-Based Microgrid**," IEEE Transactions on Power Electronics, vol. 22, 2007.

13. Salima Nemsi, Seifeddine Abdelkader Belfedhal, Linda Barazane '' **Role of Flywheel Energy Storage System in Microgrid**, Journal of Engineering Research and Technology, Volume 3, Issue 3, September 20
14. E. Hendawi, I. Bedir, '' **Analysis and simulation of three phase sinusoidal PWM Inverter fed by PV array**'', Electronic Research Institute, Egypt. 2014.
15. Jayesh M. Suryawanshi, Sunil T. Gaikwad, '' **Automatic Synchronizing Control of a Microgrid**'', University of Pune, January 2015.
16. Li-Jun Qin, Wan-Tao Yang, '' **Micro-Grid Converter Droop Control Strategy and Simulation**'', North China Electric Power University, Beijing, China.
17. Shafinaz A. Lopa, S. Hossain, M. K. Hasan, T. K. Chakraborty, '' **Design and Simulation of DC-DC Converters**'', Presidency University, Dhaka, Bangladesh, January 2016.
18. J. A. Peças Lopes, C. L. Moreira, and A. G. Madureira, '' **Defining Control Strategies for MicroGrids Islanded Operation**'', IEEE, May 2006.
19. Zeya Cai, '' **Design and Control of Islanded Microgrid**'', University of Denver, 2016.
20. Prof R. Kameswara Rao, P. Srinivas, M.V. Suresh Kuma, '' **Design and analysis of various inverters using different PWM techniques**'', Guru Nanak Institutions Hyderabad, Raghu Engineering College, 2014.
21. Nur Aisyah Jalalludin, Arwindra Rizqiawan, Goro Fujita, '' **Grid-Connected Inverter Experimental Simulation and Droop Control Implementation**'', International Journal of Electrical, Computer, Energetic, Electronic and Communication Engineering Vol. 8, No: 12, 2014.
22. Zhikang SHUAI, Shanglin MO, Jun WANG, Z. John SHEN, Wei TIAN, Yan FENG, '' **Droop control method for load share and voltage regulation in high-voltage Microgrid**'', State Grid Electric Power Research Institute, November 2015.
23. Pankaj H Zope, Pravin G.Bhangale, Prashant Sonare ,S. R.Suralkar, **''Design and Implementation of carrier based Sinusoidal PWM Inverter**'', International Journal of Advanced Research in Electrical, Electronics and Instrumentation Engineering, Vol. 1, Issue 4, October 2012.

24. Fang Lin Luo, Hong Ye, ‘’**Advanced AC/DC Inverters: Application in Renewable Energy**’’, Taylor & Francis Group, LLC, USA, 2013.
25. Fang Lin Luo, Hong Ye, ‘’ **Advanced DC/DC converters**’’, CRC Press LLC, USA, 2004.
26. Guy Seguier, Francis Labrique, ‘’**Power Electronic Converters: DC-AC Conversion’’**,
28. Muhammad Harunur Rashid**,** ‘’ **Power Electronics Handbook**’’, University of Florida, 2001.
29. Muhammad Harunur Rashid, ‘’**Power Electronics: Circuit, Devices, and application**’’, Prentice Hall, Englewood Cliffs, New Jersey.
30. Nihan Kularatna, ‘’**Power Electronics Design Handbook**’’, Butterworth-Heinemann. 1998.
31. Dorin O. Neacsu, ‘’**Power-Switching Converters**’’, Taylor & Francis Group, LLC, 2006.
32. W. Kramer, S. Chakraborty, B. Kroposki, and H. Thomas, ‘’ **Advanced Power Electronic Interfaces for Distributed Energy Systems**’’, National Renewable Energy Laboratory, March 2008.
33. H. Sira-Ramirez, R. Silva-Ortigoza, ‘’**Control Design Techniques in Power Electronic Devices**’’, Springer-Verlag London Limited, 2006
34. I. Vechiu, A. Etxeberria, H. Camblong, and J. M. Vinassa, ‘’ **Advanced Power Electronic Interface for Hybrid Energy Storage System used for Microgrids**’’, EHU-UPV, Spain.
35. Ian F. Crowley, Ho Fong Leung, ‘’**PWM Technique: A Pure Sine Wave**’’, Worcester Polytechnic Institute Major Qualifying Project, 2010-1011.
36. Suleiman M. Sharkh, Mohammad A. Abusara, Georgios I. Orfanoudakis, Babar Hussain, ‘’ **Power Electronic Converters for Microgrids**’’, John Wiley & Sons Singapore Pte. Ltd.2014.
37. Jatin A. Patel, Asst. Prof. Hardik H. Raval, ‘’ **Design of Sinusoidal Pulse Width Modulation Inverter**’’, International Journal for Technological Research in Engineering Volume 2, Issue 8, April-2015.
38. Bandana Bhutia, Dr. S.M.Ali, Narayan Tiadi, ‘’ **Design of Three Phase PWM Voltage Source Inverter for Photovoltaic Application**’’, International Journal of Innovation Research in Electrical, Electronics, Instrumentation and Control Engineering Vol. 2, Issue 4, April 2014.

39. Nur Aisyah Jalalludin, Arwindra Rizqiawan, Goro Fujita, '' **Grid-Connected Inverter Experimental Simulation and Droop Control Implementation**'', IJECEECE, Vol.8, No.12, 2014.
40. Rashad M. Kamel, Aymen Chaouachi, Ken Nagasaka, **''Detailed Analysis of Micro-Grid Stability during Islanding Mode under Different Load Conditions**'', Tokyo University of Agriculture and Technology, Kogane- shi, Tokyo, Japan, 2014.
41. Veneceslav F. Kroupa, **''Phase Locked Loop and frequency synthesis**'', John Wiley & Sons Ltd, The Atrium, Southern Gate, Chichester, West Sussex PO19 8SQ, England, 2003.
42. Garth Nash, '' **Phase-Locked Loop Design Fundamentals''**, Free scale Semiconductor. 2006
43. Richard C .Dorf, Robert H. Bishop, '' **Modern Control Systems, 5th Ed.**'', Pearson Education, Inc., Upper Saddle River, New Jersey 07458, 2011.
44. Khaled H. Ahmed, Stephen J. Finney and Barrey W. Williams, ''**Passive filter design for three phase inverter interfacing in distributed generation''**, Strathclyde University, UK, 2007.
45. Giancarlo Bertuzzi, Ugo Stefano Cinti, Emiliano Cevenini, Alessandro Nalbone, '' **Static Transfer Switch**'', Chloride Power Protection, Italy.
46. A A Salam, A Mohamed, M A Hanan, A Ayob, '' **Improved Control Strategy for Fuel Cell and Photovoltaic Inverters in Microgrid''**, Universiti Kebangsaan Malaysia,
47. Manohar Chamana, Stephen Bayne, '' **Modelling and control of directly connected and inverter interfaced sources in a Microgrid,''**, Common Wealth Edison and Texas Tech University, August 2011.
48. Matthew Surprenant, Ian Hiskens, Giri Venkataramanan, '' **Phase Locked Loop Control of Inverters in a Microgrid**,'' University of Wisconsin and University of Michigan.
49. C.X. Wen, Z.Y. Liu, Z.X. Li, '' **Droop Control of Parallel Dual-Mode Inverters Used in Micro Grid**'', Power Electronic and Motor Drive Engineering Research Centre, North China University of Technology, Chine, 2015.
50. Chitra Natesan, Senthilkumar Ajithan,, Shobana Mani,, and Prabaakaran Kandhasamy, '' **Applicability of Droop Regulation Technique in Microgrid**

- A Survey'', Anna University, Kotturpuram, Chennai, Tamil Nadu 600025, India.

51. Jakath Sri Lal Senanyak, '' **Power Dispatching of Active Generators using Droop Control in Grid connected Micro-grid**'', University of Agder, 2014.
52. Cao, Yuanzhi; Hu, Yanting; Hu, Rui; Chen, Jianfei, '' **Research on the synchronization control strategy for Microgrid-connected voltage source inverter**'', University of Chester. 2015.
53. Tine Vandoorn, Bert Renders, Frederik De Belie, Bart Meersman and Lieven Vandevelde, '' **A Voltage-Source Inverter for Microgrid Applications with an Inner Current Control Loop and an Outer Voltage Control Loop''**, Ghent University, Belgium, April 2009.
54. Volker Quaschning, '' **Understanding Renewable Energy Systems'',** Earthscan, USA, 2005.
55. John T. S. Irvine, Paul Connor, **'' Solid Oxide Fuels Cells: Facts and Figures ''**, Springer London Heidelberg New York Dordrecht, USA, 2013.
56. Professor Laurence Peter, **'' Solid Oxide Fuel Cells: From Materials to System Modelling '',** RSC Energy and Environment Series, University of Bath, UK, 2013.
57. M. Hashem Nehrir, Caisheng Wang, **'' Modelling and control of Fuel cells''**, Institute of Electrical and Electronics Engineers, Inc., 2009.
58. Roland S. Burns, '' **Advanced Control Engineering**'', Butterworth-Heinemann, Linacre House, Jordan Hill, Oxford OX2 8DP, 2001.